Electrical Activation of Pudendal Nerve Branches: Exploration of Efferent and Afferent Effects

by

Amador Cabrera Lagunas

A dissertation submitted in partial fulfillment
of the requirements for the degree of
Doctor of Philosophy
(Biomedical Engineering)
in the University of Michigan
2026

Doctoral Committee:

Associate Professor Tim M. Bruns, Chair
Associate Professor Priyanka Gupta
Associate Professor Stephen Kemp
Associate Professor Scott F. Lempka

Amador Cabrera Lagunas

lagunas@umich.edu

ORCID iD: 0000-0002-7555-4783

© Amador C. Lagunas 2026

Dedication

This dissertation is dedicated to the memory of my grandmother, Graciela Cabrera. Gracias, te extraño, te quiero.

Acknowledgements

Thank you to everyone who has been in my life for these past six years (and longer). With your support I've grown as a scientist, engineer, and person.

First, I want to thank my PhD advisor Dr. Tim Bruns. Tim has always been kind, thoughtful, and supportive. Science is hard but we should always treat others well, including ourselves. I want to thank my committee members Dr. Priyanka Gupta, Dr. Scott Lempka, and Dr. Stephen Kemp. Thank you for taking the time to teach me and work with me throughout my entire PhD.

While the personnel of the lab have changed, the culture of collaboration and curiosity has not. Thank you to my friends, who have made it a pleasure to come into the office every day. Dr. Elizabeth Bottorff and Dr. Lauren Madden showed me that one could be a great scientist in the lab and a great community organizer and volunteer outside of it. Dr. Miguel Angel Ortiz-Lopez showed me how to be a good teammate, especially in the most stressful times. Mark Nissen and Sonia Bhaskaran showed me that one must challenge assumptions to push science forward. Vanessa Pruitt, Mackenzie Moore, and Yike Liu showed me that people, especially our study participants, are the most important part of clinical research. Eric Kennedy showed me that preparation is key to staying cool under pressure. Dr. Po-Ju Chen, who I learned all my successful habits from, showed me how to be a good scientist, mentor, and person.

Thank you to my parents Hector and Araceli, for their support and selflessness. The distance and time apart was hard, but I felt your love the whole time. Finally, thank you to my wife Maaike. You have been my editor, cheerleader, and my best friend. While we were far from our families, every day in Michigan felt like home thanks to you.

Table of Contents

Dedication ii

Acknowledgements iii

List of Tables vii

List of Figures viii

Abstract xii

Chapter 1 Introduction 1

1.1 Lower Urinary Tract Anatomy 1

1.2 Pelvic Floor Innervation 3

1.2.1 The Pudendal Nerve 3

1.2.2 The Pelvic Nerve and the Hypogastric Nerve 4

1.3 Neural Control of Bladder State 5

1.4 Lower Urinary Tract Disorders & Pain 6

1.5 Treatments for LUT Dysfunction and Pelvic Pain 7

1.6 Pudendal Neuromodulation 8

1.7 Animal and Computational Models 9

1.8 Dissertation Summary 10

Chapter 2 Factors Affecting Anal Sphincter Recruitment During Intraoperative Pudendal Nerve Stimulation: An Observational Study 11

2.1 Abstract 11

2.2 Introduction 12

2.3 Materials and Methods 13

2.4 Results 15
2.5 Discussion 19
2.6 Acknowledgements 23
2.7 Supplemental Information 24
Chapter 3 Pudendal Nerve Stimulation Recruits the Urethra During Awake Human Cystometry 27
3.1 Abstract 27
3.2 Introduction 28
3.3 Materials and Methods 29
3.4 Results 31
3.5 Discussion 34
3.6 Conclusion 37
3.7 Acknowledgments 37
3.8 Supplemental Information 37
Chapter 4 Selective Neurostimulation of Small-diameter Pudendal Fibers is Feasible with a Multicontact Nerve Cuff Electrode: A Modeling Study 39
4.1 Abstract 39
4.2 Introduction 40
4.3 Methods 41
4.3.1 Nerve Processing 41
4.3.2 Cuff Specifications 42
4.3.3 Computational Modeling Details 43
4.3.4 Simulation Configurations 45
4.3.5 Data Analysis 47
4.4 Results 48
4.5 Discussion 51

4.6 Acknowledgements 55
4.7 Supplemental Figures 56
Chapter 5 Discussion 59
5.1 Summary of Clinical Results 59
5.2 Summary of Computational Modeling Results 63
5.3 Concluding Remarks 65
Appendix 67
Bibliography 69

List of Tables

Table 2-1 Summary of participant characteristics 16

Table 2-2 Linear mixed model estimating anal sphincter activation:..... 17

Supplemental Table 2-3 The significant fixed effects on EAS EMG AUC (μV*s) for a linear mixed model incorporating electrode-to-nerve distance. The data includes all monopolar trials with electrode-to-nerve distance data (N=5). 24

Supplemental Table 2-4 The significant fixed effects on EAS threshold (mA) for a linear mixed model incorporating electrode-to-nerve distance data. The data includes all monopolar trials with electrode-to-nerve distance data (N=5)..... 24

Table 3-1 Participant demographic information. 31

Supplemental Table 3-2 Median urethra pressure changes in response to low and high frequency stimulation..... 37

Table 4-1 COMSOL model meshing parameters 43

Table 4-2 FEM material conductivities 44

List of Figures

Figure 1-1: Innervation of the external anal sphincter, external urethral sphincter, and the genitalia by the pudendal nerve in a A) female and B) male pelvis. Adapted from Yang et al. 2026[19] and Hombach-Klonisch et al. 2019[20]. 2

Figure 1-2: Innervation of pelvic floor muscles by the pudendal nerve in a female pelvis. (1) ischioscavernosus muscle, (2) bulbocavernosus muscle, (3) external urethral sphincter, (4) external anal sphincter, (5) superficial transverse perineal muscle. Adapted from de Pavia et al. 2024[27]. 3

Figure 1-3: Innervation of the bladder, urethra, and external urethral sphincter by the pelvic nerve (PEL), hypogastric nerve (HGN), and pudendal nerve. The pelvic nerves are shown in green and provide parasympathetic input to the bladder wall. The hypogastric nerves are shown in blue and innervate the base of the bladder and the urethra. The pudendal nerve is shown in yellow and innervates the external urethral sphincter. The pudendal nerve generates contractions in the external urethral sphincter. The pelvic nerves generate contractions in the bladder smooth muscle. The hypogastric nerves contract urethral smooth muscle and relax bladder smooth muscle. S_1, first sacral root; PP, Pelvic plexus. Modified from de Groat et al. 2015[16]. 5

Figure 2-1: Characterization of external anal sphincter EMG activation by intraoperative monopolar pudendal nerve stimulation. Each dot represents the minimum threshold across all electrodes for an individual participant at a given pulse width. A) The threshold current required to activate the EAS for the tested pulse widths of 60, 210, and 450 μs. B) The charge per pulse at the EAS activating threshold current depending on pulse width. Box plots represent the IQR for the height of each box, with the bold central line indicating the median. Tips of whiskers extend to the value(s) within 1.5 x IQR of each box side. * indicates $p < 0.05$, ** indicates $p < 0.01$. 18

Figure 2-2: Anal sphincter response magnitude plotted against applied current for all monopolar trials across all participants. Data is separated by participant diagnosis of overactive bladder and/or urinary retention. Each trial was performed with a pulse width of 60, 210, or 450 μs and is labeled according to the legend. 19

Figure 2-3: Measured distances (in millimeters) between each electrode on the implanted quadripolar lead and the closest point of the pudendal nerve for the five participants with minimal lead migration (<5 mm). Electrodes are labeled from E0 to E3 with E0 representing the electrode most distal to the implantable pulse generator to E3 representing the electrode most proximal to the implanted pulse generator. 20

Figure 2-4: Linear regression fits between each participant's average electrode-to-nerve distance and symptomatic survey score percent change before and after receiving pudendal neuromodulation treatment. Surveys on asymptomatic functions (CRAD-8 (Bowel), FSFI (Female sexual function)) did not have relationships to electrode-to-nerve distance ($p = 0.606$, 0.706, respectively). 21

Supplemental Figure 2-5: Anal sphincter EMG and AUC Quantification procedure. (A) Example EAS EMG after signal filtering showing five consecutive responses during a single trial. Stimulation was applied at 3 Hz. (B) Each individual response in A is segmented, rectified, and aligned at the stimulation artifact. Individual traces in are in gray and the average signal is in black. (C) The shaded area under the rectified average EMG trace, between the vertical dashed lines, is the calculated area under the curve (AUC). 25

Supplemental Figure 2-6: Monopolar threshold current and charge for all participants at each tested pulse width. A) EAS threshold current for each participant. If we tested the threshold for multiple electrodes at a given pulse width then the lowest threshold is shown. B) The charge at EAS threshold for each participant. 25

Supplemental Figure 2-7: EAS activation thresholds for 210 μs pulse width monopolar and bipolar trials. A) The minimum EAS threshold for monopolar and bipolar stimulation is shown for each participant. B) Aggregated EAS thresholds across all participants for monopolar and bipolar trials. Box plots represent the inter-quartile range (25%-75%; IQR) for the height of each box, with the bold central line indicating the median. Tips of whiskers extend to the value(s) within 1.5 x IQR of each box side. 26

Supplemental Figure 2-8: The EAS response magnitude dependence on participant diagnosis of A) Overactive Bladder, B) Urinary Retention, C) Urinary Incontinence, or D) Pelvic Pain. The N value under each x-axis indicates the number of participants diagnosed with each condition out of 16 total participants. The legends in sub-figures A and B show comorbidities of Retention or Overactive Bladder, respectively. 26

Figure 3-1: Experimental setup diagram. With participants in a reclined position, a multi-channel catheter was inserted into the urethra to measure urethra and bladder pressures. The multichannel catheter was placed alongside a urodynamics catheter which was used to infuse saline into the bladder. A urodynamics system was used to record bladder, urethra, and abdominal pressures, anal sphincter EMG, and the voided volume. This figure was modified from Karram and Blaivas[132]. 29

Figure 3-2: Stimulation driven urethra pressure changes across participants. The urethra position is labeled according to each sensors relative position to the sensor with the greatest baseline pressure. A) Lower urinary tract pressure changes during stimulation at low frequency. Pressure change is calculated per stimulation pulse. B) Lower urinary tract pressure changes during stimulation at high frequency. Pressure change is the maximum difference from the baseline pressure during a tetanic contraction. 32

Figure 3-3: LUT pressures from example trials with bladder contractions in participant 2001. A) A trial with stimulation applied at 2.1 Hz and a maximum stimulation amplitude of 2V. B)

A trial with stimulation applied at 31 Hz and a maximum stimulation amplitude of 1.3V. Note the different timing dynamics of bladder pressure rise or fall as compared to urethra pressure changes. 33

Figure 3-4: A void with pudendal nerve stimulation (PNS) for participant 1002. A) Pelvic pressures and voiding response during PNS. B) Urethra pressure profiles (UPPs) from specific time points in A marked with vertical dashed lines. 35

Supplemental Figure 3-5: A void without pudendal nerve stimulation (PNS) for participant 1002. A) Pelvic pressures and voiding response during PNS. B) Urethra pressure profiles (UPPs) from specific time points in A marked with vertical dashed lines. 38

Figure 4-1: A) H&E-stained feline pudendal cross section. B) Traced perineurium from A. C) Segmented inner portion of the pudendal nerve in A. 42

Figure 4-2: Example feline pudendal nerves placed inside each of a A) 1.20 mm diameter cuff and a B) 1.91 mm diameter cuff. Both cuffs have 8 stimulation contacts. The nerve in B is too large to fit in the cuff in A. C) Example depictions of activated contacts for bipolar, guarded, and full cuff stimulation. Four different sets of contacts were tested for bipolar and guarded stimulation. The cathode occupied a unique position on the proximal row of contacts for each unique set. Cathodes are in red with an inset (-) and anodes are in blue with an inset (+). Materials in A and B are colored as follows: white: saline, pink: parylene C, yellow: epineurium, blue: endoneurium, grey: platinum contact. 43

Figure 4-3: Box plots of fascicular selectivity for the centrally placed four fiber simulation. A) Selectivity comparison across fiber diameters. b) Selectivity comparison for different stimulation configurations for each fiber diameter. The borders of each box correspond to the first and third quartiles (interquartile range [IQR]). The upper whisker extends to the largest value that is less than or equal to 1.5 times the IQR from the upper box boundary. The lower whisker extends to the smallest value than is no more than 1.5 times the IQR from the lower box boundary. Significance was examined with a post-hoc Dunn test with Bonferroni correction. *** denotes significant difference ($p < 0.001$). 49

Figure 4-4: Selectivity of 8-, 10-, and 16-contact nerve cuffs with bipolar stimulation for fascicles with afferent fiber diameters of 2, 5.7, and 7.3 μm. A) Selectivity for an 8-contact and 10-contact cuff when both are used to stimulate the same 1.2 mm nerve. B) Selectivity for an 8-contact and 16-contact cuff when both are used to stimulate the same 1.91 mm nerve. Box plots are organized as in Figure 4-3. 50

Figure 4-5: Fascicular selectivity with bipolar stimulation for the randomly placed 36-fiber experiment. Box plots are organized as in Figure 4-3. 50

Figure 4-6: Fascicular selectivity for the randomly placed 40-fiber experiment. Box plots are organized as in Figure 4-3. *** denotes significant difference ($p < 0.001$). 51

Supplemental Figure 4-7: Anti-Neurofilament 200 Antibody was used to confirm suspected fascicles contained myelinated fibers. Myelinated fibers are identified in yellow. 56

Supplemental Figure 4-8: 3D visualization of multicontact nerve cuffs. An 8-contact (A) and 10-contact (B) nerve cuff with diameters of 1.20 mm. An 8-contact (C) and 16-contact (D) nerve cuff with a diameter of 1.91 mm. 56

Supplemental Figure 4-9: The average activation threshold is minimally impacted by the A) length and B) radius of the model. A) Mean threshold is compared to a model 50 mm in length. B) Mean threshold is compared to a model 25 mm in length. The errors bars show standard deviations. Thresholds were tested for fibers with diameters of 2, 7.3, 10, and 12.8 μm. 57

Supplemental Figure 4-10: Visualization of fiber distribution within fascicles for a single nerve. Each dot represents a single modeled fiber. A) A 2, 5.7, 7.3 and 10 μm fiber were each placed at the same point in the center of each fascicle. B) Nine fibers of each diameter were placed randomly throughout each fascicle. C) 40 fibers were placed randomly throughout each fascicle. Each fiber had a diameter randomly selected from a uniform distribution between 2 and 13 μm. 57

Supplemental Figure 4-11: Fiber counts for different diameter fibers with cumulative percentage of fibers displayed on the right-hand axis. A) Afferent fiber counts for the sensory branches of the pudendal nerve (dorsal nerve to the penis and cranial urethra). B) Efferent fiber counts for the mixed branches of the pudendal nerve (external anal sphincter, deep perineal, constrictor vulvae, and bulbospongiosus). The figure was created using data from Martin, Fletcher, and Bradly, 1974[91]. 58

Supplemental Figure 4-12: Labeled nerve fascicles for the five nerves used in the study. Cross sections A and B came from the same feline and were placed in the 1.20 mm diameter cuff. Cross sections C, D, and E were placed in the 1.91 mm diameter cuff. Sample C and D came from the same feline. The diameter for each nerve is as follows: A) 1.1 mm, B) 1.1 mm, C) 1.3 mm, D) 1.4 mm, E) 1.91 mm. 58

Figure A-1: An example of an evoked bladder contraction from pudendal nerve stimulation. ... 68

Abstract

Overactive bladder (OAB) and chronic pelvic pain are prevalent debilitating disorders that can command a person's life. Even though millions of people are affected, most suffer in silence and face their symptoms alone. Pudendal neuromodulation, an off-label therapy, is one of the few treatment options that can improve symptoms for OAB and pelvic pain. Despite two decades of use in the clinic, much is still unknown about the efferent and afferent effects of pudendal neuromodulation. In this dissertation I address this gap by characterizing the physiological effects of pudendal nerve stimulation in a clinical setting and studying selective activation of pudendal afferents with computational models.

In my first aim, I quantified the association between procedural factors and anal sphincter recruitment during intraoperative pudendal nerve stimulation. We recorded external anal sphincter (EAS) activation threshold and magnitude during pudendal stimulation with three different pulse widths. We also measured the electrode-to-nerve distance for each participant. I found that a pulse width of 210 μs balanced charge and current better than 60 or 450 μs. Additionally, a larger electrode-to-nerve distance led to increased EAS threshold ($p < 0.001$) and decreased EAS magnitude ($p = 0.0011$). Our results support the continued use of clinical pudendal neuromodulation parameters and suggest better patient outcomes for smaller electrode-to-nerve distances.

In my second aim, I explored the effects of suprasensory pudendal nerve stimulation on lower urinary tract pressures in awake human participants with implanted pudendal neuromodulation devices. We applied stimulation at low and high frequencies as the bladder was filled and during voiding to examine the effects of pudendal neuromodulation. At tolerable stimulation amplitudes there were small urethra pressure increases with low frequency stimulation, and large urethra pressure increases with high frequency stimulation throughout the length of the urethra. Additionally, we report the first example of stimulation-driven bladder pressure increases in an awake non-spinal cord injured individual. Stimulation did not have a significant immediate effect on voiding efficiency or maximum flow rate, suggesting that the benefits of pudendal nerve

stimulation come from long-term changes. We show that high frequency pudendal stimulation may be useful in preventing urinary leakage and driving bladder activation.

In my third aim, I used computational modeling techniques to investigate if selective activation of sensory fascicles in the pudendal nerve was feasible. I modeled a multicontact nerve cuff, used in *in-vivo* experiments, to selectively activate afferent pudendal nerve targets in felines. I generated computational models, with 3D geometries based on feline nerve histology, populated with fiber diameters that reflect the known population distribution of afferent and efferent fascicles, something that other studies failed to do. With the simulated cuff design, fascicular selectivity is significantly dependent on the diameter of afferent axons that need to be activated to achieve therapeutic benefit. We showed that the different axon diameters for afferent and efferent fascicles cause low fascicular selectivity with our current electrode design.

This thesis expands our knowledge of the clinical effects of pudendal neuromodulation and supports the continued development of pudendal neuromodulation into an on-label therapy. The efferent effects of pudendal nerve stimulation may provide new treatment options for people with stress urinary incontinence and underactive bladder. From my interactions with individuals who benefit from pudendal neuromodulation, I know that the technology can improve the lives of many more people.

Chapter 1 Introduction

The origin of the name for the pudendal nerve comes from the Latin “pudere” denoting shame[1]. This meaning stems from the fact that the pudendal nerve innervates the genitalia[1]. The pudendal nerve also innervates other pelvic floor structures like the external anal sphincter, external urethral sphincter, and perineum[2]. Unfortunately, the undue shame originally associated with genital innervation has spread to the rest of the pelvic floor. Lower urinary tract symptoms (LUTS) and pelvic floor disorders like overactive bladder, retention, incontinence, and chronic pelvic pain are common yet seldom talked about[3–6]. People fear the stigma associated with these disorders and will change their lifestyles in response. They become less active and more isolated, resulting in a diminished quality of life[3–8]. In contrast to the word’s origins, recent scientific advancements associate the pudendal nerve with hope. When other treatment options have failed, pudendal neuromodulation has emerged as a minimally invasive, off-label treatment option for overactive bladder and chronic pelvic pain[9–11]. Continuing this success, decades of promising results from preclinical and computational experiments with pudendal neuromodulation suggest it can have a greater clinical benefit[12–15]. In this thesis I investigate how pudendal neuromodulation is working in human clinical studies and investigate if future electrode technology could improve treatment efficacy in a computational model.

1.1 Lower Urinary Tract Anatomy

While the origins of lower urinary tract symptoms are often unknown, or idiopathic, they can be the result of an issue in the lower urinary tract or the peripheral nerves that control it. Here I describe the lower urinary tract anatomy to inform how deficiencies could lead to dysfunction.

The urinary bladder and the urethra are the two components of the lower urinary tract[16,17]. They work in tandem to enable two distinct tasks: the storage and elimination of urine[17,18]. The urinary bladder is a hollow organ that stretches to store urine during continence and contracts to generate pressure that pushes urine out of the body during micturition[18]. The bladder wall is comprised of different layers that contribute to the function of the bladder[18]. The innermost layer,

the urothelium, serves as an impermeable barrier between urine and the other layers of bladder tissue, preventing irritation caused by pathogens and solutes[18]. The urothelium also sends afferent signals that communicate bladder conditions like temperature, pressure, and infection[18] to the rest of the body. The next layer is the lamina propria. It contributes to nerve signaling, cell growth, and inflammatory responses[18]. The detrusor layer consists of three overlapping layers of muscle that stretch as the bladder fills and contract to promote emptying, driving fluid out of the bladder[18].

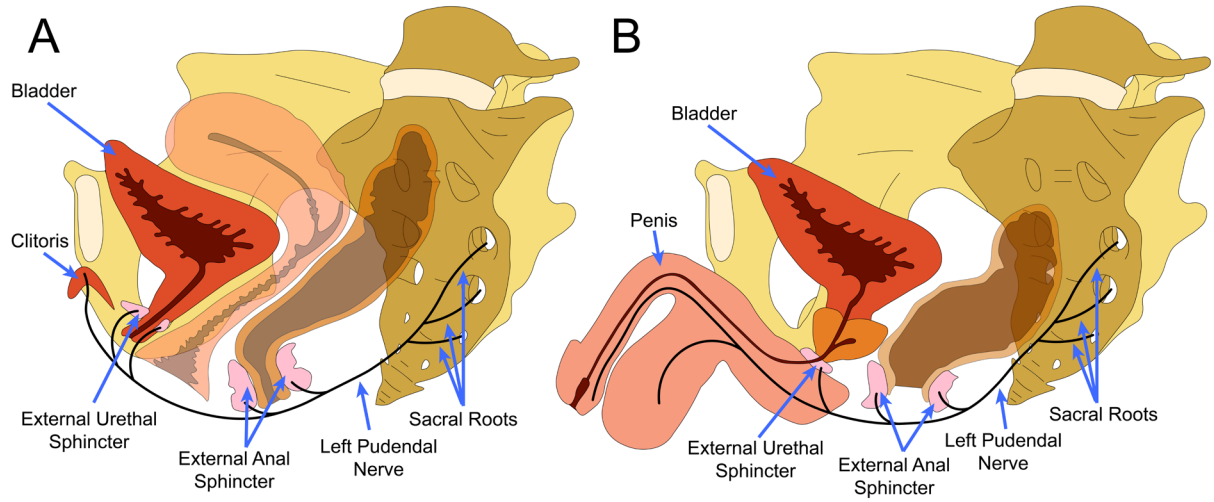


Figure 1-1: Innervation of the external anal sphincter, external urethral sphincter, and the genitalia by the pudendal nerve in a A) female and B) male pelvis. Adapted from Yang et al. 2026[19] and Hombach-Klonisch et al. 2019[20].

The urethra connects the bladder to the outside environment and works with the bladder to prevent urine leakage during storage, via urethra contraction, and facilitate urine flow during micturition, via urethra relaxation[21,22]. Similar to the bladder, the urethra is also comprised of layers of tissue with unique compositions and functions[23,24]. The first layer is the epithelium, which functions as a barrier between urine and the other urethra layers[25]. It surrounds the lumen, the space inside the urethra that urine flows through. The next layer of tissue is the lamina propria[25]. The lamina propria supports the epithelium and also contains sensory nerve endings that send sensory information from the urethra to the spinal cord[25]. Smooth muscle surrounds the lamina propria, arranged in a longitudinal layer and then a circular layer[25]. Smooth muscle comprises the internal urethral sphincter, which provides continuous, involuntary urethra tone during continence, preventing leakage. In men the internal urethral sphincter passes through the prostate[26]. Finally, striated muscles surround the smooth muscle to form the external urethral sphincter. The external

urethral sphincter is under voluntary control and contributes to urethral closure pressure and continence[23,24]. In women, the external urethral sphincter surrounds the distal half of the urethra excluding the urethral opening[23]. In men, the external urethral sphincter covers the portion of the urethra between the prostate and bulbar urethra, roughly where the urethra passes the pubic symphysis.

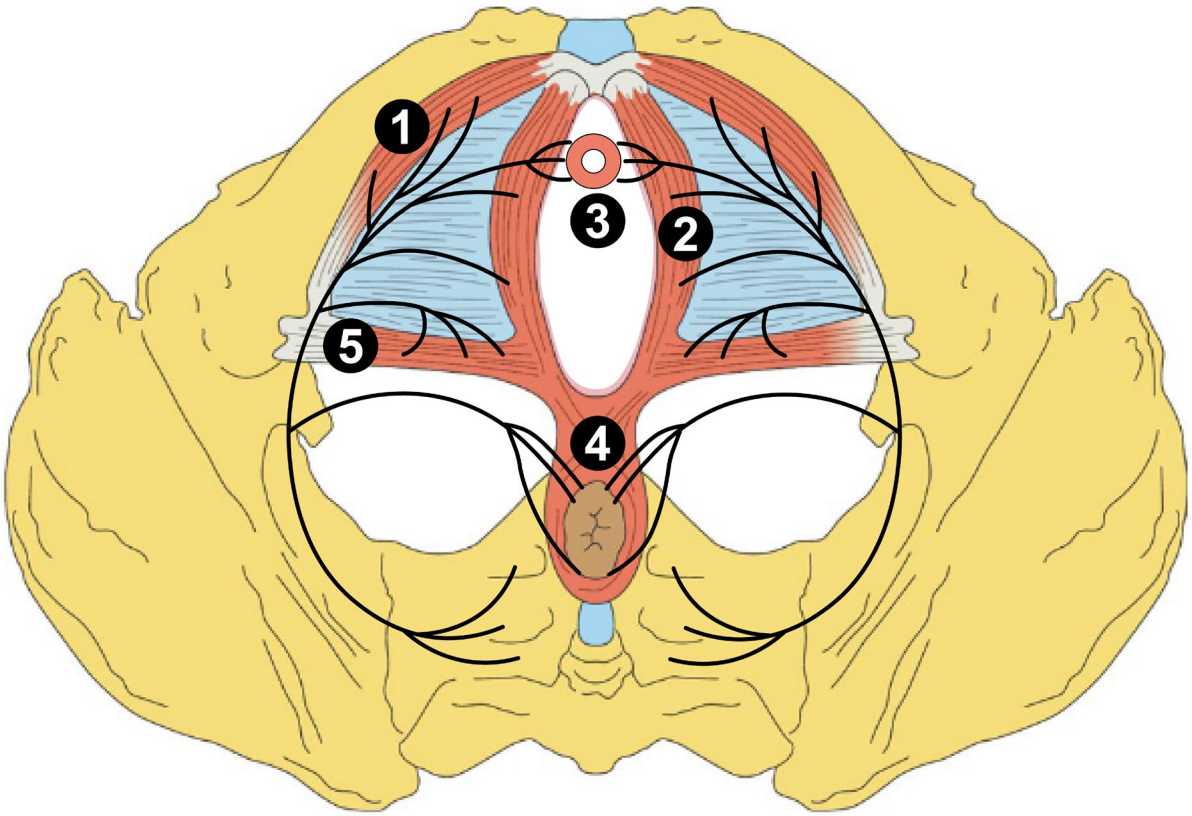


Figure 1-2: Innervation of pelvic floor muscles by the pudendal nerve in a female pelvis. (1) ischioscavernosus muscle, (2) bulbocavernosus muscle, (3) external urethral sphincter, (4) external anal sphincter, (5) superficial transverse perineal muscle. Adapted from de Pavia et al. 2024[27].

1.2 Pelvic Floor Innervation

1.2.1 The Pudendal Nerve

The pudendal nerve is a somatic mixed nerve that provides sensory and motor innervation to the external urethra sphincter, external anal sphincter, genitals, and perineurium[19,28]. Innervation

of these targets by the pudendal nerve is depicted in Figure 1-1 and Figure 1-2. The pudendal nerve is most commonly derived from the S2, S3, and S4 sacral roots. Recent studies have shown that the pudendal nerve can also originate from the L4 to the S5 roots[19]. The sacral roots combine to create a singular pudendal nerve trunk, although multiple trunk configurations are also common, which enters the pelvis through the lesser sciatic foramen and Alcock's canal[19]. From here the pudendal nerve branches to create the inferior rectal nerve, dorsal genital nerve, and perineal nerve, however there is considerable variation in way that the pudendal nerve branches diverge from the main trunk[19,28,29]. These distal branches of the pudendal nerve are represented in the main trunk of the pudendal nerve as individual fascicles or groups of fascicles[30]. The inferior rectal nerve innervates the external anal sphincter and levator ani[31]. The external anal sphincter lies at the end of the anal canal and is consciously controlled for defecation[2,32]. The dorsal genital nerve innervates the penis and clitoris in men and women respectively[33], sending afferent signals to the spinal cord and brain. The perineal nerve provides efferent motor innervation to the external urethral sphincter, bulbocavernosus muscle, and ischiocavernosus muscle. Pudendal nerve innervation of pelvic floor muscles is illustrated in Figure 1-2. The perineal nerve also provides afferent sensory innervation of the perineum and the urethra[29,34]. In women it innervates the labia majora and in men it innervates the posterior surface of the scrotum[29,34].

1.2.2 The Pelvic Nerve and the Hypogastric Nerve

The pelvic and hypogastric nerves are responsible for autonomic regulation of the bladder and urethra in addition to other pelvic targets[16,33]. Pelvic nerve afferent fibers reside in layers of the bladder wall and respond to stretching, which occurs during bladder filling, and irritation, which can be caused by infection[16]. When signals are sent from the brain to the bladder during voluntary initiation of micturition, parasympathetic fibers in the pelvic nerve produce bladder contractions in the bladder smooth muscle[16]. The hypogastric nerve is comprised of sympathetic fibers that originate in the T11 through S2 spinal cord segments and innervates the bladder and the urethra[16]. To promote continence, the hypogastric nerve relaxes the bladder smooth muscle and contracts the urethral smooth muscle[16]. Lower urinary tract innervation by the pudendal, hypogastric, and pelvic nerves is illustrated in Figure 1-3.

1.3 Neural Control of Bladder State

The lower urinary tract has two functions: urine storage and urine elimination[16,35]. Achieving both requires the coordination of the bladder, urethral sphincters, and the nerves that control them[16]. The bladder stretches as it fills and stretch-sensitive neurons relay stretch information to the central nervous system, via the pelvic nerve [16,35]. To maintain continence, spinal reflex circuits prevent the contraction of the detrusor and promote the contraction of the internal urethral sphincter, through the sympathetic nervous system and hypogastric nerve[16]. The external urethral sphincter also contributes to continence. The guarding reflex automatically contracts the external urethral sphincter in response to increased bladder pressures, thereby preventing urine leakage[36]. The external urethral sphincter can also be consciously contracted to help maintain continence. Conscious contraction of the external urethral sphincter may also suppress parasympathetic signals that promote bladder contraction[35].

When there is a conscious decision to urinate, it is important that the urethra and bladder work in unison. The pontine micturition center sends signals that initiate bladder contraction through the pelvic nerves and parasympathetic system[16,35]. Subconscious signals cause hypogastric nerve inhibition and internal urethral sphincter relaxation while the external urethral sphincter is consciously relaxed through the pudendal nerve[16,35]. If there are no obstructions then urine should flow freely through the lower urinary tract. As urine flows through the urethra it triggers a urethra-detrusor reflex that promotes continued micturition[16,37]. Once the bladder is empty, pelvic afferent firing should be minimal and the sympathetic nervous system should cause bladder relaxation and urethra contraction[16,35].

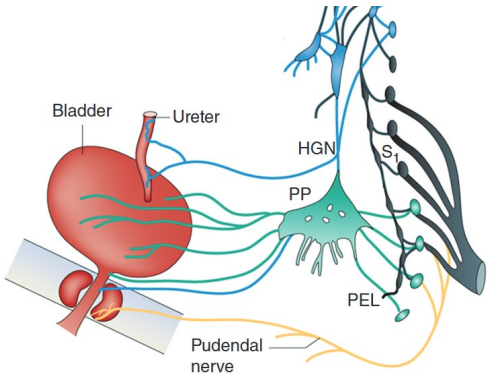


Figure 1-3: Innervation of the bladder, urethra, and external urethral sphincter by the pelvic nerve (PEL), hypogastric nerve (HGN), and pudendal nerve. The pelvic nerves are shown in green and provide parasympathetic input to the bladder wall. The hypogastric nerves are shown in blue and innervate the base of the bladder and the urethra. The pudendal nerve is shown in yellow and innervates the external urethral sphincter. The pudendal nerve generates contractions in the external urethral sphincter. The pelvic nerves generate contractions in the bladder smooth muscle. The hypogastric nerves contract urethral smooth muscle and relax bladder smooth muscle. S_1, first sacral root; PP, Pelvic plexus. Modified from de Groat et al. 2015[16].

1.4 Lower Urinary Tract Disorders & Pain

Lower urinary tract (LUT) dysfunction can lead to a variety of symptoms. Some common symptoms associated with lower urinary tract dysfunction are urinary urgency (a more intense than normal feeling to urinate), urinary frequency (needing to urinate more often), nocturia (needing to urinate multiple times throughout the night), increased post-void residual (a large amount of urine remaining in the bladder after urination is finished), and incontinence (unwanted leakage of urine). Urgency urinary incontinence is a symptom where there is involuntary loss of urine with sensations of urgency[38]. Multiple symptoms often overlap and are used to classify a particular lower urinary tract disorder or disease. Overactive bladder (OAB) is a syndrome defined as "urinary urgency, usually accompanied by frequency and nocturia, with or without urgency urinary incontinence, in the absence of urinary tract infection or other obvious pathology"[38]. Non-neurogenic chronic urinary retention is defined as "an elevated post-void residual of greater than 300 mL that has persisted for at least 6 months …"[39]. Urinary retention can be caused by bladder muscle underactivity and is sometimes referred to as underactive bladder[39]. Chronic pelvic pain is a syndrome associated with dysfunction in the pelvic region and is defined as "chronic or persistent pain perceived in structures related to the pelvis of either men or women"[6]. Chronic pelvic pain often arises in the bladder, urethra, genitalia, anal sphincter, or pudendal nerve itself[6].

Unfortunately, chronic pelvic pain, OAB, and retention can be common. One study showed that chronic pelvic pain had a prevalence of 14.8%[40]. Reported rates of OAB vary between 7% and 27% for men and 9% and 43% for women[41]. The prevalence of incontinence varies widely and differs between men and women as well. Studies report incontinence occurring in 5% to 64%[42] of women with 45% of them seeking treatment[43]. Risk factors like pregnancy and menopause[42,44] only occur in women and can partially explain the difference in prevalence rates between women and men. Men are half as likely to seek treatment and report lower rates of bothersome incontinence[43,45]. While OAB is more common in women, urinary retention is more common in men. In one study of individuals over 60, 22.1% of men and only 10.8% of women had issues with bladder emptying[46]. While both men and women face decreased bladder contractility with age, enlarged prostates in older men can increase urethra resistance and worsen retention symptoms[46]. Neurological disorders like multiple sclerosis, Parkinson's disease, and spinal cord injury can also lead to lower urinary tract dysfunction[47,48]. This dissertation focuses on non-neurogenic lower

urinary tract dysfunction, but the therapies presented may be applicable to neurogenic dysfunction as well.

1.5 Treatments for LUT Dysfunction and Pelvic Pain

There are a wide variety of treatment options for lower urinary tract dysfunction and pelvic pain. Treatment options are similar across lower urinary tract disorders and are presented by level of invasiveness[41,49]. The least invasive therapies focus on quality-of-life improvements through lifestyle changes and behavioral management. This can involve actions like wearing absorbent undergarments to reduce discomfort associated with incontinence, managing fluid intake to prevent urgency or incontinence, or improving diabetes management to improve comorbidities[49,50]. Non-invasive therapies improve the function of muscle and nerves already in the body through physical therapy[6], dedicated muscle training[50], and transcutaneous tibial nerve stimulation[6,41,50]. There are a wide range of pharmacologic therapies to treat OAB, incontinence, retention, and pelvic pain [6,39,41,49,50].

Minimally invasive therapies are procedural or clinical but with a low risk of adverse events[41]. Injection of botulinum toxin type A into the detrusor has been an effective treatment for overactive bladder and pelvic pain from pudendal neuralgia. Unfortunately, the benefits of botulinum injection fade over time, requiring re-injections at regular intervals[41,51–54]. Percutaneous tibial nerve stimulation (PTNS) is a treatment option for OAB where a needle is placed near the ankle and connected to an external neurostimulator to stimulate the tibial nerve. PTNS uses a dosing of roughly 30 minutes once a week for 12 weeks followed by regular maintenance sessions every 2-3 weeks[41,55]. Botulinum injections and PTNS are clinical procedures that require continual follow-up. Sacral and pudendal neuromodulation are surgical procedures that require device implantation but do not require frequent clinical visits afterwards. Sacral neuromodulation is a minimally invasive treatment option for OAB, retention, urge incontinence, and chronic pelvic pain[6,49,50,56]. A quadripolar lead electrode is placed in the S3 sacral foramen and connected to an implantable pulse generator to continuously stimulate the sacral nerve and improve symptoms[57].

Invasive therapies carry higher risk of adverse effects and are therefore only recommended when other treatment options are ineffective and individuals have a large reduction in quality of life because of their bladder symptoms[41]. Due to the risks associated with invasive therapies, additional minimally invasive treatment options can provide substantial patient benefit. Over the past 20 years, pudendal neuromodulation has emerged as a minimally invasive treatment option

for OAB and pelvic pain[10,11,58]. Recent guidelines for overactive bladder emphasize treatment option choice based on clinician and patient judgement[41]. This may result in more people trying minimally invasive therapies and increase the overall benefit from pudendal neuromodulation.

1.6 Pudendal Neuromodulation

In pudendal neuromodulation, an electrode is placed along the pudendal nerve to electrically stimulate the nerve and provide symptom relief[59]. A quadripolar tined lead, the same lead used in sacral neuromodulation, is placed next to the pudendal nerve using fluoroscopy and visual landmarks[11,59]. Each contact on the lead is stimulated and if an external anal sphincter contraction occurs at a low level for multiple electrodes, then the lead location is finalized[11]. Anal sphincter contraction is verified by observing a compound muscle action potential from the anal sphincter EMG[59]. The lead is then connected to an external pulse generator[11]. If patient symptoms improve by at least 50% over the following two weeks, then the lead is connected to an implantable pulse generator in a second surgical procedure, mirroring what is done in sacral neuromodulation[11].

The mechanism of action by which pudendal neuromodulation improves overactive bladder symptoms is not fully understood. It is thought to work by stimulating pudendal afferent pathways that inhibit the micturition reflex and reduce sensory signals sent to the brain[11,60–62]. Additional research suggests that pudendal neuromodulation can improve pelvic pain symptoms, like bladder hypersensitivity, by inhibiting sensory signals[63]. One 2005 cross-over study showed a patient preference for pudendal neuromodulation over sacral neuromodulation for voiding dysfunction[10], but no other studies have been done to corroborate this comparison. A possible explanation is that pudendal neuromodulation allows access to 100% of pudendal afferent fibers. Sacral neuromodulation can only activate a single sacral root, which contains approximately 60% of pudendal afferent fibers[64]. Activating more pudendal afferent fibers may improve symptom relief.

As mentioned earlier, the electrode used in pudendal neuromodulation for the past 20 years was designed for sacral neuromodulation[65]. The pudendal canal is surrounded by soft tissue while the sacral foramen is surrounded by the sacrum. The soft tissue environment of the pudendal canal may result in movement of the current lead design and a subsequent reduction in implant performance[66]. An alternate lead designed for pudendal neuromodulation could improve activation of pudendal afferent fibers and reduce lead movement. Despite 20 years of clinical use, clinical research into pudendal neuromodulation has been limited. As a result, there is still a poor

understanding of the effects of pudendal neuromodulation on the pelvic floor and urinary tract in humans. Recent advancements in sacral neuromodulation technologies have led to more clinical research[67,68]. This is not the case in pudendal neuromodulation. Most of the recent research on pudendal neuromodulation mechanisms comes from preclinical and computational models.

1.7 Animal and Computational Models

Much of our current understanding of the neural mechanisms involved in micturition comes from rodent, canine, and feline research[69–72]. Research in felines showed that stimulation of pudendal afferent fibers can evoke changes in bladder state, like bladder contractions[13,14,73]. In humans, pudendal stimulation evoked bladder contractions have been observed, but only in individuals with spinal cord injury[74–76]. High stimulation amplitudes, multiple times the magnitude required for anal sphincter contractions, are necessary to activate the afferent fibers that evoke bladder contractions[13,77]. The quadripolar lead cannot precisely control where stimulation is delivered. Off-target stimulation can result in the activation of off-target fibers and sensations of pain and discomfort. Ideally the pudendal neuromodulation electrode would be able to selectively activate only the afferent fibers that evoke bladder contractions, if that is the therapeutic goal. If bladder contractions could be evoked without pain or discomfort, more people could benefit from pudendal neuromodulation.

Mathematical models of neurons have been available for 70 years, enabling the prediction of neural responses before physical experimentation[78]. Recent advances in computational power and finite element modeling allow for the calculation of extracellular potentials in realistic 3D geometries[79]. When biophysical neuron models are combined with these extracellular potentials it allows for computational estimations of neural responses that are comparable to *in-vivo* experiments[79]. These combined computational models have been used to study the performance of a wide variety of electrode designs for multiple nerves[80–83]. Relevant to this dissertation, computational models have simulated pudendal nerve activation with multicontact nerve cuffs[12,84,85]. Multicontact nerve cuffs have been used to selectively activate fascicles in several different nerves[86–89]. Studies have shown that multicontact nerve cuffs can selectively activate pudendal fascicles as well[12,84,90].

Computational models need to be initialized with biologically relevant data to provide useful results. The pudendal nerve contains sensory and mixed fascicles which have different distributions of fiber diameters[91]. While these distributions have been observed in felines[91], they

are currently unknown in humans. Previous computational models of the pudendal nerve have not included realistic distributions of fiber dimeters for sensory and mixed fascicles[12,84,85]. This is an issue because a fiber's diameter is related to its function and activation threshold[92]. For computational models to give accurate predictions of fascicular selectivity, accurate fiber diameters need to be included.

1.8 Dissertation Summary

While pudendal neuromodulation has been in use in humans for many years, its effects on human physiology has been poorly characterized. There remain open questions on the feasibility of selective pudendal nerve activation with the underlying organization of pudendal nerve fibers. The goals of this dissertation are to characterize the effects of clinical pudendal nerve stimulation on the lower urinary tract, and use computational modeling methods, that incorporate realistic fiber diameters, to evaluate selective pudendal nerve activation with a multicontact cuff.

For the first two aims of my dissertation, I conducted clinical research investigating the effect of pudendal nerve stimulation on the pelvic floor and lower urinary tract in humans. In Chapter 2, I investigated the benefit of the stimulation pulse width currently used in pudendal neuromodulation and show that anal sphincter EMG can be used to infer electrode-to-nerve distances. In Chapter 3, I show that pudendal neuromodulation can cause observable increases in urethra pressure in humans at tolerable stimulation amplitudes. Additionally, I demonstrate the first reported example of pudendal stimulation evoked bladder contractions in an awake non-spinal cord injured individual. In Chapter 4, I evaluate the performance of a novel nerve cuff design with a computational model that incorporates realistic distributions of fiber diameters. I show that a multicontact nerve cuff placed on the feline pudendal nerve could selectively activate a small set of afferent fibers. However, achieving greater selectivity, which might be required to evoke bladder contractions without off target effects, will require design changes.

Overall, this thesis improves our understanding of the effects of pudendal neuromodulation and highlights areas to improve in its current and future application.

Chapter 2 Factors Affecting Anal Sphincter Recruitment During Intraoperative Pudendal Nerve Stimulation: An Observational Study

(Previously published in the International Urogynecology Journal, August 2025)[93]

2.1 Abstract

Introduction and Hypothesis:

The relationship between pudendal neuromodulation and patient factors is not well understood. This observational study aimed to identify and quantify physiological, demographic, and stimulation factors that significantly affect external anal sphincter (EAS) recruitment and outcomes in participants receiving pudendal neuromodulation for treatment of lower urinary tract symptoms and pelvic pain.

Methods:

Participants (N=16) provided demographic and diagnostic information upon entry to this observational study. EAS activation at different stimulation amplitudes and pulse widths was recorded during lead implantation. Magnetic resonance imaging and computed tomography were used to determine the distance of the electrodes on the implanted lead from the nerve. Linear mixed modeling was used to quantify the impact of each variable on EAS recruitment.

Results:

Participant sex, age, and body-mass index did not significantly affect EAS recruitment. Participant diagnoses had significant relationships to EAS recruitment, likely due to unbalanced group sizes. A pulse width of 210 μs required less current than 60 μs ($p = 0.005$) and less charge than 450 μs ($p = 0.02$) to activate the EAS. Increased electrode-to-nerve distance decreased the magnitude of the EAS response ($p = 0.0011$), increased the EAS activation threshold ($p < 0.001$), and was related to reduced bladder symptom improvements.

Conclusions:

Of the three tested pulse widths, 210 μs best balances current and charge for EAS recruitment. Minimizing the distance between the electrode and pudendal nerve should be a

priority during lead implantation. External sphincter activation threshold and response magnitude could be useful clinical indicators of electrode-to-nerve distance.

2.2 Introduction

Chronic pelvic pain and lower urinary tract disorders (LUTD) affect millions of people in the United States[11,94]. These conditions result in diminished physical health, mental health, and productivity[95–97] placing a large and growing burden on the healthcare system[98]. Therapy options for chronic pelvic pain and LUTD are typically grouped on their level of invasiveness including non-invasive, pharmacologic, and minimally invasive therapies like botulinum toxin injections and sacral neuromodulation[41].

When patients fail to respond to traditional therapies they are left with few options. Pudendal nerve stimulation has emerged as a minimally invasive off-label therapy for pelvic pain and LUTD, successfully improving symptoms even in people who previously failed sacral neuromodulation[9,99]. While pudendal neuromodulation most often improves symptoms, outcomes can vary and not all patients gain complete relief[100–103]. These differences in outcomes could be due to differences in patient anatomy, altered LUT function due to their symptom etiology, or treatment factors like the distance between the electrode and nerve. Aging can change nerve function[104] and therefore effectiveness at tolerable stimulation amplitudes, while body composition may affect the electrode-to-nerve distance and thus nerve recruitment with electrical stimulation. Insights into the factors which have the largest effect on nerve activation and treatment outcomes may further improve pudendal neuromodulation outcomes.

Typically, the neurostimulator implant procedure involves two surgical stages. In the stage-1 implant surgery, the stimulation lead is placed near the main trunk of the pudendal nerve and the pulse generator is placed in a later stage-2 implant surgery. Anal sphincter recruitment in response to pudendal stimulation during the stage-1 surgery is a key indicator that the lead is correctly positioned and recruiting fibers in the main trunk of the pudendal nerve[10]. However, to our knowledge, no previous study has investigated what factors influence recruitment of the anal sphincter. Our primary objective was to determine which stimulation parameters and physiological factors have a significant impact on the recruitment of the inferior rectal branch of the pudendal nerve during pudendal nerve stimulation. Our primary hypotheses were that smaller electrode-to-nerve distances, longer stimulation pulse widths, and larger stimulation amplitudes would increase pudendal nerve recruitment, as observed via anal sphincter activity. We also hypothesized that

smaller electrode-to-nerve distances and longer stimulation pulse widths would reduce nerve activation thresholds. Finally, we hypothesized that participant demographics and lower urinary tract symptoms would not be significantly related to nerve recruitment or thresholds.

2.3 Materials and Methods

Approval for this observational study was obtained from the Institutional Review Board (HUM00165005). This study was registered on ClinicalTrials.gov (NCT04236596) before commencement of study procedures. This was a single center study with all surgeries performed by the same physician.

We recruited patients 18 years of age or older receiving pudendal neuromodulation for the treatment of bladder dysfunction and/or pelvic pain. Individuals were excluded from the study if they were pregnant or planned to be pregnant during the study or were diagnosed with atonic bladder, neurogenic bladder, pudendal nerve damage, or other conditions affecting the neural circuits in control of micturition. Individuals were also ineligible if they were planning to become pregnant during the study, unable to provide consent, or unable to complete all study activities. Participants were recruited from September 2020 to June 2023. We targeted a sample size of 20 participants based on the expected number of pudendal implants in our clinical practice within that timeframe and similar human subject neuromodulation studies[105].

After providing informed consent, participants completed clinically validated surveys to assess bladder health (American Urological Association Symptom Index: AUASI [106] and Michigan Incontinence Symptom Index: M-ISI[107]), sexual function (Female Sexual Function Index-6: FSFI-6[108] or Sexual Health Inventory for Men: SHIM[109]), bowel function (Colorectal-Anal Distress Inventory-8: CRAD-8[110]), and pelvic pain (Female Genitourinary Pain Index: FGUPI[111] or Male Genitourinary Pain Index: MGUPI[111]). Just before or after the final post-op clinic visit participants completed the same set of surveys, and we calculated survey score changes. Participants underwent a pre-surgery pelvic magnetic resonance imaging (MRI) scan, data collection during their scheduled stage-1 implant surgery, and a pelvic computed tomography (CT) scan at least three weeks after the stage-2 surgery.

Data was collected during the stage-1 surgery, in which an Interstim (Medtronic, MN, USA) electrode lead was inserted near the pudendal nerve, as described in Peters 2013[59], using fluoroscopy and external anal sphincter (EAS) electromyography (EMG) to confirm lead position. Monopolar needle EMG electrodes (Ambu, MD, USA), were placed in the external anal sphincter

at the 3 and 9 o'clock positions. The needle electrodes were connected to a Cascade Elite (Cadwell, WA, USA) intraoperative neurophysiological monitor on which the EAS EMG data was recorded with a 333 hertz (Hz) sampling rate. The EMG data was filtered by the Cascade system with 3 kHz low pass and 10 Hz high pass filters, and a 60 Hz notch filter when 60 Hz noise was observable.

After lead placement, 10-second stimulation trials were performed in which the stimulation amplitude, pulse width (among 60, 210, and 450 μs), and electrode combinations were varied. The implanted lead had four electrodes (E0 to E3) that could be activated individually (monopolar referenced to a surface electrode on the ankle) or used in any bipolar combination once the external pulse generator was connected. Stimulation was performed at either 3 Hz for monopolar stimulation or 3.1 Hz for multipolar stimulation. For each electrode and pulse width combination, threshold amplitude was defined as the lowest stimulation amplitude that elicited an EAS contraction. Stimulation trials were performed at and above the threshold amplitude to a maximum of 5.5 mA. Charge per pulse was calculated by multiplying the applied current by the pulse width for a given trial.

We used volumetric imaging from both the pre-surgery MRI (3T T2 weighted pelvis scan; Ingenia 3T system, Philips, Amsterdam, the Netherlands) and post-surgery helical CT scans (L4 vertebra to the proximal femur shaft with a slice thickness of 0.625 mm; Discover CT750 HD or Revolution scanner, GE Healthcare, IL, USA) together to create patient-specific models of the pelvic anatomy. We used Mimics Research (v25.0; Materialise, Leuven, Belgium) and the Vascular Modeling Toolkit (v1.4.0; http://www.vmtk.org/) to identify and segment the pudendal nerve in the MRI scans and to identify and segment the implanted lead artifacts in the CT scan. We then used Mimics Research to co-register surface segmentations derived from the MRI and CT scans and to position the lead and nerve within the pelvis. We recreated the lead geometry from the CT artifacts using the geometry functions of COMSOL Multiphysics (v 5.6; COMSOL, Stockholm, Sweden). To measure the electrode-to-nerve distance we calculated the center-to-center distances between each electrode on the implanted lead and the closest point on the pudendal nerve, in Python (v3.7.0), using their recorded positions from the CT and MRI scans respectively. We did not blind participant study identifiers or sex during image analysis, however researchers performing segmentation were unaware of the intraoperative data collection outcomes for each participant.

For each stimulation trial, we calculated the average area under the curve (AUC) of the rectified EAS EMG for five stimulation events using MATLAB (v2021a, MathWorks, Natick, Massachusetts, USA). This value was used to quantify the magnitude of the anal sphincter contraction, as done previously[112–114]. The AUC calculation interval started 10 milliseconds after the stimulation artifact onset and continued for 100 milliseconds. This process is visually summarized in Supplemental Figure 2-5.

We performed all statistical analysis with R Statistical Software (v4.4.1; R Core Team 2024). We used a Shapiro-Wilk test to check for normality of each data set. A Kruskal-Wallis test was used to determine if groups had equal medians followed by a pairwise Mann-Whitney U test with a Bonferroni correction to determine statistically significant differences between groups. Where relevant, values are given for the median and interquartile range (IQR) or average and standard deviation. A significance level of $\alpha = 0.05$ was used. We used linear mixed models to estimate the EAS AUC and the threshold current based on participant age, sex, body mass index (BMI), lower urinary tract symptoms (overactive bladder (OAB), urinary retention, urinary incontinence, and pelvic pain), and stimulation parameters (stimulation amplitude, pulse width, electrode-to-nerve distance). We only included participants who had a lead migration distance of 5 mm or less in models incorporating electrode-to-nerve distance data, based on a comparison of each participant's stage-1 fluoroscopy images and CT images. We chose this distance because adjacent electrodes on the lead are roughly 5 mm apart. We used the R packages *lme4* and *lmerTest* to calculate the linear mixed model parameters. In the model, pulse width is a 3-level categorical variable with a 60 μs pulse width used as the baseline condition. Nerve-to-electrode distance, stimulation amplitude, age, and BMI were used as continuous variables with all other variables included as yes/no categorical variables. We used ANOVA to compare models and determine which fixed effects to include. Participants were classified as having OAB, retention, incontinence, or pelvic pain based on the diagnoses given by their examining urologist. Diagnoses of urgency urinary incontinence, stress urinary incontinence, or mixed urinary incontinence were all classified as incontinence. Diagnoses of pelvic pain, pudendal neuralgia, vulvodynia, and interstitial cystitis were all classified as pelvic pain in the statistical analysis.

2.4 Results

Of the 23 participants eligible for study inclusion, seven did not complete intraoperative data collection for a variety of reasons including: improvement of symptoms, insurance denial or

delay, unsuccessful device implantation, inability to record data due to COVID restriction, indefinite surgical postponement, or non-signature of consent form and were not included in this analysis. We did not observe a relationship between these factors and patient demographics or collected data. Patient information for the sixteen included participants is summarized in Table 2-1. One female participant had their implanted lead removed and was reenrolled.

Table 2-1 Summary of participant characteristics

Variable	Count
Sex	
Female	13
Male	3
Diagnosed Condition	
Overactive Bladder	12
Retention	5
Incontinence	7
Pelvic Pain	12
Age (years), mean (standard deviation)	55.9 (10.8)
BMI (kg/m^2), mean (standard deviation)	28.4 (3.8)

BMI body mass index

The monopolar EAS threshold current for 210 and 450 μs pulse widths were not normally distributed ($p < 0.01$) and had a median of 1.90 (IQR = 1.2), 0.75 (IQR = 0.45), and 0.55 (IQR = 0.45) mA for a pulse width of 60, 210, and 450 μs, respectively. The three pulse widths had significantly different ($p = 0.001$) median threshold levels, with the threshold current level at 60-μs significantly higher than 210 μs ($p = 0.005$) and 450 μs ($p = 0.004$) (Figure 2-1A). Similarly, the charge per pulse at EAS threshold was not normally distributed ($p < 0.001$). The median charge required for 60, 210, and 450 μs pulse widths was 114.0 (IQR = 72.0), 157.5 (IQR = 94.5), and 247.5 (IQR = 202.5) nC, respectively. These three groups did not have the same median ($p = 0.001$). There was a significant difference between the median charge required at anal sphincter threshold for 450 and 210 μs pulse widths ($p = 0.02$) and 450 and 60 μs pulse widths ($p = 0.004$) (Figure 2-1B). Supplemental Figure 2-6 provides individual participant monopolar threshold current and charge levels for each tested pulse width. In this figure it is shown that at a 210 μs

pulse width, 15 of 16 participants had EAS activation below 2 mA. There was not a significant difference between monopolar and bipolar thresholds (p = 0.98) (Supplemental Figure 2-7).

Table 2-2 Linear mixed model estimating anal sphincter activation:

Fixed Effect	Coefficient Estimate	Standard Error	95% Confidence Interval	p value
Intercept	2.73	0.69	(1.38, 4.08)	4.67e-4
Current	0.79	0.10	(0.60, 0.98)	1.5e-14
Pulse Width 210 µs	1.91	0.35	(1.23, 2.61)	8.27e-8
Pulse Width 450 µs	2.38	0.39	(1.60, 3.15)	4.22e-9
OAB yes	-2.79	0.58	(-3.91, -1.66)	2.66e-4
Retention yes	-2.28	0.56	(-3.39, -1.17)	8.94e-4

Summary of the significant fixed effects for the linear mixed model estimating EAS AUC (µV*s). The data includes all monopolar trials (N=16). A representative equation for the corresponding linear mixed model is shown in Supplemental Equation S1.
OAB overactive bladder

EAS external anal sphincter

AUC area under the curve

In a linear mixed model incorporating all monopolar trials, the estimated AUC was significantly impacted by stimulation current, stimulation pulse width, and diagnosis of OAB or urinary retention. The model coefficient estimate for each statistically significant fixed effect is given in Table 2-2. The equation used to generate the estimates is given in Supplemental Equation 2-1. Patient demographic data (BMI, age, or sex) did not have a significant fixed effect. The relationship between EAS response and applied current across pulse widths and diagnoses can be seen in Figure 2-2. The EAS AUC for each observed trial is shown in Supplemental Figure 2-8, segmented by each diagnosed condition, highlighting the overlap between OAB and retention diagnoses. Overall, we included 343 monopolar trials across sixteen participants in this model.

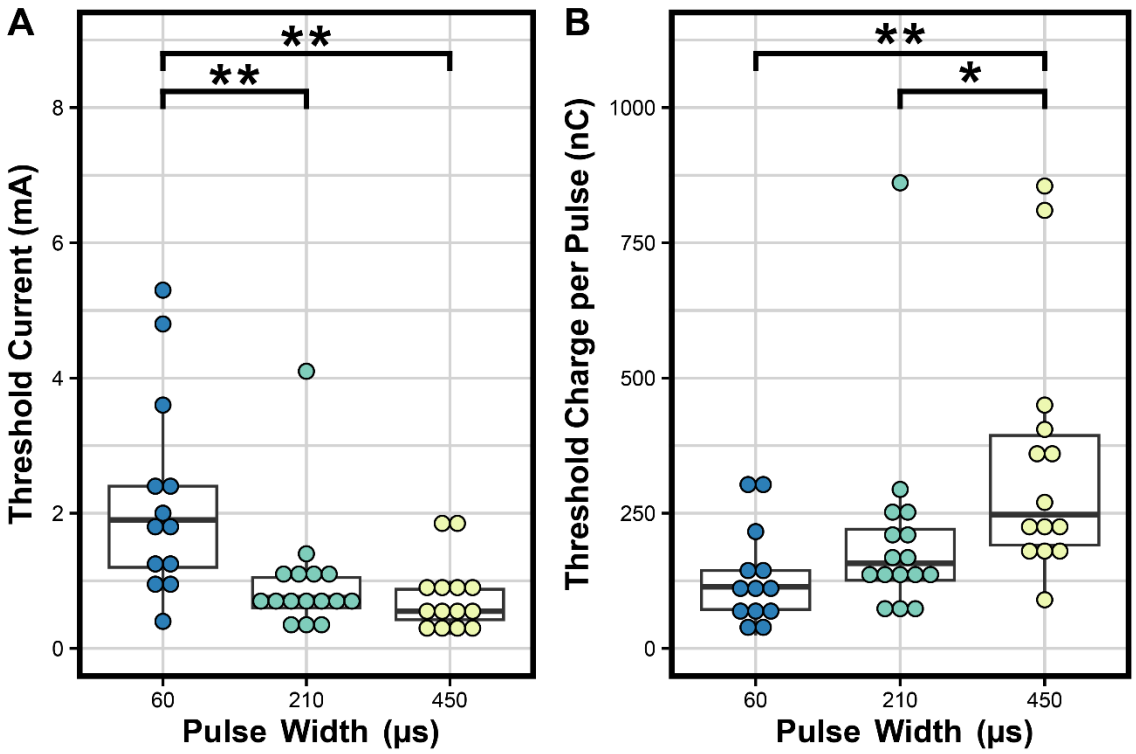


Figure 2-1: Characterization of external anal sphincter EMG activation by intraoperative monopolar pudendal nerve stimulation. Each dot represents the minimum threshold across all electrodes for an individual participant at a given pulse width. A) The threshold current required to activate the EAS for the tested pulse widths of 60, 210, and 450 µs. B) The charge per pulse at the EAS activating threshold current depending on pulse width. Box plots represent the IQR for the height of each box, with the bold central line indicating the median. Tips of whiskers extend to the value(s) within 1.5 x IQR of each box side. * indicates $p < 0.05$, ** indicates $p < 0.01$.

Eleven study participants (all female) had fluoroscopy and CT images that allowed for identifying lead migration distances. Five participants (all female) had a lead migration distance less than 5 mm, and their corresponding electrode-to-nerve distances are shown in Figure 2-3. We created two linear mixed models to investigate the impact of stimulation parameters on EAS AUC and EAS threshold for participants with valid electrode-to-nerve distances. The coefficient estimates for the fixed effect of applied current, pulse width, and electrode-to-nerve distance on EAS AUC were all statistically significant and are shown in Supplemental Table 2-3. Additionally, when controlling for other variables, each millimeter between the nerve and electrode decreased the expected EAS AUC by 0.27 µV*s (95% confidence interval [CI] = -0.41 to -0.13; p = 0.0011). A second mixed model showed that electrode-to-nerve distance and pulse width both significantly affect EAS threshold (Supplemental Table 2-4). Each millimeter between the nerve and electrode increased the expected threshold by 0.22 mA (95% CI = 0.15 to 0.29; p = 2.7e-7). We performed

linear regressions between the average electrode-to-nerve distance and change in each survey score. There was a significant relationship ($p = 0.049$) between AUASI score change and average electrode-to-nerve distance, indicating greater bladder symptom improvement with reduced electrode-to-nerve distance, but not with any other survey score change (Figure 2-4).

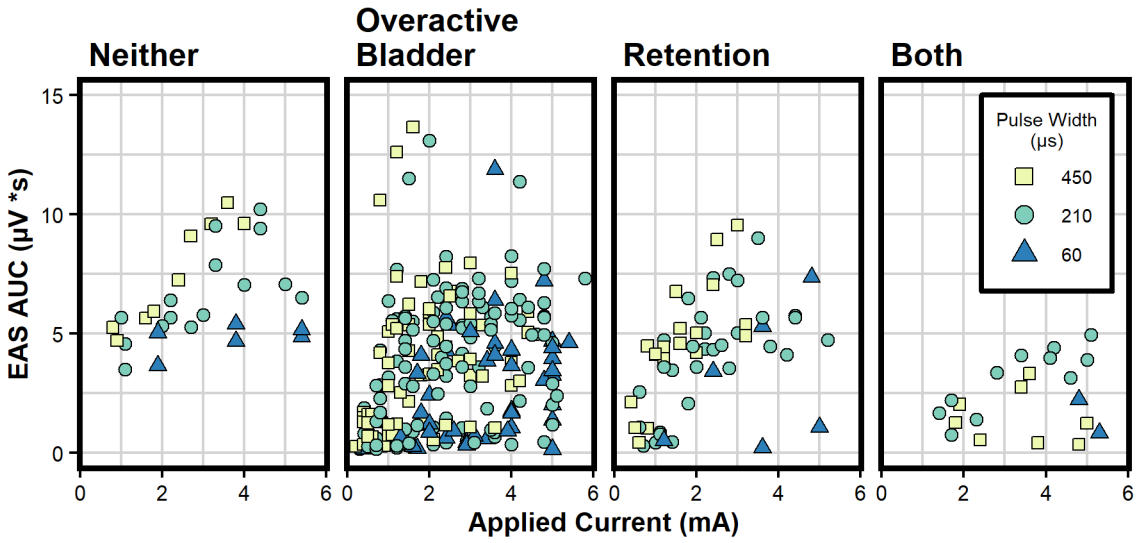


Figure 2-2: Anal sphincter response magnitude plotted against applied current for all monopolar trials across all participants. Data is separated by participant diagnosis of overactive bladder and/or urinary retention. Each trial was performed with a pulse width of 60, 210, or 450 μs and is labeled according to the legend.

2.5 Discussion

In this observational study, we examined the influence of key patient data and stimulation parameters on pudendal nerve recruitment. To our knowledge, this is the first study which investigates these relationships in human subjects.

A pulse width of 210 μs is the current standard of care for pudendal neuromodulation[115] but there is little documentation supporting this choice, particularly in human subjects. We show that when compared to 60 μs and 450 μs, a pulse width of 210 μs balances the minimum required current (Figure 2-1A) and charge (Figure 2-1B) and therefore requires less energy to recruit the pudendal nerve. These results agree with the findings of an earlier study[116] that showed a pulse width of 200 μs minimizes the energy required to activate afferent fibers of the pudendal nerve and align with the most commonly used sacral neuromodulation pulse width of 210 μs[117]

supporting the continued use of common sacral neuromodulation stimulation pulse widths in pudendal neuromodulation. Thus, our findings confirm that pulse width does not need to be adjusted for pudendal nerve stimulation, and clinicians can focus on amplitude and frequency when determining stimulation parameters.

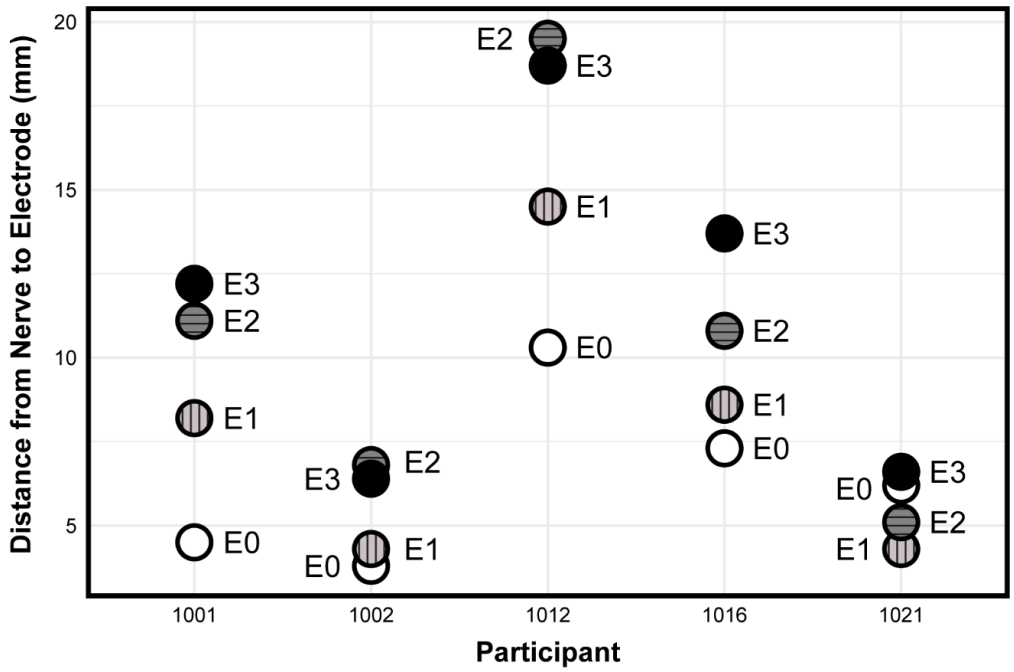


Figure 2-3: Measured distances (in millimeters) between each electrode on the implanted quadripolar lead and the closest point of the pudendal nerve for the five participants with minimal lead migration (<5 mm). Electrodes are labeled from E0 to E3 with E0 representing the electrode most distal to the implantable pulse generator to E3 representing the electrode most proximal to the implanted pulse generator.

We estimated the relationship between EAS activation and age, BMI, and LUTD diagnosis with a linear mixed model. Age, sex, BMI and diagnosis of incontinence or pelvic pain did not significantly affect anal sphincter recruitment. However, diagnosis of OAB or retention significantly reduced the EAS activation based on 95% confidence interval testing (Table 2-2). Participants with diagnoses of OAB or retention had lower EAS activation across all applied currents (Figure 2-2). If true, these results would suggest that people with these diagnoses might require more current than is typical to activate the EAS and recruit the pudendal nerve. However, it is important to note that there was an unbalanced distribution of diagnoses in our study population and diagnoses of neither OAB nor retention (n=2) or both OAB and retention (n=1) were rare. This limited the amount of data collected for these cases, shown in Supplemental Figure

2-8, and implies that the effect of certain diagnoses was mainly dependent on a few participants, limiting the generalizability of our results. Also, the model coefficient estimates for OAB and retention had large errors of 0.58 and 0.57, respectively, showing that the strength of the effect varied across participants. The model also showed that pulse width and current significantly impact EAS recruitment (Table 2-2). We saw that larger electrode-to-nerve distances were significantly related to reductions in the magnitude of the EAS response and increases in the current required to activate the EAS at threshold, as is shown in Supplemental Tables 2-3 and 2-4 and aligning with bioelectric principles. Therefore, examining changes in the EAS EMG AUC and EAS activation thresholds during intraoperative stimulation could inform estimates of the relative electrode-to-nerve distance and help clinicians optimize lead placement.

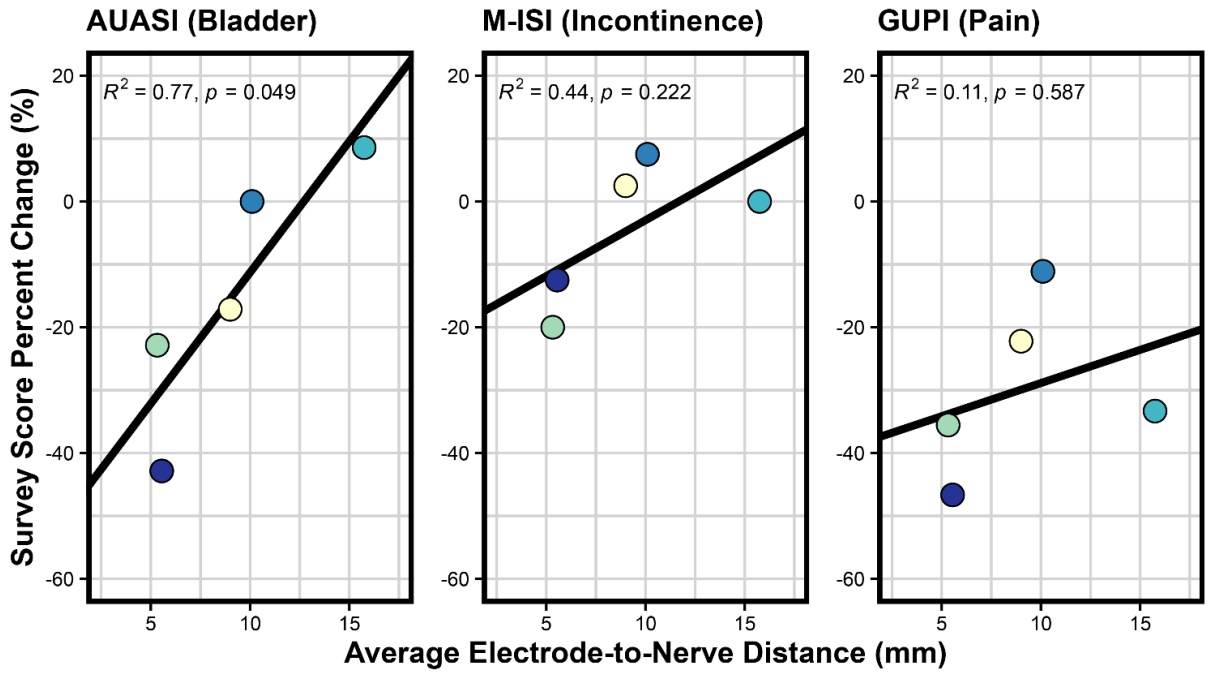


Figure 2-4: Linear regression fits between each participant's average electrode-to-nerve distance and symptomatic survey score percent change before and after receiving pudendal neuromodulation treatment. Surveys on asymptomatic functions (CRAD-8 (Bowel), FSFI (Female sexual function)) did not have relationships to electrode-to-nerve distance (p = 0.606, 0.706, respectively).

We observed a significant relationship between electrode-to-nerve distance and AUASI scores (Figure 2-4), with improved bladder outcomes when the distance was minimized. We also observed that six of eleven participants had lead migration larger than 5 mm between the stage-1

implant surgery and CT imaging. Examination of lead migration was not a primary goal of this study; however, it is not commonly reported in the literature. Future studies should specifically investigate whether lead migration has a significant relationship with the outcomes or changes in pelvic floor recruitment.

Generally, the goal when implanting a pudendal stimulation lead is to activate the anal sphincter with a current below 2 mA[118] with at least three electrodes[119]. In this study, 94% of participants had EAS activation below 2 mA with a 210 μs pulse width (Supplemental Figure 2-6). While lead implantation at the pudendal nerve is a challenging procedure, these results show that pudendal nerve stimulation can consistently activate the EAS at low current when the lead is placed by an experienced surgeon. During the implant surgery, monopolar stimulation is used to locate the nerve and adjust the position of the foramen needle or lead. However, most pudendal neuromodulation patients use bipolar electrode combinations to manage their symptoms at home. In our data, we did not see a significant difference in the threshold current for monopolar trials and bipolar trials, shown in Supplemental Figure 2-7, supporting the continued use of monopolar stimulation to confirm intraoperative lead location. We provide evidence supporting the typical use of electrodes with the lowest EAS activation threshold when performing patient programming, as our results show these electrodes are likely closest to the nerve and therefore are expected to deliver the most effective therapy.

It's important to note some limitations in this study. We did not perform an a priori power analysis to support our target sample size due to a lack of relevant effect sizes and fixed capabilities in patient recruitment. However, a post hoc power analysis suggests that we had sufficient ability to detect our observed findings. We reduced the coefficient estimate of each linear mixed model fixed effect by 20%, following good principles to avoid computing the observed power[120] and taking a more conservative approach than a 15% reduction used previously[121], and obtained a power of over 90% for each variable in the model that included 16 participants with the simr package in R[122]. The linear mixed model that related electrode-to-nerve distance to AUC magnitude obtained a power of 84.8% with 5 participants. This analysis suggests we had an adequate sample size to detect our findings. Evoked EAS responses due to stimulation were monitored live and identified manually, leaving room for human judgement errors and misidentification of threshold current. However, as the amplitude step interval was only 0.1 mA, we expect any threshold errors were minimal. The relative depth of the EAS needles was not

tracked across procedures. In general, the surgeon seeks to place the needles as deep as possible with a consistent position on opposite sides of the sphincter, however it is possible one or both needles shifted during a surgical procedure which could affect the EMG recording. Along with a relatively small sample size, there is an unbalanced grouping in the number of participants with OAB and the gender ratio of participants with OAB, which limit the generalizability of our conclusions. Additional studies should be done with larger, balanced samples sizes and diagnoses to investigate the relationship between EAS recruitment and OAB diagnosis.

This study emphasizes the benefits of a 210 μs stimulation pulse width, as compared to 60 and 450 μs, and provides support for its continued use in pudendal neuromodulation. Pudendal nerve stimulation is effective at activating the pudendal nerve and EAS in patients with a wide range of LUT symptoms and backgrounds. Minimizing the distance between the nerve and electrode is critical for recruitment of the pudendal nerve. Our results show that readily available physiological measurements like EAS threshold and AUC magnitude may be good indicators of electrode-to-nerve distance and useful for determining when that distance is minimized. Larger distances require more current to activate the nerve and may therefore reduce the battery lifespan of implanted devices and reduce the size of the therapeutic window. Future studies can utilize the data collected in this work towards a priori sample size calculations and more comprehensive designs. Additionally, future studies can more accurately determine the relationship between electrode-to-nerve distance and observed AUC response, examine how bipolar stimulation affects pudendal nerve recruitment at different distances from the electrode to the nerve, and look deeper at how LUT dysfunction may affect recruitment of the EAS with pudendal nerve stimulation. Finally, this study supports that pudendal neuromodulation has a role in treating refractory overactive bladder and pelvic pain. The relationships observed here may be similar in sacral neuromodulation, and analogous studies with patients receiving SNM are warranted.

2.6 Acknowledgements

We thank Vanessa Pruitt and Mackenzie Moore for their contributions as study coordinators and Gaurang Shah for his help in reviewing MRI scans. We also thank Kelly Ridenour and Stephanie Jones for their EMG identification expertise in the operating room. This project was funded by an award from the National Institutes of Health SPARC program (OT2OD028191).

2.7 Supplemental Information

Supplemental Table 2-3 The significant fixed effects on EAS EMG AUC (μV*s) for a linear mixed model incorporating electrode-to-nerve distance. The data includes all monopolar trials with electrode-to-nerve distance data (N=5).

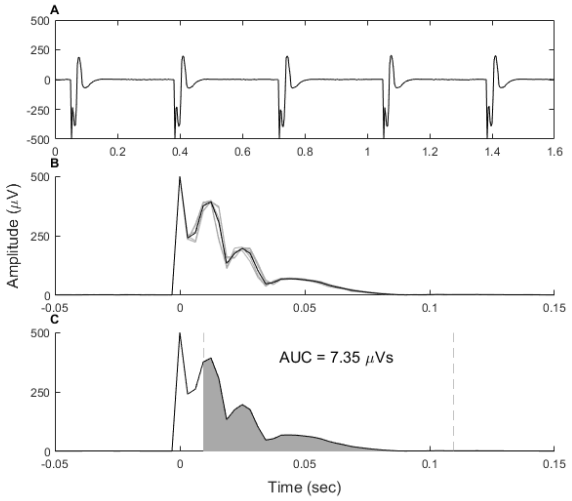
Fixed Effect	Coefficient Estimate	Standard Error	95% Confidence Interval	p-value
Intercept	0.76	0.73	(-0.68, 2.19)	0.32
Current	0.90	0.15	(0.60, 1.20)	7.3e-8
Pulse Width 210 μs	2.69	0.50	(1.71, 3.67)	5.6e-7
Pulse Width 450 μs	2.60	0.57	(1.44, 3.67)	2.2e-5
Distance	-0.27	0.07	(-0.41, -0.13)	1.1e-3

Supplemental Table 2-4 The significant fixed effects on EAS threshold (mA) for a linear mixed model incorporating electrode-to-nerve distance data. The data includes all monopolar trials with electrode-to-nerve distance data (N=5).

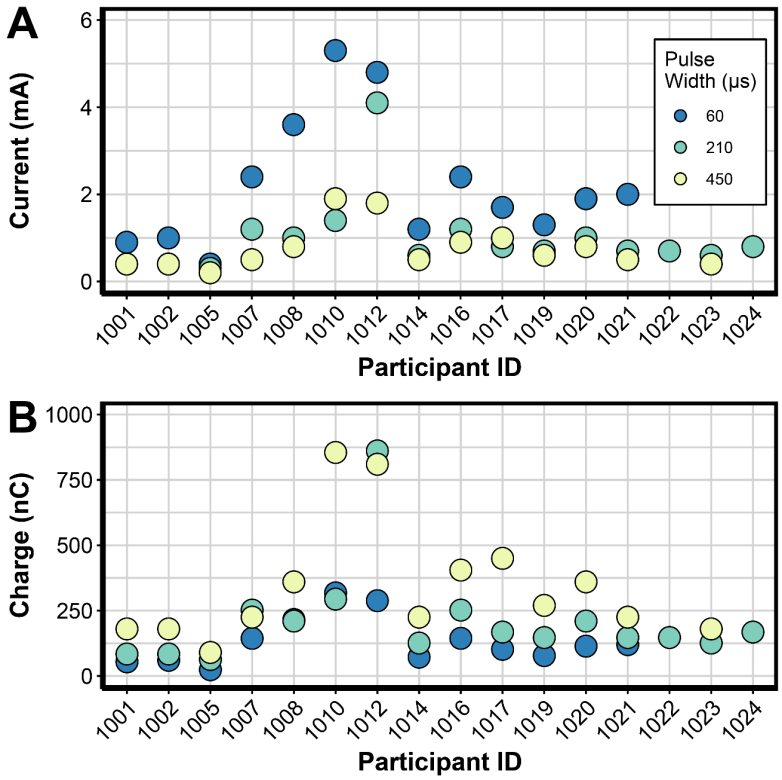
Fixed Effect	Coefficient Estimate	Standard Error	95% Confidence Interval	p-value
Intercept	0.78	0.35	(0.11, 1.46)	0.030
Pulse Width 210 μs	-0.86	0.32	(-1.49, -0.23)	0.011
Pulse Width 450 μs	-1.47	0.36	(-2.17, -0.77)	2.8e-4
Distance	0.22	0.03	(0.15, 0.29)	2.7e-7

Supplemental Equation 2-1 The equation relating the statistically significant factors in interest to the observed EAS response magnitude written in R lme4 format to generate the coefficient estimates shown in Table 2.

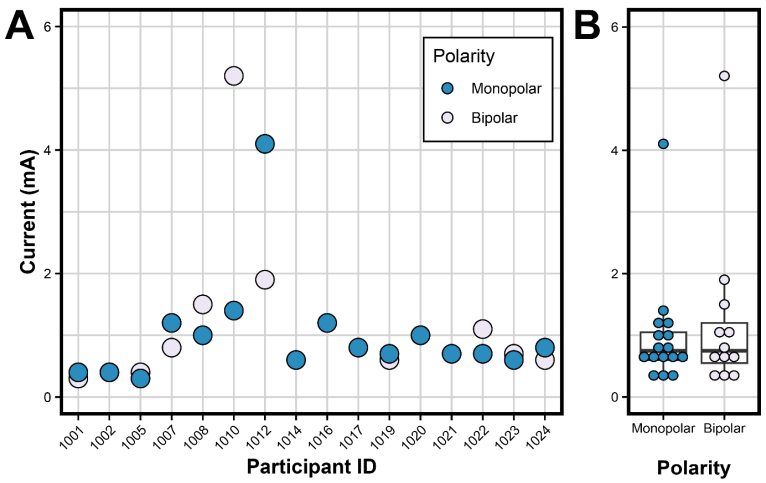
$$\boldsymbol{EAS\ AUC \sim Pulse\ Width + Current + OAB + Retention + (1|Participant)}$$



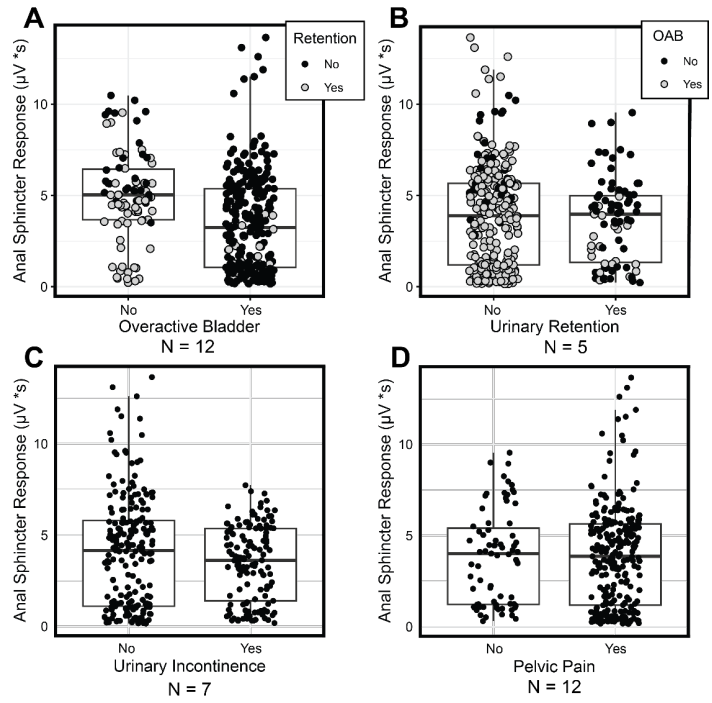
Supplemental Figure 2-5: Anal sphincter EMG and AUC Quantification procedure. (A) Example EAS EMG after signal filtering showing five consecutive responses during a single trial. Stimulation was applied at 3 Hz. (B) Each individual response in A is segmented, rectified, and aligned at the stimulation artifact. Individual traces in are in gray and the average signal is in black. (C) The shaded area under the rectified average EMG trace, between the vertical dashed lines, is the calculated area under the curve (AUC).



Supplemental Figure 2-6: Monopolar threshold current and charge for all participants at each tested pulse width. A) EAS threshold current for each participant. If we tested the threshold for multiple electrodes at a given pulse width then the lowest threshold is shown. B) The charge at EAS threshold for each participant.



Supplemental Figure 2-7: EAS activation thresholds for 210 µs pulse width monopolar and bipolar trials. A) The minimum EAS threshold for monopolar and bipolar stimulation is shown for each participant. B) Aggregated EAS thresholds across all participants for monopolar and bipolar trials. Box plots represent the inter-quartile range (25%-75%; IQR) for the height of each box, with the bold central line indicating the median. Tips of whiskers extend to the value(s) within 1.5 x IQR of each box side.



Supplemental Figure 2-8: The EAS response magnitude dependence on participant diagnosis of A) Overactive Bladder, B) Urinary Retention, C) Urinary Incontinence, or D) Pelvic Pain. The N value under each x-axis indicates the number of participants diagnosed with each condition out of 16 total participants. The legends in sub-figures A and B show comorbidities of Retention or Overactive Bladder, respectively.

Chapter 3 Pudendal Nerve Stimulation Recruits the Urethra During Awake Human Cystometry

(Submitted to MedRxiv, February 2026)[123]

3.1 Abstract

Objective:

This study aimed to characterize the activation of lower urinary tract (LUT) targets in response to pudendal nerve stimulation (PNS) in awake human participants.

Materials and Methods:

In this single center study, recruited participants had an implanted pudendal neurostimulator for treatment of their symptoms including overactive bladder, incontinence, urinary retention, and/or pelvic pain. Participants came in for a modified urodynamic study where a multichannel manometry catheter was placed in the lower urinary tract alongside a dual sensor urodynamics catheter. The bladder was filled and after each participant expressed a strong desire to void, PNS was applied and LUT pressures were measured. Participants attempted voids with the catheters in place to characterize LUT behavior and voiding efficiency with and without stimulation.

Results:

The study consisted of 15 participants including 13 women. Across 133 total trials, contractions were observed at the distal urethra 52 times (39%) and at the proximal urethra 46 times (35%). The maximum observed pressure change occurred significantly more often at the proximal urethra than the distal urethra ($p=0.007$). There was a significantly higher maximum tolerable stimulation amplitude for low frequency stimulation (2-3.1 Hz) when compared to high frequency stimulation (30-33 Hz) ($p = 0.041$). In one participant there were four instances of stimulation driven bladder contractions with an average pressure change of 24.3 cmH_2O (standard deviation = 10.5). There was not a significant difference in voiding efficiency or maximum flow rate with and without stimulation ($p=0.76$ and $p = 0.45$, respectively).

Conclusions:

PNS can affect LUT pressures at tolerable stimulation amplitudes. The absence of a direct effect of PNS on voiding characteristics suggests a similar mechanism of action as sacral neuromodulation.

3.2 Introduction

Pudendal nerve stimulation (PNS) is an off-label clinical treatment for incontinence, retention, and chronic bladder pain that has been in use for 20 years[9,10,124]. However, there is still little information on how pudendal stimulation directly affects the lower urinary tract in human subjects[11,125]. While the relationship between PNS and lower urinary tract activation has been well studied in animal models[126–128], most findings have not been verified in human subjects.

The pudendal nerve is a mixed nerve that innervates the perineum, genitals, and external urethra sphincter[60]. While PNS can cause external urethra contractions in preclinical experiments[126] and in humans under anesthesia[129], it's not clear if PNS can generate urethra contractions without bothersome pain or discomfort in awake humans. If feasible, on demand urethra contractions in humans could help treat stress urinary incontinence stemming from inadequate urethra pressure.

As a mixed nerve, the pudendal nerve contains sensory afferents[60] that contribute to bladder function through spinal reflex circuits[69,70]. Animal studies have shown that PNS can lead to bladder contractions[14,130] and there are reported cases of PNS evoked bladder contractions occurring in individuals with spinal cord injury[75,76]. However, there have not been any reported instances of PNS evoked bladder contractions in non-spinal cord injured individuals. The ability to generate bladder contractions with PNS could help people with detrusor underactivity manage their symptoms and regain some bladder control.

PNS can improve symptoms for patients with overactive bladder and retention, but the mechanism that causes symptom improvement is unclear. The effectiveness of PNS is counter intuitive as overactive bladder and retention are issues with contradictory bladder symptoms. Preclinical studies have shown that PNS can directly affect voiding and bladder function[127,131] but no studies have looked at the direct effects of PNS on voiding characteristics in human participants. A study on voiding performance with and without stimulation may improve our understanding of how PNS improves patient symptoms and help improve future therapies.

In this work we investigated direct and indirect effects of PNS on the lower urinary tract (LUT) in participants with an implanted pudendal neurostimulator. We examined the effect of PNS on urethra pressures at multiple locations, attempted to elicit reflex bladder contractions, and compared LUT dynamics during voluntary voiding with and without PNS.

3.3 Materials and Methods

Recruited participants had an implanted pudendal neurostimulator for treatment of symptoms including overactive bladder, pelvic pain, incontinence, and/or urinary retention.

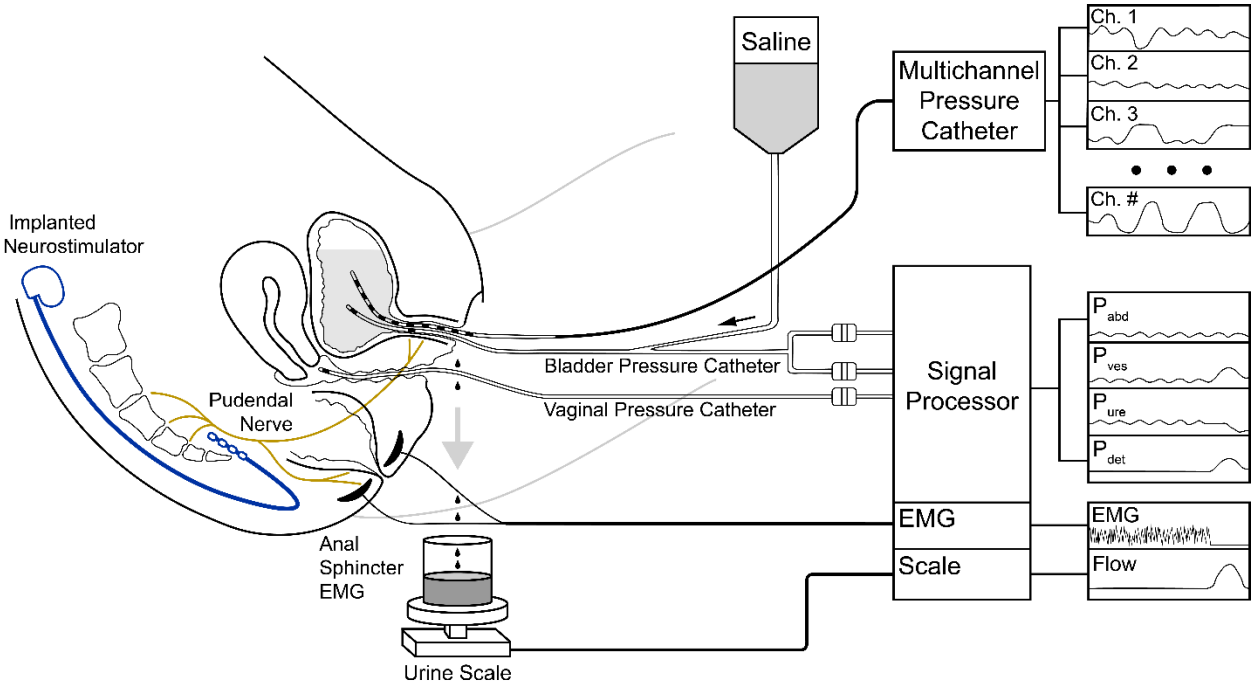


Figure 3-1: Experimental setup diagram. With participants in a reclined position, a multi-channel catheter was inserted into the urethra to measure urethra and bladder pressures. The multichannel catheter was placed alongside a urodynamics catheter which was used to infuse saline into the bladder. A urodynamics system was used to record bladder, urethra, and abdominal pressures, anal sphincter EMG, and the voided volume. This figure was modified from Karram and Blaivas[132].

A visualization of the experimental setup is shown in Figure 3-1. Each participant was seated, in a reclined position. We recorded pressures in the bladder and urethra with a 2.75 mm diameter manometry catheter (MSC-3886: Manoscan, Medtronic, MN, USA) with solid-state pressure sensors at a 7.5 mm center to center distance between adjacent sensors. We estimated the position of each pressure sensor in the LUT from the pressures recorded by the manometry catheter and from the number of the sensor located outside of the body. We identified the proximal urethra

sensor as the sensor with the highest pressure outside of the bladder. For female participants we set the distal urethra sensor as the first sensor inside the body and for male participants we set the distal urethra sensor as three sensors away distally from the proximal urethra sensor. We followed standard cystometry practice with a 7 French air-charged dual sensor catheter (CAT880: Laborie, NH, USA) placed in the LUT to record bladder pressure and urethra pressure and to infuse saline into the bladder. An abdominal catheter (CAT875: Laborie, NH, USA) was placed in the rectum (if possible) or else in the vagina to record abdominal pressure. A pair of patch electrodes were placed on opposite sides of the anal sphincter to record anal sphincter activation and electrical stimulation artifact. A uroflowmeter was placed underneath each participant to measure urine flow.

At the beginning of each testing session, we determined the sensory threshold and maximum tolerable stimulation amplitude (MTSA) at 14Hz, a commonly used stimulation frequency, or 31Hz. MTSA was determined for each electrode in a monopolar configuration with the implantable pulse generator acting as the positive return. We filled the bladder with saline and without PNS until each participant reported a strong desire to urinate. After evaluating a variety of stimulation configurations, we applied stimulation with their home program, or a program that recruited the pelvic floor, and participants attempted to void. After the first void, if the participant agreed, we conducted another filling cycle with additional trials and a second void attempt without stimulation.

During each trial we evaluated different electrode combinations within 2-3.1 Hz, referred to as low frequency here after, and within 30-33 Hz, referred to as high frequency here after, in monopolar or bipolar configurations. For each trial, the stimulation amplitude was increased to MTSA and kept there for at least ten seconds. In preclinical studies low frequency stimulation (2-5 Hz) and high frequency stimulation (20-40 Hz) can cause bladder inhibition and excitation[133–136] so these stimulation frequency ranges were chosen to see if similar results could be observed in humans. For low frequency trials the contraction amplitude was calculated by averaging the peak height for five stimulation-driven contractions. For high frequency trials the contraction amplitude was calculated by taking the difference between the maximum LUT pressure during stimulation increase and a five second average baseline before stimulation was applied. When there were multiple sensors in the distal or proximal urethra, the sensor with maximum pressure change was used in the analysis. Bladder pressures were reported from the sensor that was closest to the tip of the catheter. The bladder pressure change during voiding was calculated as the

difference between the mean bladder pressure in the ten-second interval surrounding the peak flow rate and in the ten-second interval before the void was initiated. Voiding efficiency was expressed as the ratio of voided volume to infused volume. If more fluid was voided than infused then efficiency was set at 100%[137].

We used the Shapiro-Wilk test to check if the data was normally distributed. If the data was normally distributed, then it is reported as mean with standard deviation (SD) otherwise data is reported as median with interquartile range (IQR). After confirming normality of the data, we used a Welch two sample t-test to check for a significant difference between groups. A paired t-test was used to compare bladder pressure changes during voids. A Wilcoxon rank sum test was used if data was non-normal. To evaluate statistical significance, α was set to 0.05.

3.4 Results

Table 3-1 Participant demographic information.

Participant	Sex	Age (years)	Body Mass Index (kg/m^2)
1002‡	F	64	22.3
1008	F	56	25.8
1010	F	79	30.4
1012	F	52	21.3
1016	F	46	30.7
1017*	F	64	28.0
1019	F	58	31.6
1021*	F	65	26.4
1022	F	60	36.7
1024	F	53	26.2
2001	M	34	35.9
2003	F	69	31.2
2004	M	54	30.1
2005	F	68	31.8
2006‡	F	65	23.0
N = 15	F=13	59 ± 11	28.8 ± 4.6

* Participant 1017 was re-enrolled as 1021 after receiving a new pudendal nerve stimulation implant. ‡ Participant 1002 had a second study visit and was (re)enrolled as 2006. Summary statistics are shown as mean ± standard deviation.

We collected data from 13 participants over 15 cystometry sessions. One participant was reenrolled after receiving a new pudendal stimulator on the opposite nerve. Another participant was reenrolled after a fall that affected symptom relief from the implanted stimulator. Individual participant demographic data is shown in Table 3-1.

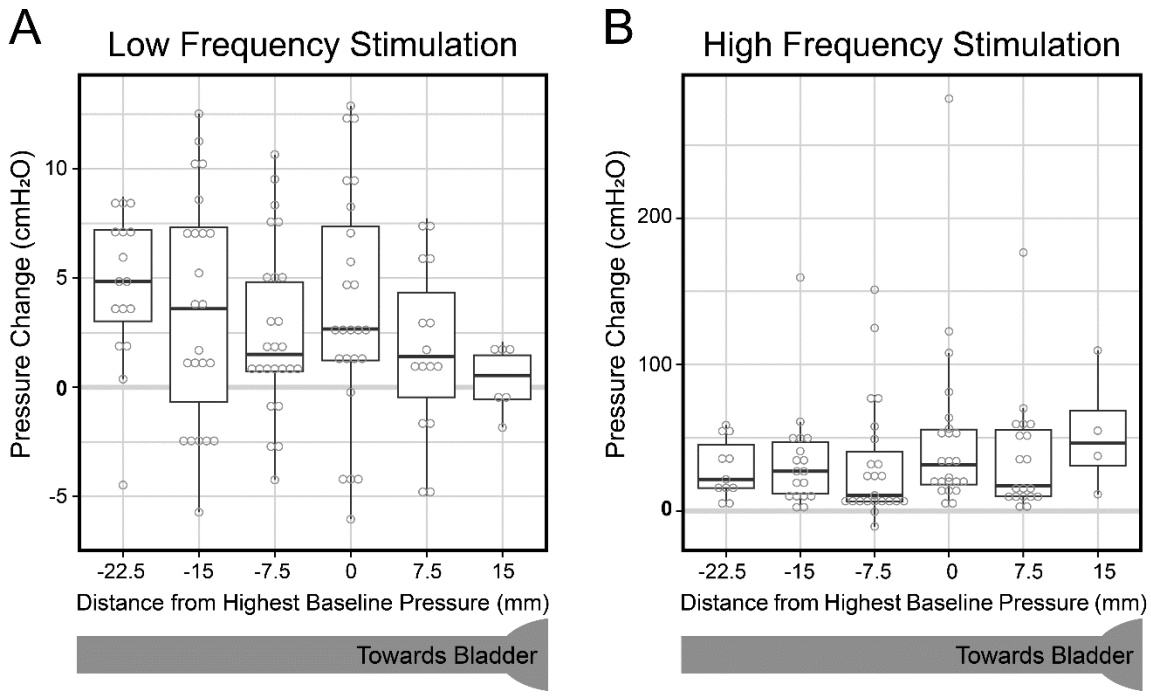


Figure 3-2: Stimulation driven urethra pressure changes across participants. The urethra position is labeled according to each sensors relative position to the sensor with the greatest baseline pressure. A) Lower urinary tract pressure changes during stimulation at low frequency. Pressure change is calculated per stimulation pulse. B) Lower urinary tract pressure changes during stimulation at high frequency. Pressure change is the maximum difference from the baseline pressure during a tetanic contraction.

Across all low and high frequency trials, for 11 cystometry sessions with voltage-controlled stimulators, the MTSA was not normally distributed (p=7.4e-9). Trials at low frequency had a median MTSA of 2.4V (IQR = 2.0) and high frequency trials had a median MTSA of 1.9V (IQR = 1.7). There was a significant difference (p=0.015) between the median MTSA for low and high frequency stimulation. Trials at low frequency with observed contractions had a median MTSA of 1.9V (IQR = 0.6) which was not significantly different (p=0.10) than trials without observed contractions which had a median MTSA of 3.5V (IQR = 3.3). Trials at high frequency with

observed contractions had a median MTSA of 1.9V (IQR = 0.6) which was not significantly different (p=0.69) than trials without observed contractions which had a median MTSA of 1.9V (IQR = 2.7).

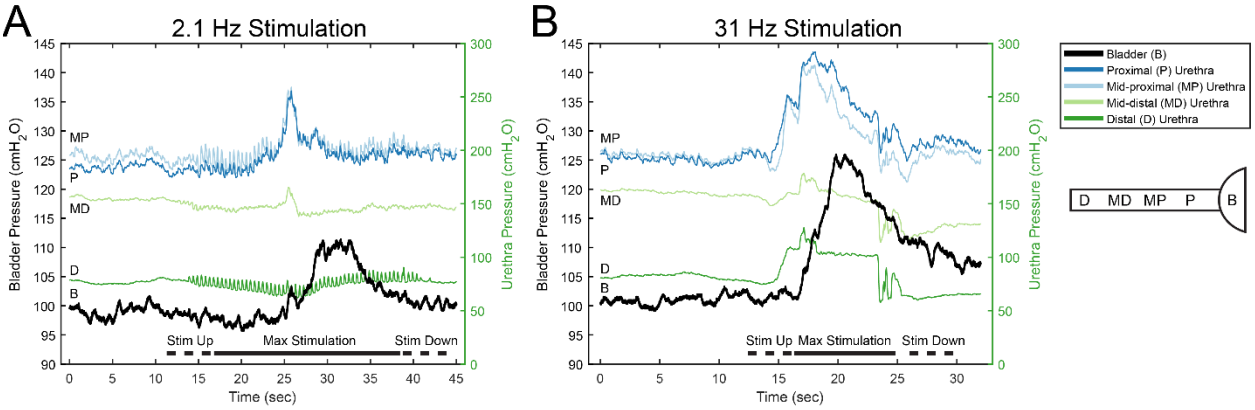


Figure 3-3: LUT pressures from example trials with bladder contractions in participant 2001. A) A trial with stimulation applied at 2.1 Hz and a maximum stimulation amplitude of 2V. B) A trial with stimulation applied at 31 Hz and a maximum stimulation amplitude of 1.3V. Note the different timing dynamics of bladder pressure rise or fall as compared to urethra pressure changes.

We observed urethra contractions in response to stimulation in 11 sessions. Across 62 low frequency trials in nine different participants, 31 trials had observable contractions at the MTSA. The number of responsive trials and the median distal and proximal pressure change for each participant are shown in Supplemental Table 3-2. When urethra contractions were observed, the maximum pressure change occurred at the distal urethra 19 times and at the proximal urethra 12 times, with no significant difference (p=0.28) in the proportion of maximum pressure at each location. For low frequency stimulation, the median stimulation evoked contraction amplitude was 2.3 cmH_2O (IQR = 3.1) at the distal urethra and 2.6 cmH_2O (IQR= 5.9) at the proximal urethra with no significant difference (p=0.53) between locations. Figure 3-2A illustrates the relationship between the location in the urethra and the observed contraction amplitude during low frequency trials. For high frequency stimulation there were urethra contractions in 24 out of 71 trials and in seven out of fifteen sessions. The maximum pressure change occurred in the distal urethra 5 times and the proximal urethra 19 times, with a significant difference (p = 0.007) in the proportion of trials with a larger contraction in the proximal urethra. For high frequency stimulation the median stimulation evoked contraction amplitude was 17.5 cmH_2O (IQR = 29.9) at the distal urethra and

33.8 cmH_2O (IQR= 41.3) at the proximal urethra with a significant difference (p=0.013) between locations. Figure 3-2B illustrates how pressure changes with urethra location for high frequency trials.

We observed four instances of stimulation driven bladder contractions in one participant (subject number 2001). The pressure traces for two example bladder contractions are shown in Figure 3-3. The mean magnitude of the bladder contraction was 24.3 cmH_2O (SD=10.5). The bladder contractions were observed with 2.1 Hz and 31Hz stimulation, with two different contacts, and at pulse widths of 210 and 450 μseconds. All contractions occurred at bladder volumes above 70 percent with monopolar stimulation or bipolar stimulation and with a MTSA at or below 2V.

There were five participants who voided both with and without stimulation. During void attempts, participants used their at home stimulation parameters. The mean voiding efficiency was 89.2% (SD=14.5%) with stimulation and 92.1% (SD=9.1%) without stimulation (p=0.76). The mean maximum flow rate was 23.3 mL/sec (SD=12.6) with stimulation and 20.3 mL/sec (SD=7.28) without stimulation (p=0.45). Figure 3-4A shows a void with stimulation and Figure 3-4B displays the urethra pressure profile before, during, and after the void. A void from the same participant without stimulation is in Supplemental Figure 3-5. Three participants who voided with and without stimulation had a pressure sensor in the bladder. In these cases, at the maximum flow rate the mean bladder pressure change during stimulation was 23.3 cmH_2O (SD = 12.6) and without stimulation was 20.3 cmH_2O (SD = 7.8), which was not significantly different (p=0.57).

3.5 Discussion

Previous studies have shown that PNS can lead to activation of the bladder and urethra in preclinical experiments and in humans under anesthesia or with spinal cord injury (SCI) [76,126,127,129,131,138,139]. This present study is the first to report urethra and bladder activation from PNS in awake, non-SCI human subjects.

We observed stimulation driven urethra contractions in 11 out of 15 cystometry sessions. Pressure changes occurred along the urethra during high and low frequency stimulation, showing that pudendal stimulation can cause urethra contractions in awake, responsive humans, as previously demonstrated under anesthesia[129]. Urethra contractions were more common with low frequency stimulation than with high frequency stimulation, occurring in more participants and more trials. While low frequency stimulation caused urethra contractions more often than high

frequency stimulation, the evoked contractions from high frequency stimulation were generally much larger and tetanic and therefore potentially more useful for preventing urine leakage. High frequency stimulation also had significantly lower maximum tolerable stimulation amplitudes even though urethra contractions did not affect participant's tolerance for stimulation. For cases where urethra contractions were not observed it is possible that high frequency stimulation resulted in continuous nerve activation which was typically more noticeable and uncomfortable for participants. This resulted in lower tolerable stimulation amplitudes, and potentially less activation of motor nerve fibers innervating the urethra. Overall, the large number of urethra contractions shows PNS is able to recruit urethra fibers effectively. However, as PNS is typically administered before motor fiber activation these results suggest symptom improvement through a mechanism involving activation of sensory afferents similar to sacral neuromodulation[140].

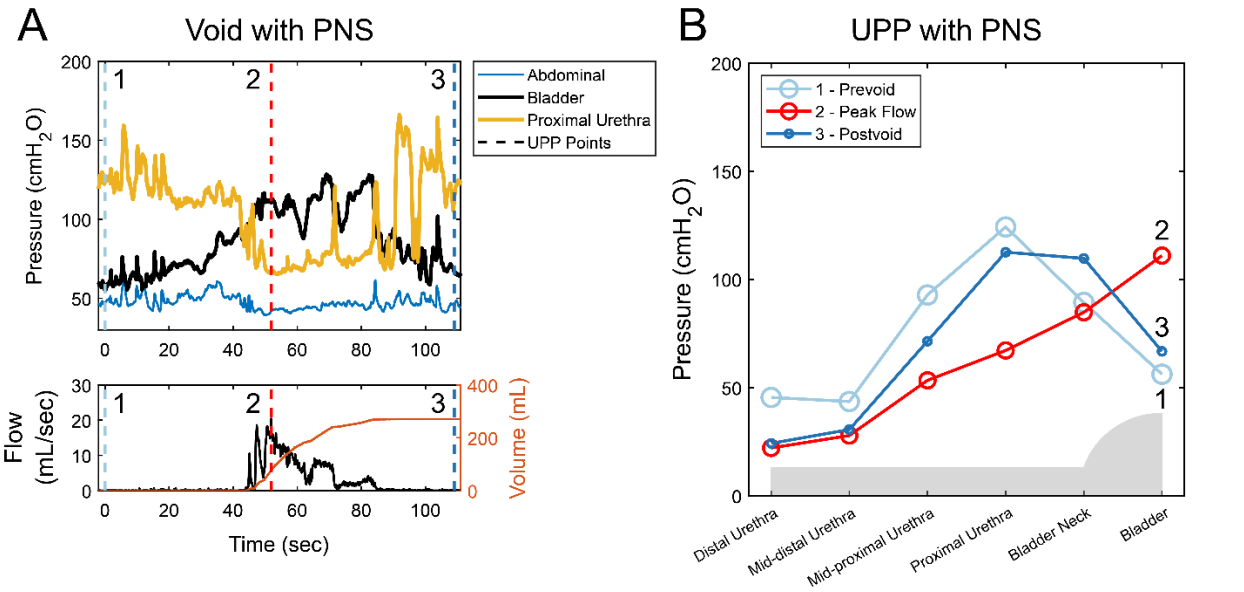


Figure 3-4: A void with pudendal nerve stimulation (PNS) for participant 1002. A) Pelvic pressures and voiding response during PNS. B) Urethra pressure profiles (UPPs) from specific time points in A marked with vertical dashed lines.

In one participant, PNS generated excitatory bladder responses in several trials. It is not clear why this participant was the only one with clear PNS-driven bladder responses, but they were especially responsive to stimulation, with a urethra response for 19 out of 21 trials. This might indicate that their implanted lead was particularly successful at recruiting pudendal nerve fibers and was able to influence the lower urinary tract reflexes that influence bladder state[131,141]. It is

important to note that in two of the trials with a bladder response the participant noted discomfort with stimulation. The level of stimulation required to activate the bladder likely activates C-fibers as well, potentially explaining why previous reports of bladder pressure changes in response to PNS occurred in people with SCI[76,142] , preclinical experiments with SCI models[127,134], or under anesthesia[14,143]. It is possible that other participants had small, stimulation driven increases in bladder pressure during PNS that were indistinguishable from background pressure oscillations.

We were able to record LUT pressures during bladder voids with and without PNS in a subset of participants. We did not see a significant effect of PNS on voiding function or dynamics. The lack of an immediate change in LUT function suggest that PNS has an indirect effect on LUT function through long term changes in nervous system networks and reflex circuits similar to the proposed mechanisms for sacral neuromodulation[144]. Our findings on the bladder and urethra behavior during voiding matched previous findings[145]. However, using the manometry catheter we observed LUT activity during voids with a level of detail not achieved before. One observation, as visualized in Figure 3-4B, is that just before voiding starts there is a large decrease in urethra pressure at the location of maximum urethra pressure. This reduction in pressure was fairly localized, only occurring in a region one to two centimeters in length. Then, during the void, there is a gradual decrease in pressure from the bladder to the end of the distal urethra, showing how LUT pressures aid in urine flow.

Collecting data from awake human participants provided some challenges. Each participant typically sensed PNS. We gradually increased stimulation amplitude as we approached the MTSA. As stimulation increased, baseline pressures could change, or participants could shift positions potentially masking out urethra contractions, particularly the sustained contractions associated with high frequency stimulation. Additionally, having two catheters in the urethra made voiding more difficult. While 14 participants attempted to void with both catheters in place, only six participants were able to complete voiding. In some voids the flow curve showed signs of restrictive flow, likely from catheterization, potentially masking any effects of stimulation. The low number of completed voids limits the strength of any conclusions on the urethra dynamics during voiding. Future studies could remove the infusion catheter before void attempts to reduce urethra restriction and achieve more consistent voiding.

3.6 Conclusion

This study demonstrates that PNS can evoke urethra and bladder contractions in awake humans which could be useful for future treatments of conditions such as stress urinary incontinence and urinary retention. Additionally, the minimal effect of PNS bladder or voiding function suggests a PNS mechanism acting through long term changes to bladder neural control circuits. Future studies should investigate whether generated urethra contractions are sufficient to prevent SUI leakage.

3.7 Acknowledgments

Thank you to Vanessa Pruitt and Mackenzie Moore for their efforts in patient recruitment. We are also thankful to the University of Michigan clinical staff for assistance during urodynamic procedures.

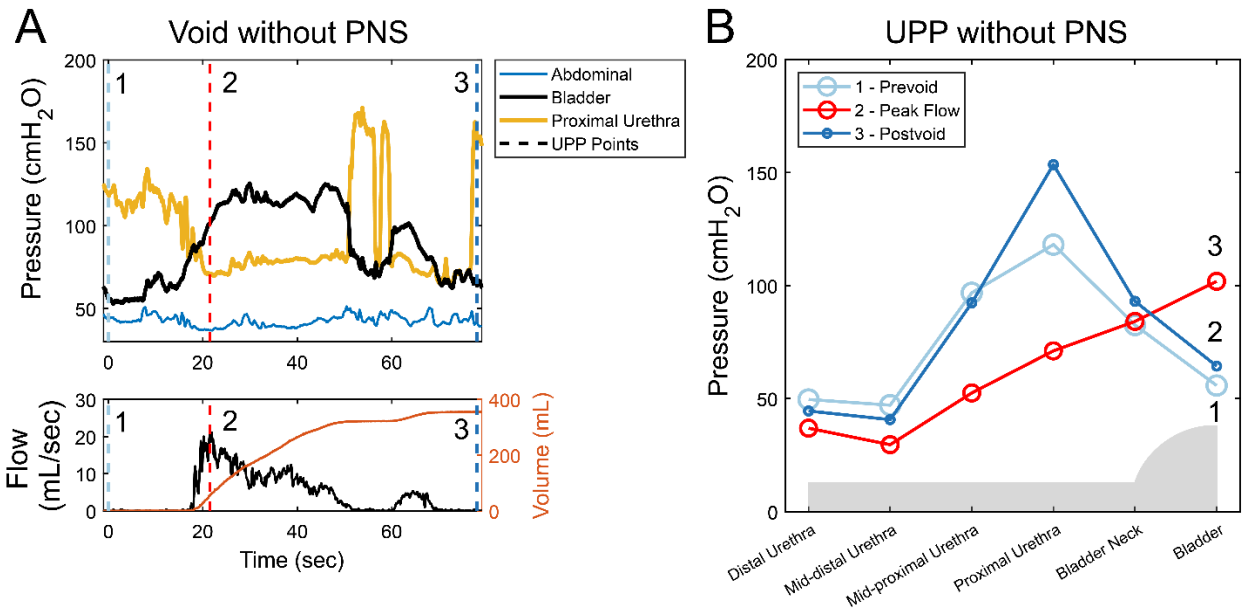
3.8 Supplemental Information

Supplemental Table 3-2 Median urethra pressure changes in response to low and high frequency stimulation.

	Low frequency Trials			High frequency Trials		
Participant	Responsive Trials / Total Trials	Median Distal Pressure Change (cmH_2O)	Median Proximal Pressure Change (cmH_2O)	Responsive Trials / Total Trials	Median Distal Pressure Change (cmH_2O)	Median Proximal Pressure Change (cmH_2O)
1002	NA	NA	NA	3/8	5.0	16.3
1008	1/3	1.5	0	1/3	10.8	9.7
1010	0/5	0	0	0/1	0	0
1012	0/4	0	0	0/5	0	0
1016	0/3	0	0	3/4	8.1	10.9
1017	2/5	-0.7	0	0/4	0	0
1019	0/3	0	0	0/3	0	0
1021	0/4	0	0	0/5	0	0
1022	4/4	6.0	1.5	0/4	0	0
1024	6/6	0.4	2.0	0/6	0	0
2001	10/11	2.5	8.3	9/10	44.9	55.6
2003	4/4	3.5	-4.2	3/4	5.8	21.3

2004	1/2	3.3	4.9	2/5	34.1	63.7
2005	1/4	0.9	0	0/4	0	0
2006	2/4	1.7	0.8	3/5	21.8	26.0

NA = not applicable, as Participant 1002 had no trials with low frequency stimulation.



Supplemental Figure 3-5: A void without pudendal nerve stimulation (PNS) for participant 1002. A) Pelvic pressures and voiding response during PNS. B) Urethra pressure profiles (UPPs) from specific time points in A marked with vertical dashed lines.

Chapter 4 Selective Neurostimulation of Small-diameter Pudendal Fibers is Feasible with a Multicontact Nerve Cuff Electrode: A Modeling Study

4.1 Abstract

Objective:

Multicontact nerve cuffs have been used to selectively activate pudendal fascicles in computational models. However, previous studies failed to account for anatomical differences between different types of pudendal fascicles. This study evaluated the fascicular selectivity of pudendal nerve stimulation with a multicontact cuff using a computational model that incorporated realistic distributions of axon diameters.

Materials and Methods:

In this computational study finite element models were created using measurements from feline pudendal nerve cross-sections processed with histology and from a custom-designed nerve cuff. A selectivity metric was calculated to quantify how many off-target fascicles in each nerve were activated while trying to activate a target fascicle. Simulations were run to determine the impact of cuff stimulation method, cuff diameter, number of contacts, simulation fiber density, and fiber diameter on the selectivity of different fiber sizes.

Results:

The study included 5 feline pudendal nerve cross sections and four different cuff designs. The cuff had two diameters and was modeled with 8, 10, or 16 contacts. In a low fiber-density model, fascicles were populated with different fiber diameters (2, 5.7, and 7.3 μm). Selectivity was significantly different ($p < 0.001$) for fascicles with different afferent fiber diameters. Within each fiber diameter, the contact arrangement used to stimulate the nerve had a significant effect on selectivity. Bipolar and guarded configurations consistently yielded a larger selectivity than a full cuff configuration ($p < 0.001$). While increasing the electrode contacts count occasionally led to a larger selectivity, the difference was not significant. A simulation with a more realistic distribution

of fiber diameters than the low fiber-density model showed a significant effect of fiber diameter on selectivity.

Conclusions:

Even when including different fiber diameters for afferent and efferent fascicles, low fiber-density models showed selectivity values that were in line with what was previously reported in the literature. However, a higher fiber-density model suggests that achieving a moderate degree of selectivity is more difficult than previously reported when fascicles have different distributions of fiber diameters. This computational model, incorporating more anatomically relevant fiber diameter distributions, shows that sensory-fascicle selectivity is challenging and suggests that advanced pudendal nerve electrode designs should be considered

4.2 Introduction

Overactive bladder (OAB) is a lower urinary tract disorder that affects millions of Americans and negatively impacts quality of life[41,146]. Individuals with OAB typically suffer from urinary urgency, urinary frequency, and can also have urinary incontinence[41]. Many therapies exist, each with their own benefits and side effects. Recent guidelines emphasize therapy choice based on shared decision making between patient and clinician. However, the guideline still recommends avoiding invasive therapies, like surgical augmentation, unless all other therapies have been considered. Any additional minimally invasive therapy for OAB could prevent patients from experiencing the significant risks associated with invasive therapies. Pudendal neuromodulation (PNM) is an off-label and minimally invasive therapy for OAB[9,115,124] that has been used clinically for over 20 years[10].

PNM is an acceptable option for individuals with OAB as it has been shown to increase bladder capacity and reduce daily incontinence episodes[115]. However, PNM has room for improvement. PNM is an off-label treatment, which limits patient access. Additionally, not all participants respond to treatment and few gain complete symptom relief[100,115]. Changes to the PNM electrode could improve therapy performance and response rate. PNM is thought to work by activating the sensory fibers in the pudendal nerve[60]. However, motor fibers can also be activated which can lead to patient discomfort. The current design of the quadripolar lead used in pudendal neuromodulation can make it difficult to selectively activate the sensory fibers in the pudendal nerve without activating motor fibers. This can limit the amount of current delivered and may limit the effectiveness of the therapy. While not widely reported, the lead used in PNM can occasionally

change position[115] which may lead to a reduction in device efficacy. An improved electrode design would allow for selective activation of afferent fascicles and minimize the risk of electrode movement.

Computational models are widely used to simulate the activation of neural tissue by stimulating electrodes[79]. They have been used to analyze the performance of electrodes specifically designed to interface with peripheral nerves like penetrating electrodes and multicontact nerve cuffs[80–83]. For the pudendal nerve, several computational studies have used a multicontact nerve cuff to selectively activate fascicles[12,84]. These models failed to differentiate between sensory fascicles and mixed fascicles. This is important because sensory fascicles have smaller fiber diameters than mixed fascicles[91]. Smaller fibers are more difficult to activate with extracellular stimulation than larger fibers[92]. Thus, selective activation of afferent axons in sensory fascicles to drive bladder state change may be more challenging than anticipated. The purpose of this study is to investigate whether selective activation of afferent sensory fascicles in the pudendal nerve is feasible with a multicontact nerve cuff that has multiple contact locations for improved current steering. We used computational modeling methods to calculate fascicular selectivity under a range of test conditions. We hypothesized that selectivity would be consistently achievable with a specific form factor multicontact nerve cuff design.

4.3 Methods

4.3.1 Nerve Processing

We collected five pudendal nerve specimens from the left (x3) and right (x2) sides of three female felines that were used in other studies[90]. Each sample was fixed in 10% neutral formalin buffered solution for 6-18 months. After fixation each sample was embedded in paraffin, sectioned, and stained with hematoxylin and eosin (Figure 4-1A). Four of the nerves also had sections stained with Anti-Neurofilament 200 antibody to identify myelinated fibers and confirm that identified fascicles contained axons (Supplemental Figure 7). Histology scans were processed in Adobe Photoshop to segment nerve epineurium and perineurium boundaries (Figure 4-1B & 4-1C). Four of the nerves were expanded with a 1.25 expansion ratio to reverse nerve shrinkage associated with histological processes, following methods reported previously[147,148]. The fifth nerve was not expanded as it would not have fit within the modeled nerve cuff. For each nerve sample the outer boundary was deformed and morphed into a circle[149]

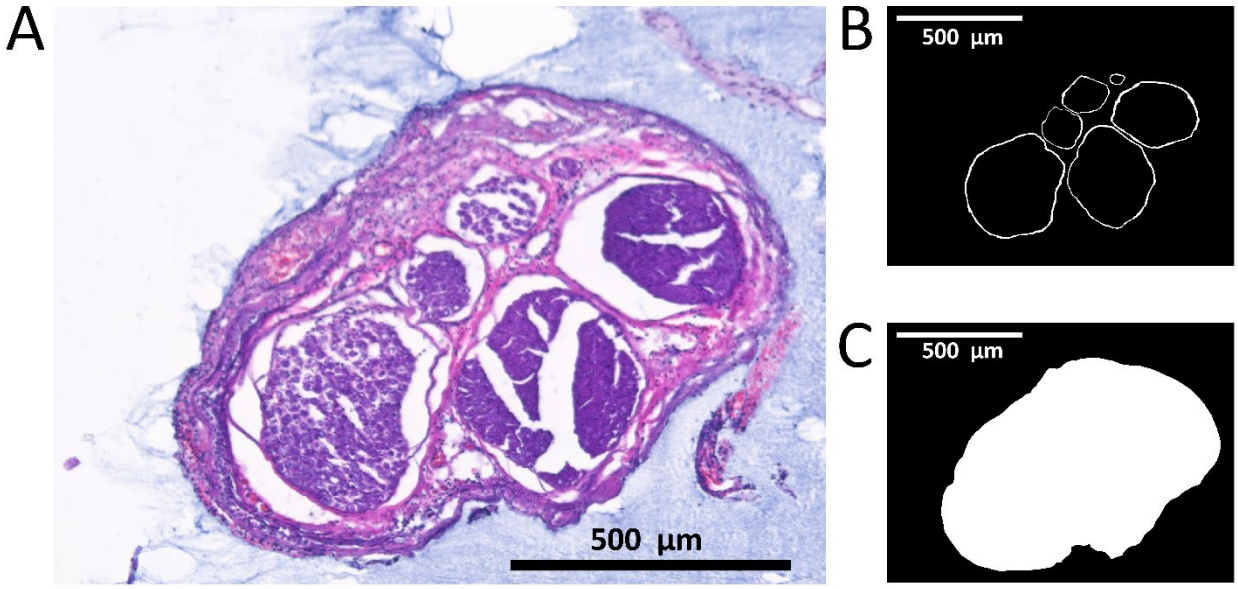


Figure 4-1: A) H&E-stained feline pudendal cross section. B) Traced perineurium from A. C) Segmented inner portion of the pudendal nerve in A.

4.3.2 Cuff Specifications

We created computational models of a custom eight-contact nerve cuff with an adjustable diameter of either 1.20 mm or 1.91 mm and a length of 5 mm, to directly match a cuff used previously *in-vivo*[90] (Figure 4-2 & Supplemental Figure 4-8A & 4-8C). There are a wide variety of cuff designs and previous research has shown that including more contacts around the nerve would increase selectivity[84]. We chose to replicate the geometry of a previously used *in-vivo* cuff so that the activation threshold of fibers in the model could be compared to motor threshold from the *in-vivo* experiments. The cuff contacts were 1.225 mm by 0.580 mm. The contacts were arranged in a two by four configuration with two rings of four contacts placed along the length of the cuff and wrapped around the perimeter of the nerve. There is a 0.23 mm gap between contact rings and a 0.17 mm gap between adjacent contacts in each ring. The base material of the cuff is 0.02 mm-thick parylene C. Each contact consisted of a 0.002 mm thick layer of platinum placed 0.01 mm deep on the inner surface of the cuff. Two alternate cuff designs were created to test how additional stimulation contacts affected selectivity (Supplemental Figure 8-B and 8-D): one with an additional contact pair on a 1.20 mm diameter cuff and one with four additional contact pairs on a 1.91 mm diameter cuff.

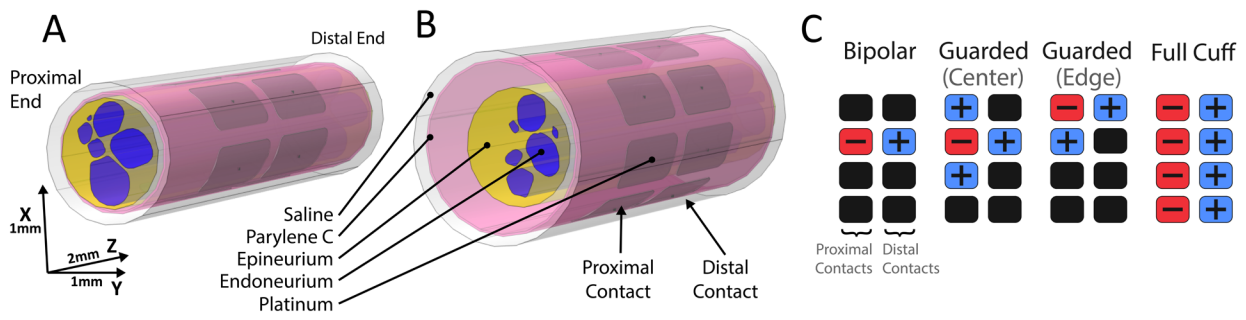


Figure 4-2: Example feline pudendal nerves placed inside each of a A) 1.20 mm diameter cuff and a B) 1.91 mm diameter cuff. Both cuffs have 8 stimulation contacts. The nerve in B is too large to fit in the cuff in A. C) Example depictions of activated contacts for bipolar, guarded, and full cuff stimulation. Four different sets of contacts were tested for bipolar and guarded stimulation. The cathode occupied a unique position on the proximal row of contacts for each unique set. Cathodes are in red with an inset (-) and anodes are in blue with an inset (+). Materials in A and B are colored as follows: white: saline, pink: parylene C, yellow: epineurium, blue: endoneurium, grey: platinum contact.

4.3.3 Computational Modeling Details

We used the ASCENT[149] package (v1.14.0) to implement the finite element model (FEM) of each nerve and nerve cuff in COMSOL (6.2) and calculate the neural response to stimulation in NEURON (8.2.6). Details for this process are given below.

Table 4-1 COMSOL model meshing parameters

Parameter	Inner Mesh	Outer Mesh
Minimum element size	10 (μm)	10 (μm)
Maximum element size	1600 (μm)	1600 (μm)
Resolution of narrow regions	1	1
Maximum element growth rate	2.2	2.5
Curvature factor	2	0.2

4.3.3.1 Model Geometry:

Processed nerve samples were used to create three-dimensional finite element models. The nerve epineurium was defined as the outer boundary of each nerve. The perineurium was modeled as a thin layer approximation using the average perineurium thickness measured from histology.

Endoneurium filled the rest of the nerve. The cross-section for each nerve was extruded to create a three-dimensional model. To minimize the gap between the nerve and nerve cuff, each nerve was placed in the smallest cuff it could fit in. The two smaller nerves (diameters 1.1, 1.1 mm) were placed in a 1.20 mm diameter cuff (Figure 4-2A). The three larger nerves (diameters 1.3, 1.4, 1.9 mm) were placed in a nerve cuff with a 1.91 mm diameter (Figure 4-2B). The diameter for each cuff replicated the diameters of the *in-vivo* experiments[90]. The nerve cuff was placed at the midpoint. The cuff was shifted laterally towards the nerve until a 10 μm gap remained between the nerve and the closest point on the nerve cuff. Saline was used to approximate bodily fluid and span any gaps between the nerve and cuff. Surrounding the saline, nerve, and nerve cuff was an outer layer of muscle represented as a cylinder. The muscle layer spanned the entire length of the nerve and had a diameter of 10 mm. To reduce the computational size of the model, it was split into two parts for COMSOL meshing (Table 4-1). The inner mesh had a diameter of 6 mm and encompassed the nerve, nerve cuff, saline, and some muscle. The outer mesh had an outer diameter of 10 mm, included the rest of the modeled muscle, and had a lower resolution meshing geometry than the inner mesh. The outer boundary of the outer mesh of the model was assigned to electrical ground.

Table 4-2 FEM material conductivities

Material	Electrical Conductivity {x, y, z} (S/m)
Saline	1.76[149]
Muscle	{0.086, 0.086, 0.35}[149,150]
Platinum	9.43*10^6[149,151]
Endoneurium	{1/6, 1/6, 1/1.75}[149,152,153]
Epineurium	1/6.3[153]
Perineurium	8.703*10^-4[149,154]
Parylene C	10^-14[155]

4.3.3.2 Electrophysiological Modeling

The conductivities for all modeled materials are shown in Table 4-2. A point current source was modeled in the middle of each platinum contact. The FEM was solved using Laplace's

equation for each contact delivering 1 mA of current. Electrical potentials were calculated to determine the threshold currents for fibers placed throughout the model. Fiber characteristics changed for different experimental configurations. Each stimulation simulation was run for 50 ms with a time step of 1 μs. At the 1 ms mark of each simulation a single biphasic pulse train was applied with a pulse width of 210 μs.

Activation threshold for a given fiber was defined as the amount of current required to activate a fiber. Threshold was detected if there was a transmembrane potential with a rising edge greater than -30 mV at 90% of the nerve length on the proximal side of the nerve (Figure 4-2). Threshold for each fiber was found using a bisection search algorithm that stopped searching after reaching an exit criteria of a 1% difference between the upper and lower bounds[149,156].

We conducted a convergence analysis to verify that the model domain was large enough to not change activation thresholds by more than 2% as compared to a larger model. We varied the model length (12.5, 25, 35 mm) and radius (5, 10 mm) and compared the mean activation threshold for fiber diameters of 2-12 μm (Supplemental Figure 4-9**)**. The final model length and radius were set to 25 mm and 5 mm respectively. These same lengths were used for all experimental configurations.

4.3.4 Simulation Configurations

4.3.4.1 Centrally Placed 4-fiber Simulation:

This simulation was created to compare fascicular activation between a sensory fascicle that contained small diameter axons and mixed fascicles that contained larger diameter axons. In this configuration the center of each fascicle was populated with four different diameter fibers, each modeled in a separate simulation as an MRG axon[157,158] (Supplemental Figure 4-10**)**. We chose fibers of 2, 5.7, 7.3, and 10 μm diameters as a representative sample of known fiber diameters in the feline pudendal nerve[91]. The 10 μm diameter axons were used to indicate activation of a mixed fascicle and the smaller diameters indicated activation of sensory fascicles.

For each of the 5 nerves, three copies were created. A nerve cuff was placed on each nerve identically for each nerve copy creating 15 models. For each set of three models utilizing the same nerve copy, the first copy had the nerve cuff rotated by 0 degrees, the second copy had the nerve cuff rotated by 120 degrees, and the third copy had the nerve cuff rotated by 240 degrees. Across each of the 15 models, stimulation was applied in bipolar, guarded, and full cuff configurations

across different contacts (see Figure 4-2c for examples). Bipolar stimulation current was delivered through pairs of proximal cathodic and distal anodic contacts aligned along the z direction and had 4 unique sets of contact combinations. Guarded stimulation was applied through a proximal cathodic contact with each adjacent contact acting as an anode and had 4 unique sets of contact combinations. For full-cuff stimulation, all proximal contacts were cathodes and all distal contacts were anodes, so only one unique set of contacts was possible. In total, 135 simulations were run for each of the four fiber diameters, across all nerves, cuff rotations, and stimulation configurations.

4.3.4.2 10 and 16 Contact Cuff Simulation

This simulation was created to evaluate how additional cuff electrode contacts can affect fascicular selectivity. In four separate simulations, a fiber with a diameter of 2, 5.7, 7.3, and 10 μm was placed in the center of each fascicle for each modeled nerve. One of the two nerves with a diameter less than 1.20 mm was randomly selected and placed inside a 10-contact cuff. The chosen nerve had 6 fascicles. One of the three nerves with a diameter greater than 1.20 mm was chosen at random and placed inside a 16-contact cuff. The chosen nerve had seven fascicles. The nerve cuffs are illustrated in Supplemental Figure 4-8. Each nerve cuff was applied to its respective nerve with a 0-degree rotation. Bipolar stimulation was applied through all 5 pairs of contacts for the 10-contact cuff and all 8 pairs of contacts for the 16-contact cuff. Selectivity was compared between the 8-, 10-, and 16-contact cuff.

4.3.4.3 Randomly Placed 36-fiber Simulation:

This simulation was created to assess if a higher density of fibers per fascicle changed fascicular selectivity. Fibers with 2, 5.7, 7.3, and 10 μm diameters were modeled with MRG axons. For each diameter, 9 fibers were placed randomly throughout each fascicle resulting in 36 total fibers per fascicle. The two smaller nerves that fit in the 1.20 mm diameter cuff were used in this simulation. Two of the larger diameters nerves, excluding the nerve with 14 fascicles, were also used in this simulation. Each of the four nerves had 8-contact cuffs applied to them with rotations of 0, 120, and 240 degrees resulting in 12 total models. Only bipolar stimulation was used in this simulation.

4.3.4.4 Randomly Placed 40-fiber Simulation:

This simulation was created to examine if a more realistic distribution of fiber diameters led to changes in fascicular selectivity[91]. Forty fibers were placed randomly in each fascicle to maximize coverage of the entire fascicular area. The fiber diameters were continuously and uniformly distributed between 2 and 13 μm[91]. The diameter of activated fibers was used to calculate the overall percentage of activated fibers in a sensory or mixed fascicle. The overall percentage of activated fibers was used to calculate the fascicular selectivity. For all five nerves, nerve cuffs were applied with rotations of 0, 120, and 240 degrees, resulting in 15 total models. Only bipolar stimulation was applied.

4.3.5 Data Analysis

We calculated the selectivity of each fascicle using a modified version of the fascicular selectivity presented in other studies and shown in Equation 1[80,83,85]. For simulations with discrete fiber sizes, the fascicular selectivity was determined for afferent fascicles populated with 2, 5.7, or 7.3 μm diameter fiber and compared to fascicles populated by a 10 μm diameter fibers. In simulations with one fiber of each fiber size per fascicle, the activation threshold for a 2, 5.7 or 7.3 μm diameter fiber in fascicle *i* is compared against the activation threshold for a 10 μm diameter fiber in every other fascicle *j*. If the threshold of the fiber in *j* is less than the threshold for the fiber in *i* then the *j*th fascicle was considered activated. The selectivity was calculated as 1 minus the ratio of activated fascicles to total nontarget fascicles (Equation 1). The selectivity ranges from 0 to 1 with 0 indicating no selectivity and 1 indicating perfect selectivity. At a selectivity of 1, all fibers in the target fascicle are activated before any 10 μm fibers in any other fascicle. For a given nerve cuff rotation and stimulation method (bipolar, guarded), if a fascicle had multiple selectivity values when stimulated by different contacts, then the highest selectivity was included in the data analysis.

Equation 1: $Selectivity_i = 1 - \frac{1}{m-1}\sum_{j=1, j\neq i}^{m} u_j$

In the simulation with 36 fibers per fascicle, the fascicular selectivity was calculated in a similar manner. For 2, 5.7, and 7.3 μm fibers in a fascicle *i*, the stimulation configuration that required the least current to activate all 9 fibers of that diameter was set as the threshold current

and was used to determine the fascicular selectivity. For every other fascicle *j,* the proportion of 10 μm fibers activated before the threshold current was calculated. These values were then averaged across fascicles and subtracted from 1 to yield the selectivity for the fascicle and fiber size of interest.

In the simulation with 40 fibers per fascicle, the fascicular selectivity was calculated for afferent fibers with diameters of 2, 3, 4, 6, and 8 μm. These fiber diameters were chosen to demonstrate how selectivity changes with the percentage of activated afferent fibers. In pudendal afferent fascicles, 91% of fibers are larger than 2 μm. Additionally, 64%, 43%, 20%, and 10% of the afferent fibers are larger than 3, 4, 6, and 8 μm respectively (Supplemental Figure 4-11A)[91]. To calculate selectivity for an on-target fascicle in a nerve, the activation threshold that activated all fibers of a set afferent fiber diameter was found. In that same nerve that same activation threshold was compared against all the activation thresholds of all fibers to find the smallest diameter fiber that was activated in every other off-target fascicle. The smallest fiber that was activated in each off-target fascicle was used to find the percentage of fibers that would be activated if the fascicle had the same fiber distribution as a mixed fascicle (Supplemental Figure 4-11B). The percentage of activated fibers for each off-target fascicle *j* was averaged using Equation 1 to calculate the selectivity for each on-target fascicle *i*.

Data was not normally distributed and reported as median with interquartile range (IQR) unless explicitly reported as mean (standard deviation; s.d.). We used a Kruskal-Wallace test and a post hoc Dunn's test with Bonferroni correction to compare selectivity between bipolar, full cuff, and guarded stimulation. To determine statistical significance, α was set to 0.05.

4.4 Results

Across the five modeled nerves there were 40 total fascicles with a mean of 8.0 (s.d. = 3.4) fascicles per nerve (Supplemental Figure 4-12). Four of the nerves had 6 or 7 fascicles and one nerve had 14 fascicles. The nerves had an average area of 1.53×10^6 μm^2 (s.d. = 0.74×10^6 μm^2) and an average diameter of 1366 μm (s.d. = 314 μm). The average fascicle area was 51.3×10^3 μm^2 (s.d. = 53.7×10^3 μm^2) with an average diameter of 221 μm (s.d. = 130 μm).

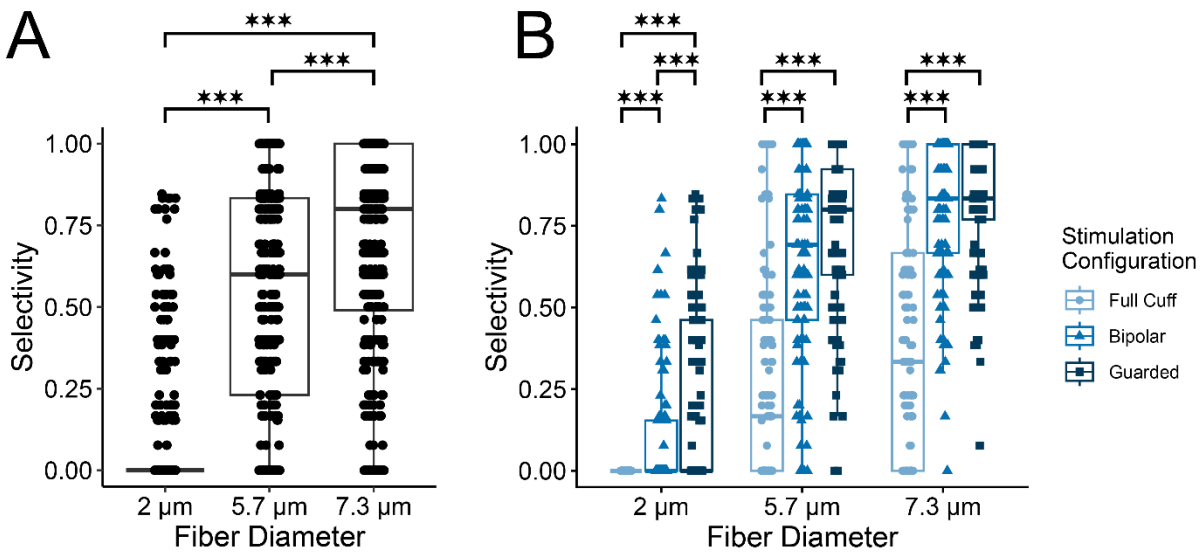


Figure 4-3: Box plots of fascicular selectivity for the centrally placed four fiber simulation. A) Selectivity comparison across fiber diameters. b) Selectivity comparison for different stimulation configurations for each fiber diameter. The borders of each box correspond to the first and third quartiles (interquartile range [IQR]). The upper whisker extends to the largest value that is less than or equal to 1.5 times the IQR from the upper box boundary. The lower whisker extends to the smallest value than is no more than 1.5 times the IQR from the lower box boundary. Significance was examined with a post-hoc Dunn test with Bonferroni correction. *** denotes significant difference ($p < 0.001$).

In the centrally placed 4-fiber simulation there was a significant difference ($p < 0.001$) between the selectivity of fascicles populated with 2, 5.7, and 7.3 µm diameter fibers (Figure 4-3A). There was also a significant difference in selectivity when comparing across stimulation configurations for each afferent fiber diameter (Figure 4-3B). For 2 µm fibers, the selectivity was significantly different between each cuff configuration (each $p < 0.001$). For both 5.7 µm and 7.3 µm fibers, the selectivity for the full cuff configuration was significantly lower than the bipolar ($p < 0.001$) and guarded ($p < 0.001$) configurations. Selectivity was not compared within stimulation configurations for different fiber diameters. With bipolar stimulation, the mean fiber activation threshold was 269 µA (s.d. = 422 µA).

In the 10- and 16-contact simulation there was not a significant difference in selectivity between the 8-contact and 10-contact cuff designs for each of the three tested fiber diameters (Figure 4-4A). There was also not a significant difference in selectivity between the 16-contact cuff and the 8-contact cuff for each fiber diameter (Figure 4-4B). In the randomly placed 36-fiber simulation there was not a significant difference in selectivity for each diameter when bipolar stimulation was applied (Figure 4-5). However, in the 36-fiber model the selectivity was lower for

5.7 and 7.3 µm fibers. With bipolar stimulation, the mean fiber activation threshold for the 36-fiber simulation was 331 µA (s.d. = 491 µA).

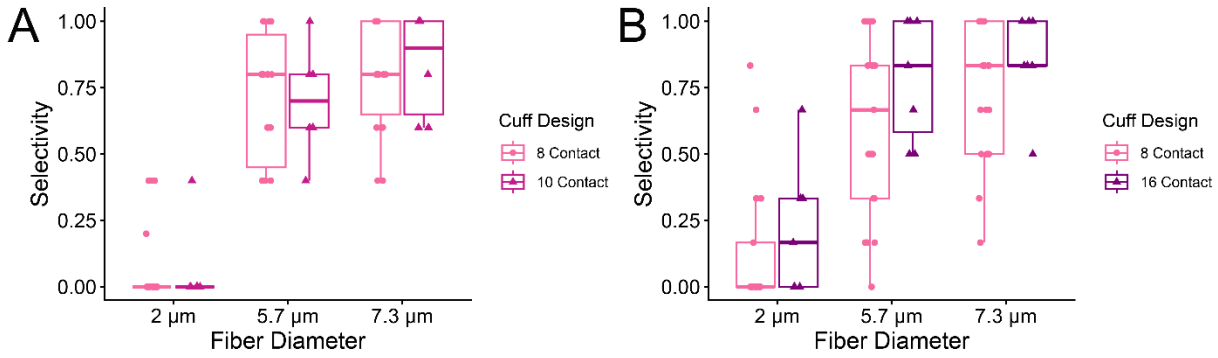


Figure 4-4: Selectivity of 8-, 10-, and 16-contact nerve cuffs with bipolar stimulation for fascicles with afferent fiber diameters of 2, 5.7, and 7.3 µm. A) Selectivity for an 8-contact and 10-contact cuff when both are used to stimulate the same 1.2 mm nerve. B) Selectivity for an 8-contact and 16-contact cuff when both are used to stimulate the same 1.91 mm nerve. Box plots are organized as in Figure 4-3.

In the randomly placed 40-fiber simulation there was a significant effect of fiber diameter on fascicular selectivity. The fascicular selectivity for bipolar stimulation was significantly dependent on the afferent fiber diameter. For diameters of 8, 6, 4, 3, and 2 µm, each fiber had a significantly lower fascicular selectivity ($p < 0.001$) than all fibers larger than itself (Figure 4-6). With bipolar stimulation, the mean fiber activation threshold for the 40-fiber stimulation was 186 µA (s.d. = 250 µA).

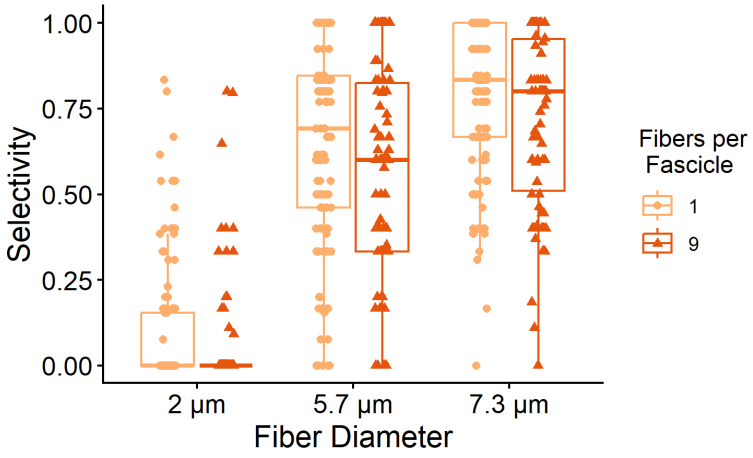


Figure 4-5: Fascicular selectivity with bipolar stimulation for the randomly placed 36-fiber experiment. Box plots are organized as in Figure 4-3.

4.5 Discussion

Overall, these results highlight a significant relationship between fiber diameter and fascicular selectivity. It is clearly possible to selectively recruit afferent pudendal fibers with a multi-contact cuff electrode. However, selectively activating a large proportion of the sensory fascicles will be difficult as it is more challenging to activate smaller diameter fibers with extra-neural stimulation. The organization of stimulating contacts plays a major role in the performance of fascicular selectively.

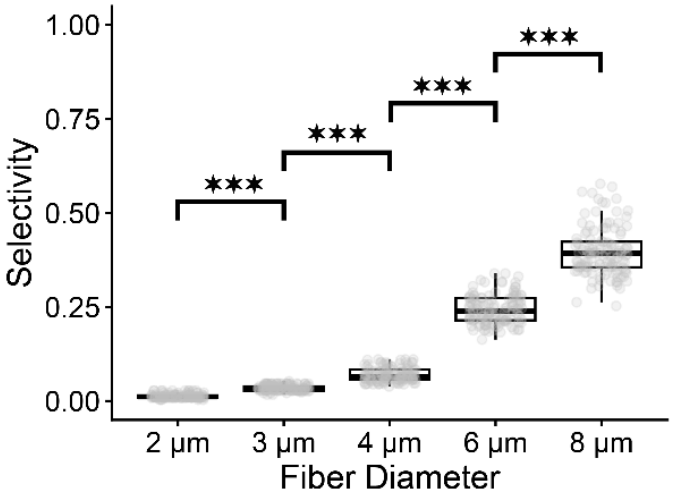


Figure 4-6: Fascicular selectivity for the randomly placed 40-fiber experiment. Box plots are organized as in Figure 4-3. *** denotes significant difference ($p < 0.001$).

There was a significant effect of fiber diameter on selectivity, greater than initially expected. It is well known that larger diameter fibers have lower stimulation thresholds[92], so it is not surprising that higher selectivities were achievable for larger diameter afferent fibers. In the model with a fiber placed at the center of each fascicle, targeted stimulation with a multicontact cuff significantly improved selective activation of afferent fibers when compared to full cuff stimulation (Figure 4-3B). Selectivities were similar for 7.3 µm fibers for bipolar and guarded configurations. The large difference between the bipolar and guarded configurations for 5.7 µm fibers suggests that better stimulation configurations can improve the selective activation of small diameter fibers. While there is a wide range of afferent fiber diameters in feline sensory pudendal

nerves, small diameter (< 5 μm) Aδ fibers make up over half of the myelinated fibers (Supplemental Figure 4-11)[159,160]. Selectivity was occasionally achievable for fascicles with 2 μm fibers, as 6% of these fascicles achieved greater than 50% selectivity with bipolar stimulation and 17% of fascicles achieved greater than 50% selectivity with guarded stimulation. However, no selectivity was achievable for most fascicles, even with more spatially focused stimulation configurations (Figure 4-3B). This is concerning because roughly 36% of afferent fibers are smaller than 3 μm[91] and its not currently known what percentage of afferent fibers need to be activated to achieve bladder activation responses seen in preclinical experiments[127]. On the other hand, it is not known how many off-target fibers can be activated before causing discomfort and limiting the amount of stimulation that can be applied. Choosing a 10 μm fiber may be too restrictive in minimizing off-target effects. Advancement in methods to improve small diameter fiber activation through manipulation of stimulation waveform characteristics may improve recruitment of these fibers[161–165]. These results likely did not depend on the number and location of fibers in each fascicle. It has been shown that the position of a fascicle relative to an electrode can affect neural activation[158,166]. A future study could investigate if sensory and mixed fascicles have different relationships between electrode-to-nerve distance and fiber activation. We did not observe a significant difference in selectivity with bipolar stimulation between the 4-fiber per fascicle model and the 36-fiber per fascicle model (Figure 4-4). However, the median selectivity for each fiber diameter of the 36-fiber model was lower. The results from the centrally placed 4-fiber simulation showed fascicular selectivity values similar to other published results[12,84], but the randomly placed 40-fiber simulation showed that fascicular selectivity may be more difficult than previously predicted.

With different distributions of fiber diameters for afferent and mixed fascicles, achieving a fascicular selectivity greater than 50% with bipolar stimulation was rare, even for fibers larger than 7 μm. If a larger percentage of afferent fibers need to be activated to see therapeutic benefits, then changes to the cuff design and stimulation techniques are needed to increase the selectivities seen in Figure 4-5. However, afferent fascicles tend to have smaller diameter fibers and more fibers than mixed fascicles[91] (Supplemental Figures 4-11A and 4-11B). At a larger fiber diameter such as 8 μm, more afferent fibers are activated than efferent fibers. Activating large diameter fibers could maximize the afferent activation while minimizing off-target efferent activation, if fibers of different sizes contribute equally to bladder activation.

The simulation generated activation thresholds varied between models but were generally similar in amplitude. The activation threshold were in the same order of magnitude as the stimulation amplitudes required to generate external anal sphincter and external urethral contractions in the related *in-vivo* experiments[90]. While the comparisons are not robust, they lend some credibility to outputs of the model. Activation thresholds for fibers were compared against one another to calculate fascicular selectivity. Therefore, the absolute values of the activation thresholds do not have to perfectly match the *in-vivo* values to yield informative results.

The average fascicular area was 1/30th of the average nerve area and there was a wide range of fascicle diameters in our nerve diameters. The feline nerve diameters used for this model are almost half the diameter of the 3.3 mm human pudendal nerve diameters used for computational models of the human pudendal nerve[12,30,84]. The feline fascicular diameters are very similar to the fascicular diameters in the human pudendal nerve, as both have an average observed fascicular diameter between 200 and 250 μm[30]. This is important because fascicular thickness is proportional to perineurium thickness, and perineurium thickness affects activation threshold[166]. The relationship between fascicle diameter and perineurium thickness is not well studied but thought to vary by species and nerve[148,167]. The ratio of fascicle thickness to perineurium thickness is likely different for humans and felines which may affect the activation thresholds. There are almost three times more fascicles in the human pudendal nerve[30] than the feline pudendal nerve, based on our feline samples. Still, anatomy can vary widely as one of the feline nerves had twice as many fascicles as the other feline nerves, highlighting the potential variation in pudendal nerve composition. We did not perform a sensitivity analysis to examine whether this high fascicle-count nerve yielded different selectivities than the other nerves. Any observed differences between the thresholds for the human and feline nerves will likely be caused by differences in the size of the nerve, thickness of perineurium, and number of fascicles rather than the size of the fascicles[158].

Previous computational research has shown that increasing the number of contacts in a cuff electrode can improve selectivity[84]. While the 10- and 16-contact cuff electrodes did have higher median selectivities than the 8-contact cuff (Figure 4-3), the difference was not significant. This is surprising because the 8-contact cuff did not completely encircle the nerve with contacts. This simulation only looked at bipolar stimulation and it is possible that another stimulation configuration could have significantly improved selectivity. The 10- and 16-contact cuffs completely encircle the nerve with contacts, which should enable the activation of more fascicles

and a lower selectivity. These results can likely be explained by the cuff and nerve geometry. To replicate the dimensions of the physical cuff, the cuff diameter was not changed. The additional contacts were placed on the empty space of the cuff which was the furthest away from the nerve. Any space between the nerve and cuff was filled with conductive fluid that may have shunted away most of the current and impeded recruitment of nearby fibers. This aligns with previous observations that the gap between the nerve and stimulation contacts needs to be minimized for effective extra-neural stimulation[168].

Minimizing the gap between the nerve and electrode is difficult for a nerve cuff with a fixed diameter. Helical and spiral nerve cuffs address this issue with spiral designs that gently encircle the nerve[169–171]. The spiral can allow some self-sizing on the nerve, placing electrodes directly on the nerve surface while minimizing compression and nerve trauma[169,170]. Current designs add more contacts to self-sizing designs[172]. These mulitcontact spiral electrodes can provide selective stimulation and minimize the electrode-to-nerve distance. Alternatively, flat interface nerve electrodes (FINE) solve the electrode to nerve gap in a different way. They reshape the nerve into a long flat cross-section to minimize the electrode-to-nerve distance and bring fascicles in the center of the nerve closer to the edges and therefore closer to the contacts[173]. These electrodes also feature multiple contacts to enable maximum selectivity[174]. Both self-sizing and FINE electrodes can reduce the gap between the nerve and nerve cuff and lead to improved selectivity.

A limitation of this study is that there were no C fibers incorporated in the model. C-fibers are not typically included in computational models of nerve stimulation unless specifically looking for activation of unmyelinated fibers[175–177]. These fibers transmit painful signals and if activated can limit the amplitude of delivered current. C fibers are also unmyelinated and have small diameters making them difficult to activate with electrical stimulation. As the majority of fibers coming from the dorsal genital nerve are myelinated[178,179], if stimulation is delivered at tolerable amplitudes, then the number of activated unmyelinated fibers should be small. Another limitation is that a random distribution was only used once for the simulations with random fiber locations. A uniform distribution would have allowed for more generalizable results. With random fiber locations there can be gaps in the nerve where no fibers reside and activation threshold cannot be calculated. A key assumption in this study is that the fascicular organization in the main trunk of the pudendal nerve mirrors the targets of distal branches. Recent studies in the vagus nerve have

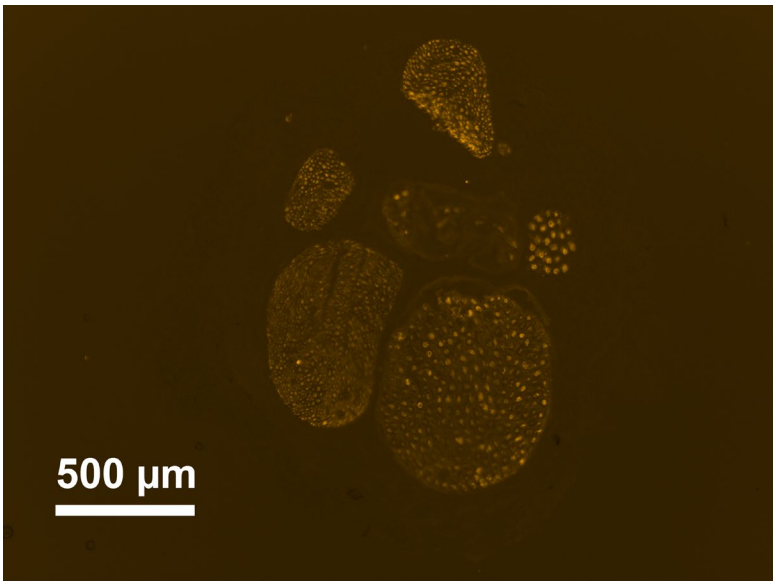
shown that there is a constant shuffling of axons between fascicles[180]. If this happens in the pudendal trunk, then selective activation of afferent fibers in fascicles that innervate sensory distal targets may be challenging. A mixing of sensory and motor fibers could limit selective activation of sensory fibers. While the cuff dimensions and nerve histology were taken from previous experiments, our results could not be directly compared to *in-vivo* experiments. This limits our ability to translate these results into relatable findings with confidence. However, we can compare the activation thresholds of fibers in this model with the activation threshold of efferent targets from the related *in-vivo* experiments. We tested a small subset of possible stimulation configurations. Optimizing the contacts used and current delivered can improve selective activation of nerve targets[84,181–184]. However, without prior knowledge of the fascicular organization, optimization can be difficult and time consuming[184]. The goal of this analysis was to demonstrate the feasible selectivity of a nerve cuff with simple stimulation configurations to replicate potential *in-vivo* settings.

This computational study suggests that achieving a high selectivity with a multicontact cuff is possible but difficult with this specific cuff design, which was utilized to compare to *in-vivo* results. Increasing the number of contacts, decreasing the circumference coverage of each contact, and minimizing the gap between each contact and the nerve could improve selectivity of the cuff. The degree of selectivity is heavily dependent on the diameter of the afferent fibers being activated and the proportion of afferent fibers that need to be activated to achieve a therapeutic benefit. Future computational studies can investigate the ability of different stimulation configurations and waveforms to improve the selective activation of pudendal afferent fascicles. More work is needed to improve cuff designs and understand the mechanisms behind stimulation driven bladder activation if a multi-contact nerve cuff is going to be used to activate the bladder.

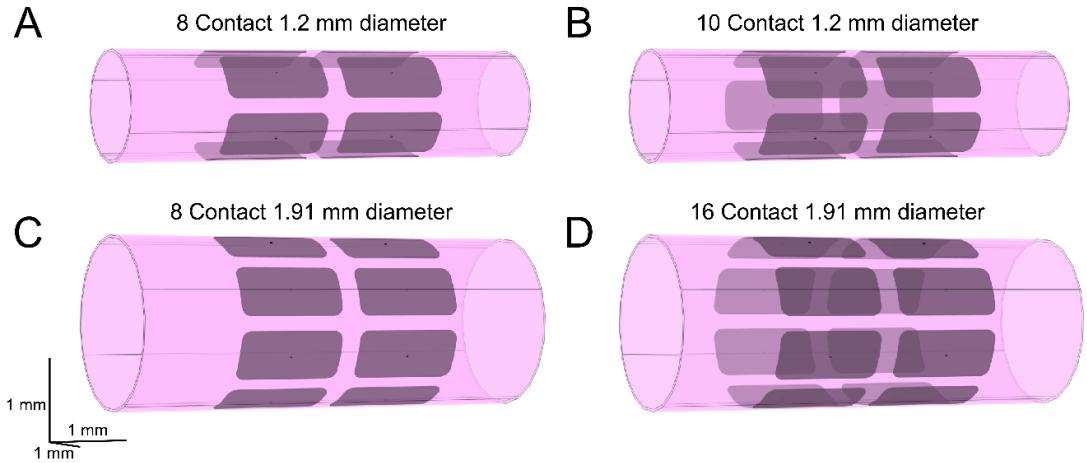
4.6 Acknowledgements

Thank you to Scott Lempka, Adrian Porras, and Liam Matthews for their help and guidance in implementing and verifying the computational models used in this study.

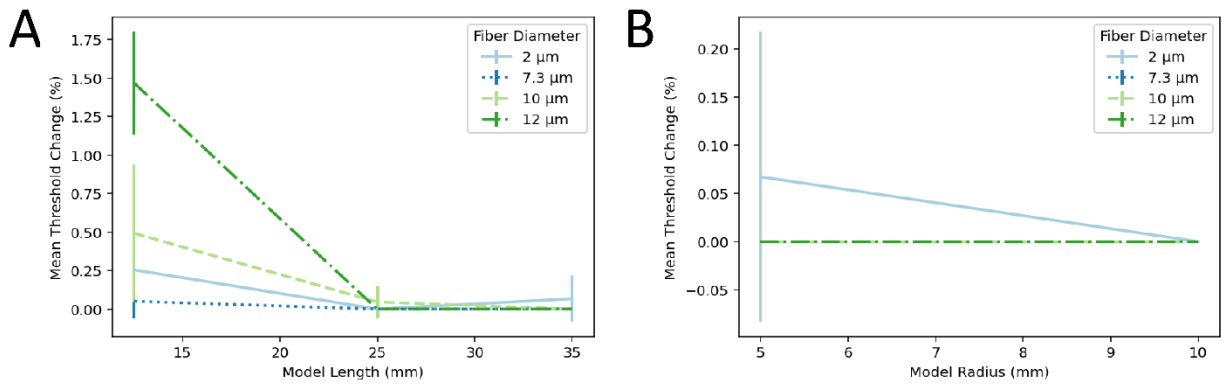
4.7 Supplemental Figures



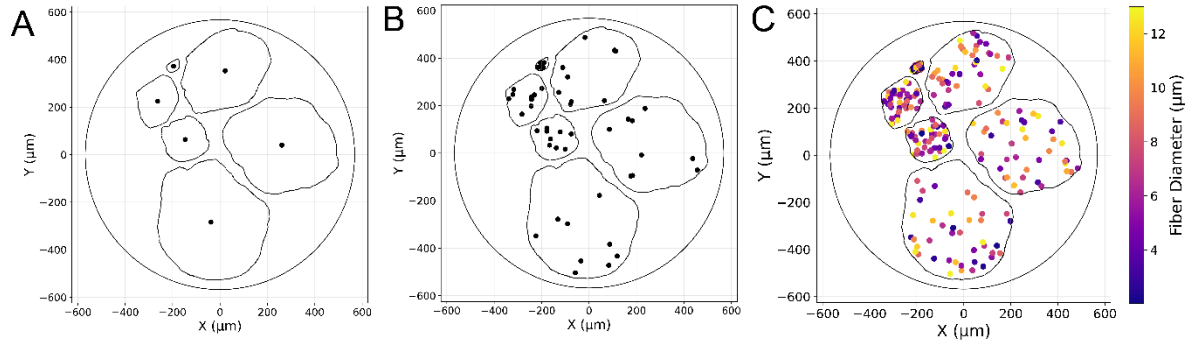
Supplemental Figure 4-7: Anti-Neurofilament 200 Antibody was used to confirm suspected fascicles contained myelinated fibers. Myelinated fibers are identified in yellow.



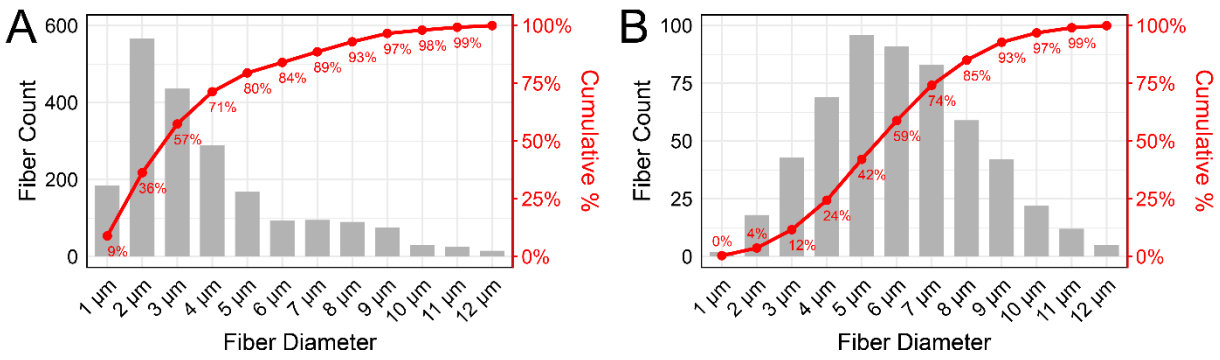
Supplemental Figure 4-8: 3D visualization of multicontact nerve cuffs. An 8-contact (A) and 10-contact (B) nerve cuff with diameters of 1.20 mm. An 8-contact (C) and 16-contact (D) nerve cuff with a diameter of 1.91 mm.



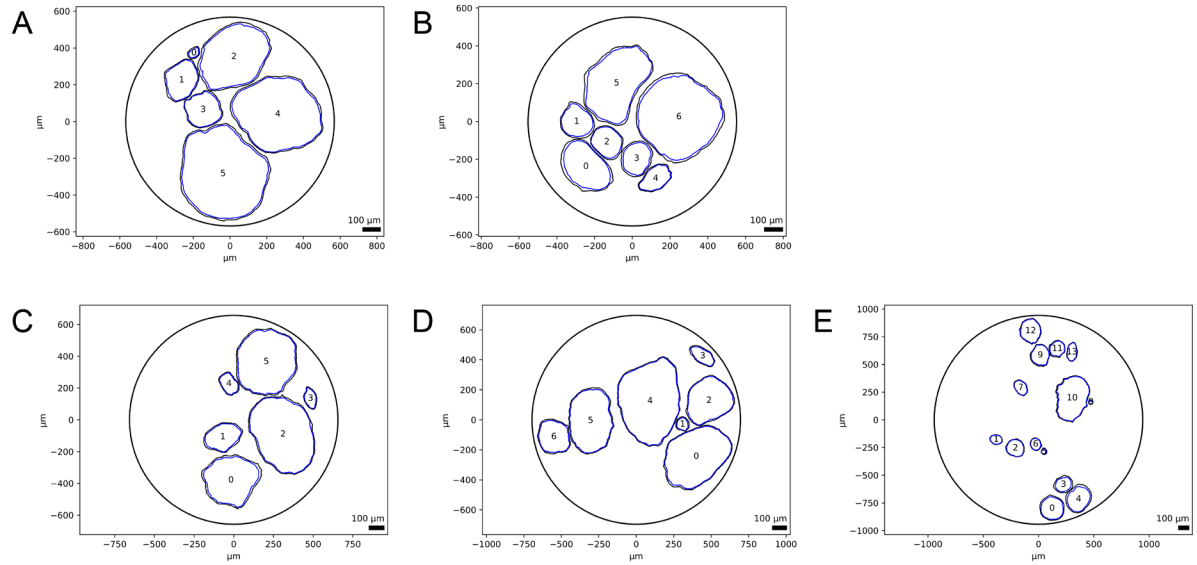
Supplemental Figure 4-9: The average activation threshold is minimally impacted by the A) length and B) radius of the model. A) Mean threshold is compared to a model 50 mm in length. B) Mean threshold is compared to a model 25 mm in length. The errors bars show standard deviations. Thresholds were tested for fibers with diameters of 2, 7.3, 10, and 12.8 µm.



Supplemental Figure 4-10: Visualization of fiber distribution within fascicles for a single nerve. Each dot represents a single modeled fiber. A) A 2, 5.7, 7.3 and 10 µm fiber were each placed at the same point in the center of each fascicle. B) Nine fibers of each diameter were placed randomly throughout each fascicle. C) 40 fibers were placed randomly throughout each fascicle. Each fiber had a diameter randomly selected from a uniform distribution between 2 and 13 µm.



Supplemental Figure 4-11: Fiber counts for different diameter fibers with cumulative percentage of fibers displayed on the right-hand axis. A) Afferent fiber counts for the sensory branches of the pudendal nerve (dorsal nerve to the penis and cranial urethra). B) Efferent fiber counts for the mixed branches of the pudendal nerve (external anal sphincter, deep perineal, constrictor vulvae, and bulbospongiosus). The figure was created using data from Martin, Fletcher, and Bradly, 1974[91].



Supplemental Figure 4-12: Labeled nerve fascicles for the five nerves used in the study. Cross sections A and B came from the same feline and were placed in the 1.20 mm diameter cuff. Cross sections C, D, and E were placed in the 1.91 mm diameter cuff. Sample C and D came from the same feline. The diameter for each nerve is as follows: A) 1.1 mm, B) 1.1 mm, C) 1.3 mm, D) 1.4 mm, E) 1.91 mm.

Chapter 5 Discussion

Lower urinary tract symptoms and chronic pelvic pain are burdensome and widespread yet seldom discussed. Pudendal neuromodulation is a currently available off-label treatment that can uniquely address both issues. However, gaps remain in our understanding of how pudendal nerve stimulation can affect the lower urinary tract and pelvic floor. In this dissertation I investigate the capability of pudendal nerve stimulation to activate afferent and efferent pudendal nerve targets. I have demonstrated that current pudendal nerve stimulation devices can evoke changes in pelvic floor targets in anesthetized and awake humans, via physiological recordings. I have also demonstrated, via biologically informed computational models of nerves and nerve cuffs, that functional selective stimulation of small afferent fibers in the pudendal nerve is feasible but difficult and dependent on currently unknown biological details.

5.1 Summary of Clinical Results

In Chapter 2 I quantified the impact of patient, surgical, and stimulation factors on external anal sphincter recruitment and patient outcomes during intraoperative pudendal nerve stimulation. This was the first study to collect patient specific data on the distance between the pudendal nerve and stimulating contacts on the implanted lead. This study used mixed modeling techniques to quantify the impact of various factors on the current required to activate the nerve and the strength of nerve activation. Based on the inverse relationship between current and distance[185], I hypothesized that reduced electrode to nerve distances would lead to better nerve recruitment and patient outcomes. My results provided evidence to support this hypothesis and showed that increased electrode-to-nerve distance is correlated with increased recruitment threshold, decreased external anal recruitment, and reduced symptom improvement. In sacral neuromodulation, the ideal lead placement will activate the sacral nerve with all four electrodes using a voltage less than two volts[186]. However, there is conflicting data on the correlation between ideal lead placement and patient outcomes[187,188]. Pudendal neuromodulation uses the same voltage target for lead placement[11]. My results suggest that the level of charge required to activate the pudendal nerve may be a better metric to guide lead placement than the number of contacts below two volts. A

post-hoc power analysis determined that the sample size was large enough to detect our findings but additional studies to support these results would be beneficial.

In current practice, live fluoroscopy and anal sphincter recruitment threshold are used to guide lead placement[11]. These methods do not inform clinicians about the exact location of the nerve. Better knowledge of the pudendal nerve's location in the pelvis could improve lead placement. Fiber tractography is one way to visualize the locations of peripheral nerves, but it is a time-intensive and labor-intensive practice[189,190]. Even if tractography was used to create a model of the pudendal nerve, there are no current methods to relate the lead locations to the mapped pudendal nerve. Therefore, it would provide little help to the clinician in minimizing electrode-to-nerve distance during the implant surgery. My results suggest that the external anal sphincter recruitment threshold and magnitude of the external anal sphincter contraction can be used as a proxy for electrode-to-nerve distance. This provides another tool that clinicians can use to guide placement of the lead. My results show that reduced electrode-to-nerve distance is significantly related to patient symptom improvement from pudendal neuromodulation. As anal sphincter recruitment is related to electrode-to-nerve distance, anal sphincter recruitment may be directly related to symptom improvement as well.

This study also provided some rarely reported information on lead migration during pudendal neuromodulation. MRI and CT scans were used to identify the location of the quadripolar lead in the pelvis. When the lead position during surgery was compared to the lead position during the CT scan a few weeks later, there were several occurrences where the lead position shifted by one contact or greater. While lead migration is uncommon when reported[9,66], this poses an interesting question about the severity of lead migration for pudendal implants. A follow-up study could do CT imaging to evaluate the rate and severity of lead migration in pudendal neuromodulation. Scans could be done before surgery, immediately after lead implantation, and several months after. After a few months enough scarring should have occurred to prevent further lead migration[66,191,192]. In these same studies it would be very interesting to have participants complete symptom surveys before and after device implantation, as we did in our study. Symptom change could be compared to electrode-to-nerve distance and lead migration with a larger sample size. More research on the causes of adverse events like lead migration and a more streamlined implantation process, potentially informed by results from this aim, could increase physician and industry interest in this therapy. A deeper understanding of pudendal neuromodulation would be

very important for attempts to promote pudendal neuromodulation as an FDA approved therapy for lower urinary tract symptoms and pelvic pain.

I quantified the impact that participant factors and diagnoses had on anal sphincter recruitment. In my results there was not a significant relationship between participant age, BMI, or sex and anal sphincter recruitment, indicating that pudendal nerve stimulation can activate the nerve equally well across patients. Additionally, there was a significant reduction in anal sphincter recruitment when patients had diagnoses of overactive bladder and retention, but not incontinence or pelvic pain. At first glance this seems to indicate that patients with overactive bladder and retention may have underlying issues with nerve activation. This is not surprising because both overactive bladder and small fiber neuropathy, which can damage peripheral nerves, are comorbidities of diabetes[41,193]. However, this study had an unbalanced distribution of participants with and without overactive bladder or retention, so I cannot make this claim with confidence. A future study could focus on recording anal sphincter activation from pudendal nerve stimulation in individuals with pelvic pain and without overactive bladder or retention. Anal sphincter activation was observed in every patient with a successful lead placement. The relative ease in activating the efferent fibers that control the external anal sphincter indicated that activating other efferent branches of the pudendal nerve might be possible as well. All the lead implantation surgeries had local or general anesthesia; therefore, it is not clear if enough stimulation can be delivered to activate efferent targets before discomfort occurs in an awake and non-anesthetized individual.

I provided evidence to support the continued use of current stimulation parameters in pudendal neuromodulation. The same implanted pulse generator is used in sacral neuromodulation and pudendal neuromodulation[11,115]. It is common to use the same stimulation parameters for both as well[115,117]. However, there is no published evidence specifically validating the use of sacral parameters in pudendal neuromodulation. When looking at the maximum (450 μs), minimum (60 μs), and standard (210 μs) pulse width for pudendal neuromodulation, the standard pulse width provides a better balance of threshold current and threshold charge, two important parameters for device longevity. The progress made in my first aim represents only a first step towards a better understanding of how well nerve recruitment works in pudendal nerve stimulation. Where Chapter 2 goes into detail about the effects of pudendal nerve stimulation on the external anal sphincter in

the operating room, Chapter 3 investigates the impact of pudendal nerve stimulation on the lower urinary tract in awake, responsive individuals.

In Chapter 3 I characterized lower urinary tract pressure changes from pudendal nerve stimulation in awake non-spinal cord injured human participants, which has not been previously reported. Reflexive contraction of the external urethral sphincter has been demonstrated in individuals with spinal cord injury via stimulation of pudendal branches[194]. We hypothesized that pudendal nerve stimulation at tolerable amplitudes could drive measurable changes in the lower urinary tract. We used a multichannel catheter capable of recording multiple pressures along the bladder and urethra simultaneously. I demonstrated that stimulation at tolerable amplitudes could cause direct motor responses in the urethra. The urethra contractions occurred with low and high frequency stimulation in most individuals. High frequency stimulation generated tetanic urethral contractions with large increases in pressure. As external urethra contraction contributes to continence during stress[195], high frequency stimulation could be useful for preventing urine leakage[90,126]. Urethra contractions were not observed in every individual. In these cases, the electrode may have been closer to off-target fascicles than the fascicles that go to the external urethral sphincter. During pudendal stimulation, the fibers in the closest fascicles are activated first, which may have led to discomfort and pain from activation of fibers in the off-target fascicles before the urethra could be recruited. To ensure that pudendal nerve stimulation can consistently generate urethra contractions large enough to prevent leakage, off target activation needs to be minimized during lead implantation. A future study could have patients use stimulation configurations that recruit the urethra at home to learn if urethral recruitment has any bearing on symptom improvement.

As a part of our experimental procedure, participants attempted to void with and without pudendal stimulation. We observed how the lower urinary tract pressure changed in real-time during a void with multiple sensors in the bladder and urethra. This is not possible with traditional methods for a micturitional urethra pressure profile[196,197]. We observed a clear drop in mid-urethral pressures, an increase in bladder pressure, and a continuous and consistent drop in pressure from the bladder to the outer urethral opening. This shows that the entirety of the lower urinary tract is altered during voiding and demonstrates the role of the urethra in maintaining continence[198]. Stimulation had no significant effect on voiding efficiency or flowrate, though the sample sizes were small which limits confidence in the findings. These results suggest stimulation works

through long term changes in central nervous system pathways rather than immediate changes in urethra or detrusor pressure[66]. Large long-term clinical studies with stimulation at 14 Hz and tolerable stimulation amplitudes would be beneficial to learn if there are measurable physiological changes in the LUT after pudendal neuromodulation.

This project has the first reported instance of a stimulation-driven reflexive bladder response in a non-spinal cord injured individual. Previous examples of stimulation evoked bladder contractions occurred in humans with spinal cord injuries[74,76]. Of the 13 tested individuals in our study, only one demonstrated stimulation driven bladder contractions. I hypothesize that this occurred because most individuals felt discomfort before enough charge could be delivered to activate the afferent fibers that drive bladder reflexes. With the current stimulation lead, fine control over the activation of nerve fibers is difficult or impossible. Electrode design changes could enable selective activation of afferent fibers. This finding hints at the underdeveloped potential of pudendal neuromodulation to treat bladder issues. The ability to control bladder state could improve symptoms from overactive bladder and retention and help those who require catheterization manage their bladder level. Chapters 2 and 3 showed the potential and the limit of current devices to treat lower urinary tract dysfunction. One major issue noted in both chapters is that the current electrode design has a limited ability to change how stimulation affects the nerve after the lead is placed. Chapter 4 highlighted the challenges of selective stimulation for a new design that may enable more control over stimulation within the nerve.

5.2 Summary of Computational Modeling Results

In Chapter 4 I use a computational model to analyze the performance of a multicontact cuff electrode on the feline pudendal nerve. While previous computational studies on pudendal nerve stimulation determined selectivity for generic fascicles in the pudendal nerve[12,84,85], they did not account for anatomical differences between sensory and mixed fascicles[91]. I incorporated these anatomical differences in my model and showed that selective activation of sensory fascicles is still possible. However, activating a large percentage of fibers in sensory fascicles without also activating fibers in mixed fascicles was not achievable with the tested methods. The number and type of afferent fibers that need to be activated to cause bladder responses is not yet known[199]. If a large percentage of the afferent fiber population needs to be activated to achieve therapeutic benefit, then an alternate design and more complex stimulation methods will need to be used. While previous studies have shown that increasing the number of contacts can improve selectivity,

they have diminishing returns[84,200,201]. Future modeling work could evaluate the impact of additional contacts while incorporating relevant anatomical data. One of the largest hurdles in the development of selective nerve cuffs is a lack of fundamental anatomical knowledge for humans. While work was done to count the distribution of fiber diameters in the feline pudendal nerve[91], this has not been done for the human pudendal nerve. Fiber diameters and fiber types have been measured in the human vagus nerve[202] and fiber number has been counted in the human spinal roots[203]. Therefore, techniques are available to measure fiber properties, but they have not been applied to the pudendal nerve. Any research that can fill this knowledge gap would be a boon to the field. When the pudendal anatomy is better understood it can be tested against alternate electrode designs to deliver selective activation.

I modeled two additional nerve cuffs, one with 10 contacts and another with 16, to investigate how additional cuff contacts would impact selectivity. While I hypothesized that selectivity would be increased with more contacts, there was no significant difference in selectivity between either cuff and the original 8-contact cuff. Each cuff had a fixed diameter which resulted in a gap between the cuff and the nerve. The nerve cuffs were shifted towards the nerve so that the original 8 contacts were within 10 micrometers of the nerve. However, as the additional contacts for the 10- and 16-contact cuff were placed on the other side of the nerve cuff, they were moved further away from the nerve when the cuff was shifted towards the nerve. Therefore, a large gap formed between the additional contacts and the nerve which likely allowed for more current to be shunted away, reducing activation of nearby fascicles[204]. The cuff size could have been modified to eliminate the gap between the nerve and the nerve cuff. However, the cuff diameters were restricted to align with the true cuff dimensions from the *in-vivo* study to gain insights into its performance. This modeling study illustrated the importance of the close fit between the nerve and the nerve cuff. The diameter of the pudendal nerve will likely not be known before the nerve is surgically accessed. To ensure that the nerve cuff is appropriately sized, either multiple sizes of cuff will need to be available, or the cuff will need to be resizable. In the computational model most fibers had activation thresholds in the same order of magnitude as the thresholds for visual muscle contractions in the related animal experiments[90]. Future studies could use other nerve cuffs from the literature and examine their fascicular selectivity with the pudendal fiber diameters used in chapter 4. Future studies could also create more robust comparisons between computational and *in-vivo* results. The exact position of nerve cuffs relative to each nerve need to be precisely

recorded with imaging and selective staining, or by using micro CT if the cuff contacts are nonmetallic[205]. Additionally, nerve imaging or histology could be used to identify fiber sizes and the distribution of afferent and efferent fascicles in the main trunk of the nerve.

5.3 Concluding Remarks

Overall, this thesis has improved our understanding of the effects of pudendal nerve stimulation on the lower urinary tract. While this therapy has been in use for over 20 years, there are still ways to improve its current clinical application, and opportunities to develop more effective devices. To expand access to pudendal neuromodulation, larger studies with longer follow-up times are needed to verify the relationship between electrode-to-nerve distance and patient outcomes. The same implantation technique was used for all participants mentioned in this paper but alternate approaches exist[66,206,207]. Additional large-scale studies are needed to compare techniques and determine a universal approach that would facilitate widespread adoption of pudendal neuromodulation. This could make pudendal neuromodulation more accessible to clinicians and therefore more widely available to patients. More widespread clinician adoption and more industry supported clinical studies could support FDA approval of pudendal neuromodulation. I showed that urethra and bladder contractions can occur during pudendal nerve stimulation in human subjects. We need more studies to demonstrate if stimulation driven lower urinary tract pressure increases can be an effective treatment for stress urinary incontinence or provide on demand bladder contraction. Multicontact nerve cuffs are clearly effective at selectively activating large fibers and driving efferent responses[172,205,208]. However, using them to selectively activate afferent fibers in the pudendal nerve is a difficult task. Updates need to be made to the cuff design that eliminate the electrode-to-nerve gap and alternate stimulation methods should be tested to improve selective activation of afferent fibers in the pudendal nerve. After verification of cuff designs in computational models and acute experiments, chronic implant of a nerve cuff in a large animal model could be done to see if the cuff can drive bladder pressure change over the life of the implant.

The future of neuromodulation for treatment of lower urinary tract dysfunction is exciting. Established medical device manufactures[209,210], startups[211,212], and research labs[90,213] are continuing to innovate. Continued industry investment is needed to fund more clinical studies and translate lab results into human treatments. If pudendal neuromodulation were more widely available and FDA approved, it could help more people receive the symptom relief they need. To

support this, most of the data from my second and third chapters is publicly available for use in future research[214]. I hope that my work can contribute to the development of this exciting and important field.

Appendix: Ovine Preclinical Experiment

A.1 Introduction

Animal experiments are widely used to study the lower urinary tract[13,14,72]. Sheep are a common animal model for studying the effects of neuromodulation on the lower urinary tract[215,216]. In this appendix I present data collected in a sheep using pudendal nerve stimulation to drive bladder contractions.

A.2 Methods

The experiment was prepared as described in Ortiz-Lopez, 2026[90]. After surgical access of the pudendal nerve and placement of a multicontact nerve cuff, the animal was switched to α-chloralose for anesthesia. Studies have shown that α-chloralose is minimally inhibitory towards autonomic reflexes[217]. The bladder was filled until leakage was observed. The pudendal nerve was stimulated at and above anal sphincter threshold for different combinations of contacts on the pudendal nerve cuff. The volume of urine released during each trial was recorded.

A.3 Results

At high amplitudes above the anal sphincter activation threshold, stimulation evoked bladder contractions occurred. As shown in Figure A-1 stimulation sometimes led to urethra contractions which increased bladder pressure and slowed or halted urine flow.

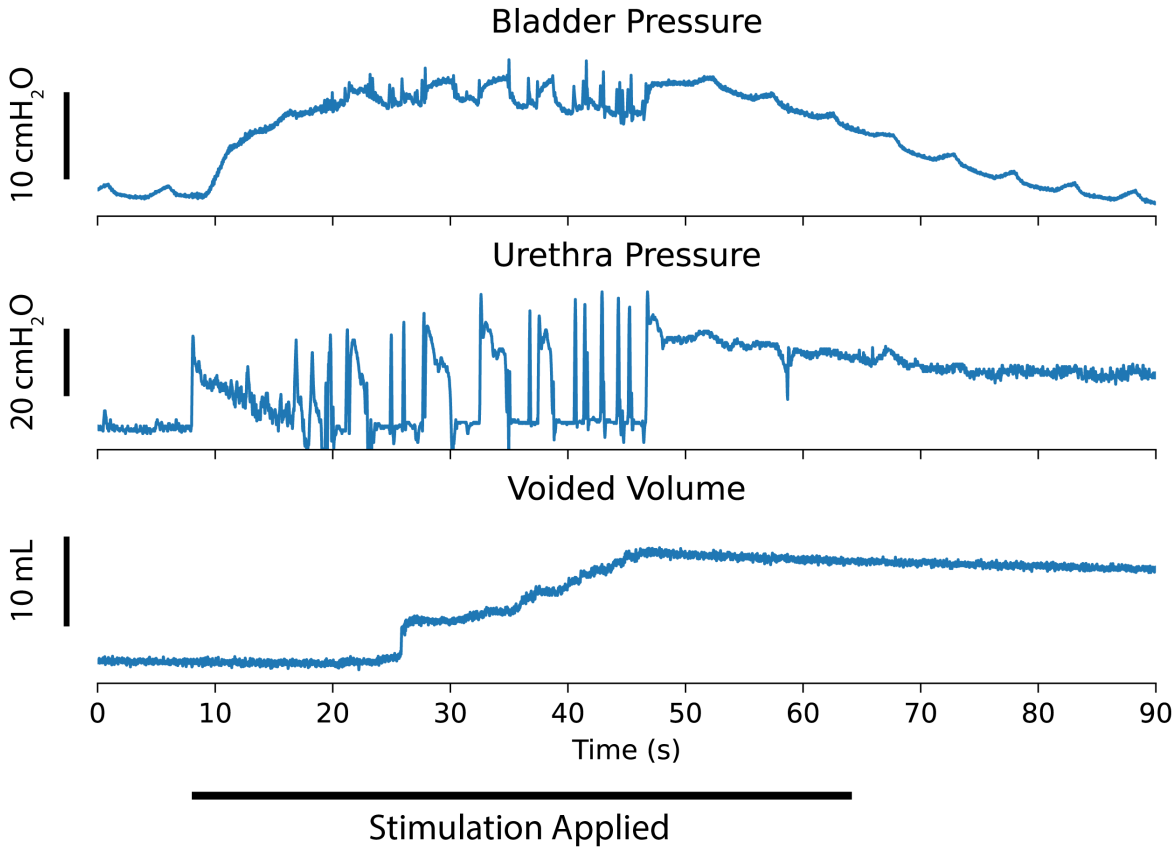


Figure A-1: An example of an evoked bladder contraction from pudendal nerve stimulation.

A.4 Discussion

Evoked bladder contractions from pudendal stimulation have been observed in smaller animal models. We demonstrated that evoked bladder contractions from pudendal stimulation are possible in sheep. However, across seven experiments in sheep only one demonstrated bladder contractions. More work needs to be done to consistently evoke bladder contractions in an anesthetized ovine animal model.

Bibliography

1. Moxham B, Pais D, Plaisant O, Kramer B. Moving beyond the use of anatomical terms derived from the Latin word pudere — An opinion piece. *Ann Anat - Anat Anz*. 2026;264:152773. doi:10.1016/j.aanat.2025.152773

2. Thakar R, Fenner DE, Hong CX. Anatomy of the Pelvic Floor, Perineum and Anal Sphincter. In: Sultan AH, Thakar R, Lewicky-Gaupp C, eds. *Pelvic Floor, Perineal, and Anal Sphincter Trauma During Childbirth*. Springer International Publishing; 2024:1-16. doi:10.1007/978-3-031-43095-4_1

3. Brodsky CN, Sitto HM, Wittmann D, et al. "There is a lot of shame that comes with this": A qualitative study of patient experiences of isolation, embarrassment, and stigma associated with overactive bladder. *Neurourol Urodyn*. 2024;43(8):1817-1825. doi:10.1002/nau.25557

4. Hawken N, Hakimi Z, Aballéa S, Nazir J, O. Odeyemi IA, Toumi M. Elicitation of Health-related Quality-of-life Concepts Associated with Overactive Bladder: A Qualitative Study. *J Health Econ Outcomes Res*. 2016;4(2):127-140. doi:10.36469/9816

5. Qudah S, Abufaraj M, Farah R, et al. The prevalence of overactive bladder and its impact on the quality of life: A cross-sectional study. *Arab J Urol*. 2024;22(1):39-47. doi:10.1080/2090598X.2023.2221403

6. D. Engeler, A.P. Baranowski, B. Berghmans, et al. EAU Guidelines on Chronic Pelvic Pain. In: EAU Guidelines Office; 2025. http://uroweb.org/guidelines/compilations-of-all-guidelines/

7. Sewell M, Churilov L, Mooney S, Ma T, Maher P, Grover SR. Chronic pelvic pain – pain catastrophizing, pelvic pain and quality of life. *Scand J Pain*. 2018;18(3):441-448. doi:10.1515/sjpain-2017-0181

8. Coyne KS, Zhou Z, Thompson C, Versi E. The impact on health-related quality of life of stress, urge and mixed urinary incontinence. *BJU Int*. 2003;92(7):731-735. doi:10.1046/j.1464-410X.2003.04463.x

9. Peters KM, Killinger KA, Boguslawski BM, Boura JA. Chronic pudendal neuromodulation: Expanding available treatment options for refractory urologic symptoms: Chronic Pudendal Neuromodulation. *Neurourol Urodyn*. 2010;29(7):1267-1271. doi:10.1002/nau.20823

10. Peters KM, Feber KM, Bennett RC. Sacral versus pudendal nerve stimulation for voiding dysfunction: A prospective, single-blinded, randomized, crossover trial. *Neurourol Urodyn*. 2005;24(7):643-647. doi:10.1002/nau.20174

11. Gracely A, Gupta P. Pudendal neuromodulation for pelvic pain. *Curr Bladder Dysfunct Rep*. 2020;15(3):113-120. doi:10.1007/s11884-020-00588-y

12. Ciotti F, Valle G, Pedrocchi A, Raspopovic S. A Computational Model of the Pudendal Nerve for the Bioelectronic Treatment of Sexual Dysfunctions. In: *2021 10th International IEEE/EMBS Conference on Neural Engineering (NER)*. IEEE; 2021:267-270. doi:10.1109/NER49283.2021.9441309

13. McGee MJ, Yoo PB, Grill WM. Selective co-stimulation of pudendal afferents enhances reflex bladder activation. In: *2011 Annual International Conference of the IEEE Engineering in Medicine and Biology Society*. IEEE; 2011:1057-1060. doi:10.1109/IEMBS.2011.6090246

14. Bruns TM, Bhadra N, Gustafson KJ. Variable Patterned Pudendal Nerve Stimuli Improves Reflex Bladder Activation. *IEEE Trans Neural Syst Rehabil Eng*. 2008;16(2):140-148. doi:10.1109/TNSRE.2007.914460

15. Yoo PB, Grill WM. Minimally-invasive electrical stimulation of the pudendal nerve: A pre-clinical study for neural control of the lower urinary tract. *Neurourol Urodyn*. 2007;26(4):562-569. doi:10.1002/nau.20376

16. de Groat WC, Griffiths D, Yoshimura N. Neural Control of the Lower Urinary Tract. In: Terjung R, ed. *Comprehensive Physiology*. 1st ed. Wiley; 2014:327-396. doi:10.1002/cphy.c130056

17. de Groat WC, Yoshimura N. Anatomy and physiology of the lower urinary tract. In: *Handbook of Clinical Neurology*. Vol 130. Elsevier; 2015:61-108. doi:10.1016/B978-0-444-63247-0.00005-5

18. Stoffel JT. Neuroanatomy and Neurophysiology. In: Martins FE, Holm HV, Sandhu J, McCammon KA, eds. *Female Genitourinary and Pelvic Floor Reconstruction*. Springer International Publishing; 2022:1-22. doi:10.1007/978-3-030-71112-2_3-1

19. Yang J, Webb KE, Carrington EV, et al. Anatomical Variation of the Pudendal Nerve and Related Structures. *Eur Urol Open Sci*. 2026;85:71-81. doi:10.1016/j.euros.2026.01.015

20. Hombach-Klonisch S, Klonisch T, Peeler J, eds. *Sobotta Clinical Atlas of Human Anatomy*. 1st edition. Elsevier; 2019. https://www.clinicalkey.com/#!/browse/book/3-s2.0-C20150000260

21. Mahadevan V. Anatomy of the lower urinary tract. *Surg Oxf*. 2019;37(7):351-358. doi:10.1016/j.mpsur.2019.04.009

22. Jung J, Ahn HK, Huh Y. Clinical and Functional Anatomy of the Urethral Sphincter. *Int Neurourol J*. 2012;16(3):102. doi:10.5213/inj.2012.16.3.102

23. Pipitone F, Sadeghi Z, DeLancey JOL. Urethral function and failure: A review of current knowledge of urethral closure mechanisms, how they vary, and how they are affected by life events. *Neurourol Urodyn*. 2021;40(8):1869-1879. doi:10.1002/nau.24760

24. Huisman AB. Aspects on the anatomy of the female urethra with special relation to urinary continence. *Contrib Gynecol Obstet*. 1983;10:1-31.

25. Ferreira A, Duarte Cruz C. The urethra in continence and sensation: Neural aspects of urethral function. *Neurourol Urodyn*. 2021;40(3):744-752. doi:10.1002/nau.24632

26. Mangera A, Osman NI, Chapple CR. Anatomy of the lower urinary tract. *Surg Oxf*. 2013;31(7):319-325. doi:10.1016/j.mpsur.2013.04.013

27. De Paiva AMF, Cervantes GV, De Paula Andres M, Abrão MS, De Almeida Barbosa P. Pelvic Floor. In: Salomão Ayroza H, Ayroza Ribeiro P, eds. *Atlas of Laparoscopic Gynecological Anatomy*. Springer International Publishing; 2024:63-79. doi:10.1007/978-3-031-63520-5_4

28. Zapletal J, Nanka O, Halaska MJ, et al. Anatomy of the pudendal nerve in clinically important areas: a pictorial essay and narrative review. *Surg Radiol Anat*. Published online January 19, 2024. doi:10.1007/s00276-023-03285-7

29. Mahakkanukrauh P, Surin P, Vaidhayakarn P. Anatomical study of the pudendal nerve adjacent to the sacrospinous ligament. *Clin Anat*. 2005;18(3):200-205. doi:10.1002/ca.20084

30. Gustafson KJ, Zelkovic PF, Feng AH, Draper CE, Bodner DR, Grill WM. Fascicular anatomy and surgical access of the human pudendal nerve. *World J Urol*. 2005;23(6):411-418. doi:10.1007/s00345-005-0032-4

31. Salimoglu S, Kilinc G, Calik B. Anatomy of the Colon, Rectum, and Anus. In: Engin O, ed. *Colon Polyps and Colorectal Cancer*. Springer International Publishing; 2021:1-22. doi:10.1007/978-3-030-57273-0_1

32. Bharucha a. e. Pelvic floor: anatomy and function. *Neurogastroenterol Motil*. 2006;18(7):507-519. doi:10.1111/j.1365-2982.2006.00803.x

33. Alkatout I, Wedel T, Pape J, Possover M, Dhanawat J. Review: Pelvic nerves – from anatomy and physiology to clinical applications. *Transl Neurosci*. 2021;12(1):362-378. doi:10.1515/tnsci-2020-0184

34. Gyorfi MJ, Abd-Elsayed A. Pudendal nerve blockade for persistent genital arousal disorder (PGAD): A clinical review and case report. *Pain Pract*. 2024;24(6):852-855. doi:10.1111/papr.13362

35. Viktrup L, Bump RC. Simplified neurophysiology of the lower urinary tract. *Prim Care Update OBGYNS*. 2003;10(5):261-264. doi:10.1016/S1068-607X(03)00043-X

36. Park JM, Loom DAB, Uire EJM. The guarding reflex revisited. *Br J Urol*. Published online 1997. doi:10.1046/j.1464-410x.1997.00488.x

37. Kuru M. Nervous Control of Micturition. *Physiol Rev*. 1965;45(3):425-494. doi:10.1152/physrev.1965.45.3.425

38. Haylen BT, De Ridder D, Freeman RM, et al. An International Urogynecological Association (IUGA)/International Continence Society (ICS) joint report on the terminology for female pelvic floor dysfunction. *Int Urogynecology J*. 2010;21(1):5-26. doi:10.1007/s00192-009-0976-9

39. Stoffel JT, Peterson AC, Sandhu JS, Suskind AM, Wei JT, Lightner DJ. AUA White Paper on Nonneurogenic Chronic Urinary Retention: Consensus Definition, Treatment Algorithm, and Outcome End Points. *J Urol*. 2017;198(1):153-160. doi:10.1016/j.juro.2017.01.075

40. Ayorinde AA, Bhattacharya S, Druce KL, Jones GT, Macfarlane GJ. Chronic pelvic pain in women of reproductive and post-reproductive age: a population-based study. *Eur J Pain*. 2017;21(3):445-455. doi:10.1002/ejp.938

41. Cameron AP, Chung DE, Dielubanza EJ, et al. The AUA/SUFU Guideline on the Diagnosis and Treatment of Idiopathic Overactive Bladder. *J Urol*. Published online April 23, 2024:10.1097/JU.0000000000003985. doi:10.1097/JU.0000000000003985

42. Fok CS, Gotlieb R, Nakib N. Epidemiology, Definitions, and Cost of Incontinence in Women. In: Cameron AP, ed. *Female Urinary Incontinence*. Springer International Publishing; 2022:3-17. doi:10.1007/978-3-030-84352-6_1

43. Harris SS, Link CL, Tennstedt SL, Kusek JW, McKinlay JB. Care Seeking and Treatment for Urinary Incontinence in a Diverse Population. *J Urol*. 2007;177(2):680-684. doi:10.1016/j.juro.2006.09.045

44. Aoki Y, Brown HW, Brubaker L, Cornu JN, Daly JO, Cartwright R. Urinary incontinence in women. *Nat Rev Dis Primer*. 2017;3(1):17042. doi:10.1038/nrdp.2017.42

45. Daugirdas SP, Markossian T, Mueller ER, Durazo-Arvizu R, Cao G, Kramer H. Urinary incontinence and chronic conditions in the US population age 50 years and older. *Int Urogynecology J*. 2020;31(5):1013-1020. doi:10.1007/s00192-019-04137-y

46. Van Koeveringe GA, Vahabi B, Andersson KE, Kirschner-Herrmans R, Oelke M. Detrusor underactivity: A plea for new approaches to a common bladder dysfunction. *Neurourol Urodyn*. 2011;30(5):723-728. doi:10.1002/nau.21097

47. Tudor KI, Sakakibara R, Panicker JN. Neurogenic lower urinary tract dysfunction: evaluation and management. *J Neurol*. 2016;263(12):2555-2564. doi:10.1007/s00415-016-8212-2

48. Ginsberg DA, Boone TB, Cameron AP, et al. The AUA/SUFU Guideline on Adult Neurogenic Lower Urinary Tract Dysfunction: Diagnosis and Evaluation. *J Urol*. 2021;206(5):1097-1105. doi:10.1097/JU.0000000000002235

49. Cameron AP, ed. *Female Urinary Incontinence*. Springer International Publishing; 2022. doi:10.1007/978-3-030-84352-6

50. Agboola A, Khunda A, Kershaw V, Ballard P, Shawer S. Overactive bladder syndrome: an updated review of diagnostic and therapeutic modalities. *Obstet Gynaecol Reprod Med*. Published online February 2026:S1751721426000163. doi:10.1016/j.ogrm.2026.02.007

51. Denys P, Castaño Botero JC, Vita Nunes RL, et al. AbobotulinumtoxinA is effective in patients with urinary incontinence due to neurogenic detrusor overactivity regardless of spinal cord injury or multiple sclerosis etiology: Pooled analysis of two phase III randomized studies (CONTENT1 and CONTENT2). *Neurourol Urodyn*. 2023;42(1):153-167. doi:10.1002/nau.25062

52. Del Popolo G, Filocamo MT, Li Marzi V, et al. Neurogenic Detrusor Overactivity Treated with English Botulinum Toxin A: 8-Year Experience of One Single Centre. *Eur Urol*. 2008;53(5):1013-1020. doi:10.1016/j.eururo.2007.09.034

53. Caroço T, Bollens R, Portugal D. Botulinum toxin injection of the piriformis muscle for refractory pudendal neuralgia after decompression surgery: case report. *Pain Manag*. Published online September 9, 2025:1-6. doi:10.1080/17581869.2025.2555162

54. Basol G, Kale A, Gurbuz H, Gundogdu EC, Baydilli KN, Usta T. Transvaginal pudendal nerve blocks in patients with pudendal neuralgia: 2-year follow-up results. *Arch Gynecol Obstet*. 2022;306(4):1107-1116. doi:10.1007/s00404-022-06621-1

55. Kobashi K, Nitti V, Margolis E, et al. A Prospective Study to Evaluate Efficacy Using the Nuro Percutaneous Tibial Neuromodulation System in Drug-Naïve Patients With Overactive Bladder Syndrome. *Urology*. 2019;131:77-82. doi:10.1016/j.urology.2019.06.002

56. Thomas L, Hashim H. Sacral neuromodulation for voiding dysfunction and urinary retention. *Continence*. Published online July 2024:101337. doi:10.1016/j.cont.2024.101337

57. Hashim H, Thomas L, Siegel SW. Sacral Neuromodulation. In: Goldman HB, Zillioux J, eds. *Complications of Urogynecology and Reconstructive Pelvic Surgery*. Springer Nature Switzerland; 2025:367-380. doi:10.1007/978-3-032-00339-3_32

58. Carmel M, Lebel M, Tu LM. Pudendal nerve neuromodulation with neurophysiology guidance: a potential treatment option for refractory chronic pelvi-perineal pain. *Int Urogynecology J*. 2010;21(5):613-616. doi:10.1007/s00192-009-1054-z

59. Peters KM. Pudendal Neuromodulation for Sexual Dysfunction. *J Sex Med*. 2013;10(4):908-911. doi:10.1111/jsm.12138

60. van Kerrebroeck PEV, Smits MAC. Pudendal Nerve Stimulation. In: Badlani GH, ed. *Minimally Invasive Therapy for Urinary Incontinence and Pelvic Organ Prolapse*. Current Clinical Urology. Springer New York; 2014:177-181. doi:10.1007/978-1-4939-0008-4_15

61. Yamanishi T, Kaga K, Fuse M, Shibata C, Uchiyama T. Neuromodulation for the Treatment of Lower Urinary Tract Symptoms. *LUTS Low Urin Tract Symptoms*. 2015;7(3):121-132. doi:10.1111/luts.12087

62. Evolving types of pudendal neuromodulation for lower urinary tract dysfunction. *Cent Eur J Urol*. Published online 2024. doi:10.5173/ceju.2023.86

63. Ness TJ, DeWitte C, McNaught J, Clodfelder-Miller B, Su X. Spinal mechanisms of pudendal nerve stimulation-induced inhibition of bladder hypersensitivity in rats. *Neurosci Lett*. 2018;686:181-185. doi:10.1016/j.neulet.2018.08.041

64. Huang JC, Deletis V, Vodusek DB, Abbott R. Preservation of Pudendal Afferents in Sacral Rhizotomies. *Neurosurgery*. 1997;41(2):411-415. doi:10.1097/00006123-199708000-00015

65. Tilborghs S, De Wachter S. Sacral neuromodulation for the treatment of overactive bladder: systematic review and future prospects. *Expert Rev Med Devices*. 2022;19(2):161-187. doi:10.1080/17434440.2022.2032655

66. Gilleran JP, Gaines N. Pudendal Neuromodulation. In: Gilleran JP, Alpert SA, eds. *Adult and Pediatric Neuromodulation*. Springer International Publishing; 2018:89-104. doi:10.1007/978-3-319-73266-4_7

67. Huri E, Hashim H, Zillioux J, Averbeck MA, McAchran S, Goldman H. Sacral neuromodulation update in 2024: Insights from the ICS workshop 2023. *Continence*. 2024;12:101705. doi:10.1016/j.cont.2024.101705

68. Benson K, McCrery R, Taylor C, et al. One-year outcomes of the ARTISAN-SNM study with the Axonics System for the treatment of urinary urgency incontinence. *Neurourol Urodyn*. 2020;39(5):1482-1488. doi:10.1002/nau.24376

69. Barrington FJF. THE NERVOUS MECHANISM OF MICTURITION. *Q J Exp Physiol*. 1914;8(1):33-71. doi:10.1113/expphysiol.1914.sp000171

70. Barrington FJF. THE COMPONENT REFLEXES OF MICTURITION IN THE CAT: PARTS I AND II. *Brain*. 1931;54(2):177-188. doi:10.1093/brain/54.2.177

71. Shen JD, Chen SJ, Chen HY, Chiu KY, Chen YH, Chen WC. Review of Animal Models to Study Urinary Bladder Function. *Biology*. 2021;10(12):1316. doi:10.3390/biology10121316

72. Fry CH, Daneshgari F, Thor K, et al. Animal models and their use in understanding lower urinary tract dysfunction. *Neurourol Urodyn*. 2010;29(4):603-608. doi:10.1002/nau.20903

73. Woock JP, Yoo PB, Grill WM. Activation and inhibition of the micturition reflex by penile afferents in the cat. *Am J Physiol-Regul Integr Comp Physiol*. 2008;294(6):R1880-R1889. doi:10.1152/ajpregu.00029.2008

74. Kennelly MJ, Arena KC, Shaffer N, et al. Electrical Stimulation of the Urethra Evokes Bladder Contractions in a Woman With Spinal Cord Injury. *J Spinal Cord Med*. 2010;33(3):261-265. doi:10.1080/10790268.2010.11689704

75. Kennelly MJ, Bennett ME, Grill WM, Grill JH, Boggs JW. Electrical stimulation of the urethra evokes bladder contractions and emptying in spinal cord injury men: Case studies. *J Spinal Cord Med*. 2011;34(3):315-321. doi:10.1179/2045772311Y.0000000012

76. Yoo PB, Klein SM, Grafstein NH, et al. Pudendal nerve stimulation evokes reflex bladder contractions in persons with chronic spinal cord injury. *Neurourol Urodyn*. 2007;26(7):1020-1023. doi:10.1002/nau.20441

77. Bruns TM, Gustafson KJ, Bhadra N. Reflex bladder activation via pudendal nerve and intraurethral stimulation depends on stimulation pattern and location. In: *2008 30th Annual International Conference of the IEEE Engineering in Medicine and Biology Society*. IEEE; 2008:2760-2763. doi:10.1109/IEMBS.2008.4649774

78. Hodgkin AL, Huxley AF. A quantitative description of membrane current and its application to conduction and excitation in nerve. *J Physiol*. 1952;117(4):500-544. doi:10.1113/jphysiol.1952.sp004764

79. Liang L, Damiani A, Del Brocco M, et al. A systematic review of computational models for the design of spinal cord stimulation therapies: from neural circuits to patient-specific simulations. *J Physiol*. 2023;601(15):3103-3121. doi:10.1113/JP282884

80. Zelechowski M, Valle G, Raspopovic S. A computational model to design neural interfaces for lower-limb sensory neuroprostheses. *J NeuroEngineering Rehabil*. 2020;17(1):24. doi:10.1186/s12984-020-00657-7

81. Yousif N, Vaizey CJ, Maeda Y. Mapping the current flow in sacral nerve stimulation using computational modelling. *Healthc Technol Lett*. 2019;6(1):8-12. doi:10.1049/htl.2018.5030

82. Helmers SL, Begnaud J, Cowley A, et al. Application of a computational model of vagus nerve stimulation. *Acta Neurol Scand*. 2012;126(5):336-343. doi:10.1111/j.1600-0404.2012.01656.x

83. Raspopovic S, Capogrosso M, Micera S. A Computational Model for the Stimulation of Rat Sciatic Nerve Using a Transverse Intrafascicular Multichannel Electrode. *IEEE Trans Neural Syst Rehabil Eng*. 2011;19(4):333-344. doi:10.1109/TNSRE.2011.2151878

84. Kent AR, Grill WM. Model-based analysis and design of nerve cuff electrodes for restoring bladder function by selective stimulation of the pudendal nerve. *J Neural Eng*. 2013;10(3):036010. doi:10.1088/1741-2560/10/3/036010

85. Ciotti F, Cimolato A, Valle G, Raspopovic S. Design of an adaptable intrafascicular electrode (AIR) for selective nerve stimulation by model-based optimization. Alber M, ed. *PLOS Comput Biol*. 2023;19(5):e1011184. doi:10.1371/journal.pcbi.1011184

86. Brill NA, Naufel SN, Polasek K, et al. Evaluation of high-density, multi-contact nerve cuffs for activation of grasp muscles in monkeys. *J Neural Eng*. 2018;15(3):036003. doi:10.1088/1741-2552/aa8735

87. Polasek KH, Hoyen HA, Keith MW, Tyler DJ. Human Nerve Stimulation Thresholds and Selectivity Using a Multi-contact Nerve Cuff Electrode. *IEEE Trans Neural Syst Rehabil Eng*. 2007;15(1):76-82. doi:10.1109/TNSRE.2007.891383

88. Tarler MD, Mortimer JT. Selective and independent activation of four motor fascicles using a four contact nerve-cuff electrode. *IEEE Trans Neural Syst Rehabil Eng*. 2004;12(2):251-257. doi:10.1109/TNSRE.2004.828415

89. Navarro X, Valderrama E, Stieglitz T, Schüttler M. Selective fascicular stimulation of the rat sciatic nerve with multipolar polyimide cuff electrodes. *Restor Neurol Neurosci*. 2001;18(1):9-21.

90. Ortiz-Lopez M, Lagunas AC, Akmal H, Bruns TM. Selective Motor Stimulation of the Pudendal Nerve Using Multi-Contact Cuff Electrodes: A Pre-Clinical Study in Feline and Ovine Models. *Neurourol Urodyn*. Published online June 2, 2026:nau.70328. doi:10.1002/nau.70328

91. Martin WD, Fletcher TF, Bradley WE. Innervation of feline perineal musculature. *Anat Rec*. 1974;180(1):15-29. doi:10.1002/ar.1091800104

92. Rattay F. Analysis of models for extracellular fiber stimulation. *IEEE Trans Biomed Eng*. 1989;36(7):676-682. doi:10.1109/10.32099

93. Lagunas A, Chen PJ, Ruiz L, et al. Factors Affecting Anal Sphincter Recruitment During Intraoperative Pudendal Nerve Stimulation: An Observational Study. *Int Urogynecology J*. Published online 2025. doi:10.1007/s00192-025-06238-3

94. Marinkovic SP. New technologies in the management of overactive bladder: current research and future prospects. *Ther Adv Urol*. 2019;11:1756287219844669. doi:10.1177/1756287219844669

95. Coyne KS, Wein AJ, Tubaro A, et al. The burden of lower urinary tract symptoms: evaluating the effect of LUTS on health-related quality of life, anxiety and depression: EpiLUTS. *BJU Int*. 2009;103:4-11. doi:10.1111/j.1464-410X.2009.08371.x

96. Eapen R, Radomski S. Review of the epidemiology of overactive bladder. *Res Rep Urol*. Published online June 2016:71. doi:10.2147/RRU.S102441

97. Huang G, Le AL, Goddard Y, et al. A Systematic Review of the Cost of Chronic Pelvic Pain in Women. *J Obstet Gynaecol Can*. 2022;44(3):286-293.e3. doi:10.1016/j.jogc.2021.08.011

98. Puckrein G, Walker D, Xu L, Congdon P, Gooch K. The Prevalence and Forecast Prevalence of Overactive Bladder in the Medicare Population. *Clin Med Insights Urol*. 2019;12:117956111984746. doi:10.1177/1179561119847464

99. Possover M. A Novel Implantation Technique for Pudendal Nerve Stimulation for Treatment of Overactive Bladder and Urgency Incontinence. *J Minim Invasive Gynecol*. 2014;21(5):888-892. doi:10.1016/j.jmig.2014.03.026

100. Jottard K, Bruyninx L, Bonnet P, Mathieu N, De Wachter S. Pilot study: pudendal neuromodulation combined with pudendal nerve release in case of chronic perineal pain syndrome. The ENTRAMI technique: early results. *Int Urogynecology J*. 2021;32(10):2765-2770. doi:10.1007/s00192-020-04565-1

101. Peters KM, Killinger KA, Jaeger C, Chen C. Pilot Study Exploring Chronic Pudendal Neuromodulation as a Treatment Option for Pain Associated with Pudendal Neuralgia: Neuromodulation and Pudendal Neuralgia. *LUTS Low Urin Tract Symptoms*. 2015;7(3):138-142. doi:10.1111/luts.12066

102. Heinze K, Hoermann R, Fritsch H, Dermietzel R, van Ophoven A. Comparative pilot study of implantation techniques for pudendal neuromodulation: technical and clinical outcome in first 20 patients with chronic pelvic pain. *World J Urol*. 2015;33(2):289-294. doi:10.1007/s00345-014-1304-7

103. Meier KM, Vecellio PM, Killinger KA, Boura JA, Peters KM. Pudendal Neuromodulation is Feasible and Effective After Pudendal Nerve Entrapment Surgery. *J Sex Med*. 2022;19(6):995-1001. doi:10.1016/j.jsxm.2022.03.219

104. Verdú E, Ceballos D, Vilches JJ, Navarro X. Influence of aging on peripheral nerve function and regeneration. *J Peripher Nerv Syst*. 2000;5(4):191-208. doi:10.1111/j.1529-8027.2000.00026.x

105. George AT, Dudding TC, Gurmany S, Kamm MA, Nicholls RJ, Vaizey CJ. Pudendal Nerve Stimulation for Bowel Dysfunction in Complete Cauda Equina Syndrome. *Ann Surg*. 2014;259(3):502-507. doi:10.1097/SLA.0b013e31828e7602

106. Barry MJ, Fowler FJ, O'leary MP, et al. The American Urological Association Symptom Index for Benign Prostatic Hyperplasia. *J Urol*. 2017;197(2S). doi:10.1016/j.juro.2016.10.071

107. Suskind AM, Dunn RL, Morgan DM, DeLancey JOL, McGuire EJ, Wei JT. The Michigan incontinence symptom index (M-ISI): A clinical measure for type, severity, and bother related to urinary incontinence: Incontinence Symptom Index. *Neurourol Urodyn*. 2014;33(7):1128-1134. doi:10.1002/nau.22468

108. Isidori AM, Pozza C, Esposito K, et al. Original Research—Outcomes Assessment: Development and Validation of a 6-Item Version of the Female Sexual Function Index (FSFI) as a Diagnostic Tool for Female Sexual Dysfunction. *J Sex Med*. 2010;7(3):1139-1146. doi:10.1111/j.1743-6109.2009.01635.x

109. Rosen R, Cappelleri J, Smith M, Lipsky J, Peña B. Development and evaluation of an abridged, 5-item version of the International Index of Erectile Function (IIEF-5) as a diagnostic tool for erectile dysfunction. *Int J Impot Res*. 1999;11(6):319-326. doi:10.1038/sj.ijir.3900472

110. Barber MD, Walters MD, Bump RC. Short forms of two condition-specific quality-of-life questionnaires for women with pelvic floor disorders (PFDI-20 and PFIQ-7). *Am J Obstet Gynecol*. 2005;193(1):103-113. doi:10.1016/j.ajog.2004.12.025

111. Clemens JQ, Calhoun EA, Litwin MS, et al. Validation of a Modified National Institutes of Health Chronic Prostatitis Symptom Index to Assess Genitourinary Pain in Both Men and Women. *Urology*. 2009;74(5):983-987.e3. doi:10.1016/j.urology.2009.06.078

112. Gregory WT, Lou JS, Stuyvesant A, Clark AL. Quantitative Electromyography of the Anal Sphincter After Uncomplicated Vaginal Delivery: *Obstet Gynecol*. 2004;104(2):327-335. doi:10.1097/01.AOG.0000134527.07034.81

113. Stålberg E, van Dijk H, Falck B, et al. Standards for quantification of EMG and neurography. *Clin Neurophysiol*. 2019;130(9):1688-1729. doi:10.1016/j.clinph.2019.05.008

114. Su X, Cutinella M, Koppes S, Agran JE, Dinsmoor DA. Electromyographic Responses Across Different Pulse-Widths of Sacral Neuromodulation in Sheep. *Neuromodulation Technol Neural Interface*. 2019;22(6):684-689. doi:10.1111/ner.12779

115. Herroelen S, Knowles C, Kerrigan-Smith J, Noone T, Denison T, De Wachter S. Pudendal nerve stimulation for treatment of lower urinary tract symptoms: A systematic review of safety, technical feasibility and clinical efficacy. *Continence*. 2024;11:101685. doi:10.1016/j.cont.2024.101685

116. Plevnik S, Vodušek DB, Vrtačnik P, Janež J. Optimization of pulse duration for electrical stimulation in treatment of urinary incontinence. *World J Urol*. 1986;4(1):22-23. doi:10.1007/BF00326736

117. Lehur PA, Sørensen M, Dudding TC, et al. Programming Algorithms for Sacral Neuromodulation: Clinical Practice and Evidence—Recommendations for Day-to-Day Practice. *Neuromodulation Technol Neural Interface*. 2020;23(8):1121-1129. doi:10.1111/ner.13117

118. Vodušek DB, Plevnik S, Vrtačnik P, Janež J. Detrusor inhibition on selective pudendal nerve stimulation in the perineum. *Neurourol Urodyn*. 1987;6(5):389-393. doi:10.1002/nau.1930060506

119. Gilleran JP, Alpert SA, eds. *Adult and Pediatric Neuromodulation*. Springer International Publishing; 2018. doi:10.1007/978-3-319-73266-4

120. Hoenig JM, Heisey DM. The Abuse of Power: The Pervasive Fallacy of Power Calculations for Data Analysis. *Am Stat*. 2001;55(1):19-24. doi:10.1198/000313001300339897

121. Kumle L, Võ MLH, Draschkow D. Estimating power in (generalized) linear mixed models: An open introduction and tutorial in R. *Behav Res Methods*. 2021;53(6):2528-2543. doi:10.3758/s13428-021-01546-0

122. Green P, MacLeod CJ. SIMR : an R package for power analysis of generalized linear mixed models by simulation. Nakagawa S, ed. *Methods Ecol Evol*. 2016;7(4):493-498. doi:10.1111/2041-210X.12504

123. Lagunas AC, Chen PJ, Bruns T, Gupta P. Pudendal nerve stimulation recruits the urethra during awake human cystometry. *medRxiv*. Preprint posted online February 23, 2026. doi:10.64898/2026.02.18.26346494

124. Spinelli M, Malaguti S, Giardiello G, Lazzeri M, Tarantola J, Hombergh UVD. A new minimally invasive procedure for pudendal nerve stimulation to treat neurogenic bladder: Description of the method and preliminary data. *Neurourol Urodyn*. 2005;24(4):305-309. doi:10.1002/nau.20118

125. Hoang Roberts L, Vollstedt A, Gilleran J, Peters KM. Bladder Dysfunction and Pelvic Pain: The Role of Sacral, Tibial, and Pudendal Neuromodulation. In: Martins FE, Holm HV, Sandhu J, McCammon KA, eds. *Female Genitourinary and Pelvic Floor Reconstruction*. Springer International Publishing; 2022:1-19. doi:10.1007/978-3-030-71112-2_15-1

126. Thor KB, Langdale CL, Karicheti V, Grill WM. Characterization of bilateral, pudendal nerve-evoked, urethral rhabdosphincter contractions in anesthetized cats. *Continence*. 2022;1:100006. doi:10.1016/j.cont.2022.100006

127. Yoo PB, Woock JP, Grill WM. Bladder activation by selective stimulation of pudendal nerve afferents in the cat. *Exp Neurol*. 2008;212(1):218-225. doi:10.1016/j.expneurol.2008.04.010

128. Liu J, Grayden DB, Keast JR, John SE. Endovascular stimulation of the pudendal nerve using a stent-mounted electrode array. *J Neural Eng*. Published online July 19, 2024. doi:10.1088/1741-2552/ad6590

129. Chen P, Lagunas AC, Soriano V, Gupta P, Bruns TM. Perineal and Rectal Nerve Recruitment Order Varies During Pudendal Neurostimulator Implant Surgery. *Neurourol Urodyn*. Published online February 10, 2025:nau.70010. doi:10.1002/nau.70010

130. Tai C, Smerin SE, De Groat WC, Roppolo JR. Pudendal-to-bladder reflex in chronic spinal-cord-injured cats. *Exp Neurol*. 2006;197(1):225-234. doi:10.1016/j.expneurol.2005.09.013

131. McGee MJ, Grill WM. Selective co-stimulation of pudendal afferents enhances bladder activation and improves voiding efficiency: Co-Stimulation of Pudendal Afferents Improves Voiding. *Neurourol Urodyn*. 2014;33(8):1272-1278. doi:10.1002/nau.22474

132. Karram MM, Blaivas J. Urodynamics: Cystometry and Urethral Function Tests. In: *Urogynecology and Reconstructive Pelvic Surgery*. Elsevier; 2007:78-101. doi:10.1016/B978-0-323-02902-5.50013-7

133. Boggs JW, Wenzel BJ, Gustafson KJ, Grill WM. Spinal Micturition Reflex Mediated by Afferents in the Deep Perineal Nerve. *J Neurophysiol*. 2005;93(5):2688-2697. doi:10.1152/jn.00978.2004

134. Tai C, Wang J, Wang X, De Groat WC, Roppolo JR. Bladder inhibition or voiding induced by pudendal nerve stimulation in chronic spinal cord injured cats. *Neurourol Urodyn*. 2007;26(4):570-577. doi:10.1002/nau.20374

135. Bruns TM, Bhadra N, Gustafson KJ. Intraurethral stimulation for reflex bladder activation depends on stimulation pattern and location. *Neurourol Urodyn*. 2009;28(6):561-566. doi:10.1002/nau.20703

136. Guo W, Shapiro K, Wang Z, et al. Restoring both continence and micturition after chronic spinal cord injury by pudendal neuromodulation. *Exp Neurol*. 2021;340:113658. doi:10.1016/j.expneurol.2021.113658

137. Abrams. Bladder outlet obstruction index, bladder contractility index and bladder voiding efficiency: three simple indices to define bladder voiding function. *BJU Int*. 1999;84(1):14-15. doi:10.1046/j.1464-410x.1999.00121.x

138. Giannotti A, Musco S, Miragliotta V, et al. Swine Pudendal Nerve as a Model for Neuromodulation Studies to Restore Lower Urinary Tract Dysfunction. *Int J Mol Sci*. 2024;25(2):855. doi:10.3390/ijms25020855

139. Hokanson JA, Langdale CL, Sridhar A, Grill WM. Stimulation of the sensory pudendal nerve increases bladder capacity in the rat. *Am J Physiol-Ren Physiol*. 2018;314(4):F543-F550. doi:10.1152/ajprenal.00373.2017

140. Krhut J, Kobberø H, Kanaan R, Fode M, Poulsen M, Zvara P. The mechanism of action of neuromodulation in the treatment of overactive bladder. *Nat Rev Urol*. Published online December 9, 2024. doi:10.1038/s41585-024-00967-8

141. Danziger ZC, Grill WM. Sensory feedback from the urethra evokes state-dependent lower urinary tract reflexes in rat: State-dependent lower urinary tract reflexes. *J Physiol*. 2017;595(16):5687-5698. doi:10.1113/JP274191

142. Gustafson KJ, Creasey GH, Grill WM. A urethral afferent mediated excitatory bladder reflex exists in humans. *Neurosci Lett*. 2004;360(1-2):9-12. doi:10.1016/j.neulet.2004.01.001

143. Woock JP, Yoo PB, Grill WM. Mechanisms of reflex bladder activation by pudendal afferents. *Am J Physiol-Regul Integr Comp Physiol*. 2011;300(2):R398-R407. doi:10.1152/ajpregu.00154.2010

144. De Wachter S, Vaganee D, Kessler TM. Sacral Neuromodulation: Mechanism of Action. *Eur Urol Focus*. 2020;6(5):823-825. doi:10.1016/j.euf.2019.11.018

145. Yalla SV, Resnick NM. Initiation of Voiding in Humans: The Nature and Temporal Relationship of Urethral Sphincter Responses. *J Urol*. 1997;157(2):590-595. doi:10.1016/S0022-5347(01)65212-1

146. Dmochowski RR, Newman DK. Impact of overactive bladder on women in the United States:results of a national survey. *Curr Med Res Opin*. 2007;23(1):65-76. doi:10.1185/030079907X159533

147. Buytaert J, Goyens J, De Greef D, Aerts P, Dirckx J. Volume Shrinkage of Bone, Brain and Muscle Tissue in Sample Preparation for Micro-CT and Light Sheet Fluorescence Microscopy (LSFM). *Microsc Microanal*. 2014;20(4):1208-1217. doi:10.1017/S1431927614001329

148. Andreis FR, Metcalfe B, Al Muhammadee Janjua T, et al. On the Relationship Between Fascicle Diameter and Perineurium Thickness in the Ulnar Nerve of Pigs. In: *2023 11th International IEEE/EMBS Conference on Neural Engineering (NER)*. IEEE; 2023:1-4. doi:10.1109/NER52421.2023.10123782

149. Musselman ED, Cariello JE, Grill WM, Pelot NA. ASCENT (Automated Simulations to Characterize Electrical Nerve Thresholds): A pipeline for sample-specific computational modeling of electrical stimulation of peripheral nerves. Schneidman-Duhovny D, ed. *PLOS Comput Biol*. 2021;17(9):e1009285. doi:10.1371/journal.pcbi.1009285

150. Gielen FLH, Wallinga-de Jonge W, Boon KL. Electrical conductivity of skeletal muscle tissue: Experimental results from different musclesin vivo. *Med Biol Eng Comput*. 1984;22(6):569-577. doi:10.1007/BF02443872

151. Solids: comparison with experiment. In: *Understanding the Properties of Matter*. 2nd ed. CRC Press; 2020:175-260. doi:10.1201/9781315274751

152. Ranck Jr. JB, BeMent SL. The specific impedance of the dorsal columns of cat: An anisotropic medium. *Exp Neurol*. 1965;11(4):451-463. doi:10.1016/0014-4886(65)90059-2

153. Pelot NA, Behrend CE, Grill WM. Modeling the response of small myelinated axons in a compound nerve to kilohertz frequency signals. *J Neural Eng*. 2017;14(4):046022. doi:10.1088/1741-2552/aa6a5f

154. Weerasuriya A, Spangler RA, Rapoport SI, Taylor RE. AC impedance of the perineurium of the frog sciatic nerve. *Biophys J*. 1984;46(2):167-174. doi:10.1016/S0006-3495(84)84009-6

155. Hassler C, Von Metzen R, Stieglitz T. Deposition Parameters Determining Insulation Resistance and Crystallinity of Parylene C in Neural Implant Encapsulation. In: Vander Sloten J, Verdonck P, Nyssen M, Haueisen J, eds. *4th European Conference of the International Federation for Medical and Biological Engineering*. Vol 22. IFMBE Proceedings. Springer Berlin Heidelberg; 2009:2439-2442. doi:10.1007/978-3-540-89208-3_585

156. Musselman ED, Raha I, Pelot NA, Grill WM. Scaling of vagus nerve stimulation parameters does not achieve equivalent nerve responses across species. *Bioelectron Med*. 2025;11(1):11. doi:10.1186/s42234-025-00174-9

157. McIntyre CC, Richardson AG, Grill WM. Modeling the Excitability of Mammalian Nerve Fibers: Influence of Afterpotentials on the Recovery Cycle. *J Neurophysiol*. 2002;87(2):995-1006. doi:10.1152/jn.00353.2001

158. Davis CJ, Musselman ED, Grill WM, Pelot NA. Fibers in smaller fascicles have lower activation thresholds with cuff electrodes due to thinner perineurium and smaller cross-sectional area. *J Neural Eng*. 2023;20(2):026032. doi:10.1088/1741-2552/acc42b

159. Halata Z, Munger BL. The neuroanatomical basis for the protopathic sensibility of the human glans penis. *Brain Res*. 1986;371(2):205-230. doi:10.1016/0006-8993(86)90357-4

160. Tajkarimi K, Burnett AL. The Role of Genital Nerve Afferents in the Physiology of the Sexual Response and Pelvic Floor Function. *J Sex Med*. 2011;8(5):1299-1312. doi:10.1111/j.1743-6109.2011.02211.x

161. Epstein S, Chang J, Johnston D, Paydarfar D. Size principles governing selective neuromodulation and recruitment order of nerve fibers. *Curr Opin Biomed Eng*. 2025;34:100583. doi:10.1016/j.cobme.2025.100583

162. Grill WM, Mortimer JT. Stimulus waveforms for selective neural stimulation. *IEEE Eng Med Biol Mag*. 1995;14(4):375-385. doi:10.1109/51.395310

163. Bhadra N, Grünewald V, Creasey G, Mortimer JT. Selective suppression of sphincter activation during sacral anterior nerve root stimulation. *Neurourol Urodyn*. 2002;21(1):55-64. doi:10.1002/nau.2068

164. Koldewijn EL, Rijkhoff NJM, Van Kerrebroeck PhEV, Debruyne FMJ, Wijkstra H. Selective Sacral Root Stimulation for Bladder Control: Acute Experiments in an Animal Model. *J Urol*. 1994;151(6):1674-1679. doi:10.1016/S0022-5347(17)35343-0

165. Lertmanorat Z, Durand DM. A Novel Electrode Array for Diameter-Dependent Control of Axonal Excitability: A Simulation Study. *IEEE Trans Biomed Eng*. 2004;51(7):1242-1250. doi:10.1109/TBME.2004.827347

166. Grinberg Y, Schiefer MA, Tyler DJ, Gustafson KJ. Fascicular Perineurium Thickness, Size, and Position Affect Model Predictions of Neural Excitation. *IEEE Trans Neural Syst Rehabil Eng*. 2008;16(6):572-581. doi:10.1109/TNSRE.2008.2010348

167. Pelot NA, Goldhagen GB, Cariello JE, et al. Quantified Morphology of the Cervical and Subdiaphragmatic Vagus Nerves of Human, Pig, and Rat. *Front Neurosci*. 2020;14:601479. doi:10.3389/fnins.2020.601479

168. Brucker-Hahn MK, Zander HJ, Will AJ, et al. Evoked compound action potentials during spinal cord stimulation: effects of posture and pulse width on signal features and neural activation within the spinal cord. *J Neural Eng*. 2023;20(4):046028. doi:10.1088/1741-2552/aceca4

169. Tarver WB, George RE, Maschino SE, Holder LK, Wernicke JF. Clinical Experience with a Helical Bipolar Stimulating Lead. *Pacing Clin Electrophysiol*. 1992;15(10):1545-1556. doi:10.1111/j.1540-8159.1992.tb02933.x

170. Naples GG, Mortimer JT, Scheiner A, Sweeney JD. A spiral nerve cuff electrode for peripheral nerve stimulation. *IEEE Trans Biomed Eng*. 1988;35(11):905-916. doi:10.1109/10.8670

171. Christie BP, Freeberg M, Memberg WD, et al. "Long-term stability of stimulating spiral nerve cuff electrodes on human peripheral nerves." *J NeuroEngineering Rehabil*. 2017;14(1):70. doi:10.1186/s12984-017-0285-3

172. Paggi V, Fallegger F, Serex L, et al. A soft, scalable and adaptable multi-contact cuff electrode for targeted peripheral nerve modulation. *Bioelectron Med*. 2024;10(1):6. doi:10.1186/s42234-023-00137-y

173. Leventhal DK, Durand DM. Chronic Measurement of the Stimulation Selectivity of the Flat Interface Nerve Electrode. *IEEE Trans Biomed Eng*. 2004;51(9):1649-1658. doi:10.1109/TBME.2004.827535

174. Brill NA, Naufel SN, Polasek K, et al. Evaluation of high-density, multi-contact nerve cuffs for activation of grasp muscles in monkeys. *J Neural Eng*. 2018;15(3):036003. doi:10.1088/1741-2552/aa8735

175. Pelot NA, Catherall DC, Thio BJ, et al. Excitation properties of computational models of unmyelinated peripheral axons. *J Neurophysiol*. 2021;125(1):86-104. doi:10.1152/jn.00315.2020

176. Maxion A, Kutafina E, Dohrn MF, et al. A modelling study to dissect the potential role of voltage-gated ion channels in activity-dependent conduction velocity changes as identified in small fiber neuropathy patients. *Front Comput Neurosci*. 2023;17:1265958. doi:10.3389/fncom.2023.1265958

177. Grill WM, Pelot NA. Computational modeling of autonomic nerve stimulation: Vagus et al. *Curr Opin Biomed Eng*. 2024;32:100557. doi:10.1016/j.cobme.2024.100557

178. Tunçkol E, Heim C, Brunk I, Vida I, Brecht M. Innervation pattern and fiber counts of the human dorsal nerve of clitoris. *Sci Rep*. 2024;14(1):23060. doi:10.1038/s41598-024-72898-8

179. Uloko M, Isabey EP, Peters BR. How many nerve fibers innervate the human glans clitoris: a histomorphometric evaluation of the dorsal nerve of the clitoris. *J Sex Med*. 2023;20(3):247-252. doi:10.1093/jsxmed/qdac027

180. Upadhye AR, Kolluru C, Druschel L, et al. Fascicles split or merge every ~560 microns within the human cervical vagus nerve. *J Neural Eng*. Published online September 29, 2022. doi:10.1088/1741-2552/ac9643

181. Fisher LE, Tyler DJ, Triolo RJ. Optimization of selective stimulation parameters for multi-contact electrodes. *J NeuroEngineering Rehabil*. 2013;10:25. doi:10.1186/1743-0003-10-25

182. Tao W, Wang Z, Lu X, Gao Y. Effects of different configurations of multi-contact cuff electrode on recruitment characteristics of nerve stimulation. In: *2015 7th International IEEE/EMBS Conference on Neural Engineering (NER)*. IEEE; 2015:498-501. doi:10.1109/NER.2015.7146668

183. Brill N, Tyler D. Optimizing nerve cuff stimulation of targeted regions through use of genetic algorithms. In: *2011 Annual International Conference of the IEEE Engineering in Medicine and Biology Society*. IEEE; 2011:5811-5814. doi:10.1109/IEMBS.2011.6091438

184. Dali M, William L, Tigra W, et al. Relevance of selective neural stimulation with a multicontact cuff electrode using multicriteria analysis. Cymbalyuk G, ed. *PLOS ONE*. 2019;14(7):e0219079. doi:10.1371/journal.pone.0219079

185. Plonsey R, Barr RC. Sources and Fields. In: *Bioelectricity*. Springer US; 2007:23-43. doi:10.1007/978-0-387-48865-3_2

186. Morgan TN, Pace N, Mohapatra A, et al. Sacral Neuromodulation: Determining Predictors of Success. *Urology*. 2021;153:124-128. doi:10.1016/j.urology.2020.06.023

187. Gilleran JP, Killinger K, Boura J, Peters KM. Number of active electrodes at time of staged tined lead interstim implant does not impact clinical outcomes. *Neurourol Urodyn*. 2016;35(5):625-629. doi:10.1002/nau.22766

188. Pizarro-Berdichevsky J, Gill BC, Clifton M, et al. Motor Response Matters: Optimizing Lead Placement Improves Sacral Neuromodulation Outcomes. *J Urol*. 2018;199(4):1032-1036. doi:10.1016/j.juro.2017.11.066

189. Haakma W, Hendrikse J, Uhrenholt L, et al. Multicenter reproducibility study of diffusion MRI and fiber tractography of the lumbosacral nerves. *J Magn Reson Imaging*. 2018;48(4):951-963. doi:10.1002/jmri.25964

190. Van Der Jagt PKN, Dik P, Froeling M, et al. Architectural configuration and microstructural properties of the sacral plexus: A diffusion tensor MRI and fiber tractography study. *NeuroImage*. 2012;62(3):1792-1799. doi:10.1016/j.neuroimage.2012.06.001

191. Anderson JM, Rodriguez A, Chang DT. Foreign body reaction to biomaterials. *Semin Immunol*. 2008;20(2):86-100. doi:10.1016/j.smim.2007.11.004

192. Polikov VS, Block ML, Fellous JM, Hong JS, Reichert WM. In vitro model of glial scarring around neuroelectrodes chronically implanted in the CNS. *Biomaterials*. 2006;27(31):5368-5376. doi:10.1016/j.biomaterials.2006.06.018

193. Sène D. Small fiber neuropathy: Diagnosis, causes, and treatment. *Joint Bone Spine*. 2018;85(5):553-559. doi:10.1016/j.jbspin.2017.11.002

194. Reitz A, Schmid DM, Curt A, Knapp PA, Schurch B. Afferent fibers of the pudendal nerve modulate sympathetic neurons controlling the bladder neck. *Neurourol Urodyn*. 2003;22(6):597-601. doi:10.1002/nau.10134

195. Venema PL, Heesakkers JPfa, De Vries AM, Van Koeveringe GA. The female urethral closure mechanism during physical stress. *Neurourol Urodyn*. 2024;43(7):1647-1654. doi:10.1002/nau.25489

196. Jain S, Agarwal MM, Mavuduru R, Singh SK, Mandal AK. Micturitional Urethral Pressure Profilometry for the Diagnosis, Grading, and Localization of Bladder Outlet Obstruction in Adult Men: A Comparison With Pressure-flow Study. *Urology*. 2014;83(3):550-555. doi:10.1016/j.urology.2013.10.012

197. Yalla SV, Sharma GVRK, Barsamian EM. Micturitional Static Urethral Pressure Profile: A Method of Recording Urethral Pressure Profile During Voiding and the Implications. *J Urol*. 1980;124(5):649-656. doi:10.1016/S0022-5347(17)55598-6

198. Hokanson JA, DeLancey JOL. Urethral failure is a critical factor in female urinary incontinence. Now what? *Neurourol Urodyn*. 2022;41(2):532-538. doi:10.1002/nau.24875

199. Danziger ZC, Grill WM. Sensory and circuit mechanisms mediating lower urinary tract reflexes. *Auton Neurosci*. 2016;200:21-28. doi:10.1016/j.autneu.2015.06.004

200. Zariffa J, Nagai MK, Daskalakis ZJ, Popovic MR. Influence of the Number and Location of Recording Contacts on the Selectivity of a Nerve Cuff Electrode. *IEEE Trans Neural Syst Rehabil Eng*. 2009;17(5):420-427. doi:10.1109/TNSRE.2009.2023301

201. Choi AQ, Cavanaugh JK, Durand DM. Selectivity of multiple-contact nerve cuff electrodes: a simulation analysis. *IEEE Trans Biomed Eng*. 2001;48(2):165-172. doi:10.1109/10.909637

202. Kronsteiner B, Carrero-Rojas G, Reissig LF, et al. Characterization, number, and spatial organization of nerve fibers in the human cervical vagus nerve and its superior cardiac branch. *Brain Stimulat*. 2024;17(3):510-524. doi:10.1016/j.brs.2024.04.016

203. Liu Y, Zhou X, Ma J, Ge Y, Cao X. The diameters and number of nerve fibers in spinal nerve roots. *J Spinal Cord Med*. 2015;38(4):532-537. doi:10.1179/1079026814Z.000000000273

204. Cheng C, Foxworthy GE, Fridman GY. A Cuff Lead for Delivering Ionic Direct Current (iDC) to Block Neural Activities of Sciatic Nerve*. In: *2023 45th Annual International Conference of the IEEE Engineering in Medicine & Biology Society (EMBC)*. IEEE; 2023:1-4. doi:10.1109/EMBC40787.2023.10340183

205. Bailey ZK, Nairac Z, Cuttaz EA, et al. Neuromodulation of a peripheral nerve using fully polymeric cuff electrodes: understanding predictability of selective stimulation. *J Neural Eng*. 2026;23(1):016032. doi:10.1088/1741-2552/ae44d0

206. Schmidt RA. Technique of pudendal Nerve Localization for Block or Stimulation. *J Urol*. 1989;142(6):1528-1531. doi:10.1016/S0022-5347(17)39150-4

207. Jottard K, Bonnet P, Bruyninx L, Ploteau S, De Wachter S. The ENTRAMI technique: Endoscopic transgluteal minimal invasive technique for implantation of a pudendal electrode under full visual control: A cadaver study. *Neurourol Urodyn*. 2019;38(1):130-134. doi:10.1002/nau.23850

208. Lienemann S, Donahue MJ, Zötterman J, Farnebo S, Tybrandt K. A Soft and Stretchable Multielectrode Cuff for Selective Peripheral Nerve Stimulation. *Adv Mater Technol*. 2023;8(6):2201322. doi:10.1002/admt.202201322

209. PMA supplement. Published online July 30, 2020. https://www.accessdata.fda.gov/scripts/cdrh/cfdocs/cfpma/pma.cfm?id=P970004S302

210. Pezzella A, McCrery R, Lane F, et al. Two-year outcomes of the ARTISAN-SNM study for the treatment of urinary urgency incontinence using the Axonics rechargeable sacral neuromodulation system. *Neurourol Urodyn*. 2021;40(2):714-721. doi:10.1002/nau.24615

211. Neuromod Prize announces two Phase 3 winners at HLTH 2025. Neuromod Prize. October 20, 2025. https://www.neuromodprize.com/phase-3-winners-announced/

212. TREATMENT OF OAB SYMPTOMS USING NEUSPERA'S ULTRA-MINIATURIZED SYSTEM: 6-MONTH RESULTS OF THE SANS-UUI PHASE II STUDY. Podium presented at: SUFU; March 1, 2025.

213. Jian J, Wang J, Shen B, et al. Pudendal Nerve Block by Adaptively Stepwise Increasing the Intensity of High-Frequency (10 kHz) Biphasic Stimulation. *Neuromodulation Technol Neural Interface*. Published online April 2023:S1094715923001496. doi:10.1016/j.neurom.2023.03.015

214. Lagunas AC, Rowan S, Chen PJ, et al. Human pudendal nerve mapping dataset. Published online 2025. doi:10.26275/PC8R-R3IU

215. Su X, Brink T, Nickles A, Nelson DE. Neuromodulation on Bladder Capacity in Conscious Sheep. *J Med Devices*. 2014;8(2):020924. doi:10.1115/1.4027023

216. Prager J, Metcalfe B, Sadrafshari S, Taylor J, Donaldson N, Granger N. Baseline cystometric parameters in conscious and anesthetized sheep: experimental data and

systematic review. *Am J Vet Res*. 2024;85(12):ajvr.24.06.0173. doi:10.2460/ajvr.24.06.0173

217. Xu JJ, Yousuf Z, Ouyang Z, et al. Anesthetic agents affect urodynamic parameters and anesthetic depth at doses necessary to facilitate preclinical testing in felines. *Sci Rep*. 2020;10(1):11401. doi:10.1038/s41598-020-68395-3